ΠΑΝΕΠΙΣΤΗΜΙΟ ΚΡΗΤΗΣ

ΤΜΗΜΑ ΒΙΟΛΟΓΙΑΣ

FOUNDATION FOR RESEARCH AND TECHNOLOGY - HELLAS
INSTITUTE OF MOLECULAR BIOLOGY AND BIOTECHNOLOGY

ΙΔΡΥΜΑ ΤΕΧΝΟΛΟΓΙΑΣ ΚΑΙ ΕΡΕΥΝΑΣ
ΙΝΣΤΙΤΟΥΤΟ ΜΟΡΙΑΚΗΣ ΒΙΟΛΟΓΙΑΣ ΚΑΙ ΒΙΟΤΕΧΝΟΛΟΓΙΑΣ

ΔΙΔΑΚΤΟΡΙΚΗ ΔΙΑΤΡΙΒΗ

Η ΙΣΟΡΡΟΠΗΜΕΝΗ ΑΠΟΘΗΚΕΥΣΗ ΚΑΙ ΑΠΟΙΚΟΔΟΜΗΣΗ ΤΩΝ ΑΓΓΕΛΙΟΦΟΡΩΝ RNAs ΡΥΘΜΙΖΕΙ ΤΗΝ ΟΜΟΙΟΣΤΑΣΗ ΤΩΝ ΜΙΤΟΧΟΝΔΡΙΩΝ, ΤΗ ΓΗΡΑΝΣΗ ΚΑΙ ΤΗΝ ΑΝΘΕΚΤΙΚΟΤΗΤΑ ΣΕ ΣΥΝΘΗΚΕΣ ΣΤΡΕΣ ΣΤΟ ΝΗΜΑΤΩΔΗ *Caenorhabditis elegans*

ΙΩΑΝΝΑ ΔΑΣΚΑΛΑΚΗ

ΗΡΑΚΛΕΙΟ

ΦΕΒΡΟΥΑΡΙΟΣ 2020

UNIVERSITY OF CRETE

BIOLOGY DEPARTMENT

FOUNDATION FOR RESEARCH AND TECHNOLOGY - HELLAS
INSTITUTE OF MOLECULAR BIOLOGY AND BIOTECHNOLOGY

FOUNDATION OF RESEARCH AND TECHNOLOGY
INSTITUTE OF MOLECULAR BIOLOGY AND
BIOTECHNOLOGY

PHD THESIS

BALANCED mRNA STORAGE AND DEGRADATION REGULATES MITOCHONDRIAL HOMEOSTASIS, AGEING AND STRESS RESISTANCE IN *Caenorhabditis elegans*

IOANNA DASKALAKI

HERAKLION

FEBRUARY 2020

Supervisor

Nektarios Tavernarakis
Chairman of the Board of Directors at the Foundation for Research and Technology-Hellas (FORTH), Professor at the Medical School of the University of Crete, Heraklion, Greece and affiliated group leader, IMBB-FORTH, Heraklion, Crete, Greece.

Advisory Committee

Christos Delidakis
Professor at the Biology Department of the University of Crete, Heraklion, Greece and affiliated group leader, IMBB-FORTH, Heraklion, Crete, Greece.

Achilleas Gravanis
Professor at the Medical School of the University of Crete, Heraklion, Greece and affiliated group leader, IMBB-FORTH, Heraklion, Crete, Greece.

Nektarios Tavernarakis
Chairman of the Board of Directors at the Foundation for Research and Technology-Hellas (FORTH) and Professor at the Medical School of the University of Crete, Heraklion, Greece and affiliated group leader, IMBB-FORTH, Heraklion, Crete, Greece.

Thesis Committee

Despina Alexandraki
Professor at the Biology Department of the University of Crete, Heraklion, Greece and affiliated group leader, IMBB-FORTH, Heraklion, Crete, Greece.

Christos Delidakis
Professor at the Biology Department of the University of Crete, Heraklion, Greece and affiliated group leader, IMBB-FORTH, Heraklion, Crete, Greece.

George A. Garinis
Professor at the Biology Department, University of Crete, Heraklion, Greece and affiliated group leader, IMBB-FORTH, Heraklion, Crete, Greece.

Achilleas Gravanis
Professor at the Medical School of the University of Crete, Heraklion, Greece and affiliated group leader, IMBB-FORTH, Heraklion, Crete, Greece.

Joseph Papamatheakis
Professor Emeritus at the Biology Department of the University of Crete, Heraklion, Greece and affiliated group leader, IMBB-FORTH, Heraklion, Crete, Greece.

Charalampos G. Spilianakis
Assistant Professor at the Biology Department of the University of Crete, Heraklion, Greece and affiliated group leader, IMBB-FORTH, Heraklion, Crete, Greece.

Nektarios Tavernarakis
Chairman of the Board of Directors at the Foundation for Research and Technology-Hellas (FORTH) and Professor at the Medical School of the University of Crete, Heraklion, Greece and affiliated group leader, IMBB-FORTH, Heraklion, Crete, Greece.

Thesis submitted in fulfilment of the requirements for the degree of doctor of Philosophy at University of Crete by the authority of the Supervisor Prof. Nektarios Tavernarakis and the members of the Advisory Committee, in the presence of the Thesis Committee appointed by the Academic Board to be defended in public on Wednesday 19 February 2020 at 12 a.m. in the Conference room, 3d floor, Physics Department.

Ευχαριστίες

Πηγαίνοντας πίσω στο χρόνο και αναπαράγοντας τις στιγμές που έζησα τα τελευταία χρόνια, αισθάνομαι ότι το διδακτορικό ήταν ένα ταξίδι. Ένα περιπετειώδες ταξίδι από την «άγνοια» στη «σοφία». Την «σοφία» που μέχρι σήμερα έχω καταφέρει να αποκτήσω και εύχομαι να έχω την τύχη να αποκτήσω ακόμη περισσότερη στο μέλλον.

Γι' αυτή την εμπειρία θα ήθελα αρχικά να ευχαριστήσω τον Νεκτάριο Ταβερναράκη, ο οποίος ουσιαστικά έδωσε το πράσινο φως για να ξεκινήσω το διδακτορικό μου υπό την επίβλεψή του. Τον ευχαριστώ θερμά όχι μόνο για την στήριξη του αλλά και γιατί αποτελεί λαμπρό παράδειγμα για εμένα. Αποτελεί ένα πρότυπο που μου δίνει τη δύναμη και αισιοδοξία.

Ταυτόχρονα, το ίδιο μεγάλο ευχαριστώ θα ήθελα πω στη Μαίρη Μαρκάκη, η οποία με έμαθε πάρα πολλά και ήταν δίπλα μου όποτε το χρειαζόμουν. Όλα αυτά τα χρόνια ήταν το πιο κοντινό μου άτομο στο εργαστήριο, το άτομο που ακόμα και με μια ματιά μπορούσε να καταλάβει αν είμαι χαρούμενη ή αν κάτι με προβληματίζει. Είναι η αδυναμία μου στο εργαστήριο..

Στην συνέχεια θα ήθελα να ευχαριστήσω την Αγγέλα Πασπαράκη για τις υπέροχες φωτογραφίες confocal, πολλές από τις οποίες νομίζω ότι έχουν και καλλιτεχνική πέραν της επιστημονικής τους αξίας!! Επίσης πάντα φρόντιζε να μην μου λείψει τίποτα!!! Ευχαριστώ πολύ για όλα (καρδούλα).

Στην συνέχεια θα ήθελα να ευχαριστήσω ιδιαίτερα την Ειρήνη Λιονάκη και τον Ηλία Γκίκα για την όμορφη συνεργασία που έχουμε τα τελευταία χρόνια, η οποία μου έδωσε την ευκαιρία να μάθω πολλά νέα πράγματα. Επίσης τους ευχαριστώ για τις απίστευτα εποικοδομητικές, ανοιχτές και χωρίς πλαίσια συζητήσεις που έχουμε για επιστημονικά θέματα οι οποίες πραγματικά με συναρπάζουν και με εμπνέουν. Τους ευχαριστώ επίσης και για την εμπιστοσύνη, το πνεύμα συνεργασίας και την ανιδιοτέλειά τους.

Επίσης θα ήθελα να ευχαριστήσω και τα υπόλοιπα μέλη του εργαστηρίου για τις εμπειρίες που μοιραστήκαμε και την γνώση που ανταλλάξαμε. Συγκεκριμένα θα ήθελα να ευχαριστήσω τη Διονυσία Πετράτου, την Andrea Princz, την Περσεφόνη Φραγκιαδάκη, την Χριστίνα Πλουμή, την Μαργαρίτα Παπανδρέου, την Αγγελική Σωτηρίου, την Μάρθα Γκικόλαι, τον Κώστα Κουνάκη, τον Θάνο Μεταξάκη, τον Κώστα Παλικαρά, τον Νίκο Χαρμπίλα και τον Γιώργο Κωνσταντινίδη.

Πολύ συμαντικό ρόλο έπαιξαν επίσης τα μέλη της τριμελούς συμβουλευτικής μου επιτροπής Χρήστος Δελιδάκης και Αχιλλέας Γραβάνης που με στήριξαν και με συμβούλευαν κατά τη διάρκεια του διδακτορικού μου. Θα ήθελα επίσης να

ευχαριστήσω τα υπόλοιπα μέλη της επταμελούς μου επιτροπής τα οποία έχουν συμβάλει σε αυτή την πορεία ο καθένας με τον τρόπο του ήδη από τα έτη που φοιτούσα στο Τμήμα Βιολογίας του Πανεπιστημίου Κρήτης. Αρχικά τον Ιωσήφ Παπαματθαιάκη δίπλα στο οποίο έκανα τα πρώτα μου βήματα και πάντα αποτελούσε μέντορα για εμένα, την Δέσποινα Αλεξανδράκη, τον Γιώργο Γαρίνη και τον Χαράλαμπο Σπηλιανάκη.

Τέλος, θα ήθελα να ευχαριστήσω ιδιαιτέρως τον πιο κοντινό μου άνθρωπο, τον Ηλία Γκίκα, την οικογένεια μου και τους φίλους μου που με την αγάπη και την υπομονή τους όχι μόνο κατανόησαν την «απουσία» μου αλλά ήταν πάντα «παρών». Δεν υπάρχουν λόγια που να μπορούν να περιγράψουν την συνεισφορά τους.

Περίληψη

Ο αριθμός των μιτοχονδρίων σε συνδυασμό με την λειτουργία τους αποτελούν σημαντικούς ρυθμιστές της υγείας των ατόμων αλλά και του προσδόκιμου ζωής αυτών σε ποικίλους οργανισμούς, από απλούς όπως ο νηματώδης *C. elegans* έως και πολύ πολύπλοκους όπως είναι ο άνθρωπος. Συγκεκριμένα, η διατάραξή τους συσχετίζεται συχνά με παθολογικές καταστάσεις όπως τα λυσοσωμικά αθροιστικά νοσήματα, η καρδιαγγειακή νόσος, ο νευροεκφυλισμός και σακχαρώδης διαβήτης τύπου 2, μεταξύ άλλων. Ο αριθμός των μιτοχονδρίων ελέγχεται στενά από δύο αντίθετες διαδικασίες, την βιογένεση των μιτοχονδρίων και τη μιτοφαγία. Σε αντίθεση με τη μιτοφαγία, η οποία έχει μελετηθεί εκτεταμένα, οι μηχανισμοί μιτοχονδριακής βιογένεσης εξακολουθούν να είναι ως επί το πλείστον ανεξερεύνητοι. Η ημι-αυτόνομη φύση των μιτοχονδρίων καθιστά τη βιογένεσή τους μια πολύπλοκη διαδικασία που βασίζεται στον συντονισμό σηματοδότησης από τα μιτοχόνδρια προς τον πυρήνα και από τον πυρήνα προς τα μιτοχόνδρια. Η τοπική μετάφραση των μεταγραφημάτων μιτοχονδριακών πρωτεϊνών που κωδικοποιούνται από το πυρηνικό DNA (NEMTTs) κοντά στα μιτοχόνδρια, είναι θεμελιώδης για τη βιογένεση των μιτοχονδρίων. Παρόλο που αναμένεται ότι κυτταροπλασματικοί παράγοντες θα πρέπει κυρίως να ρυθμίζουν την τοπική μετάφραση υπό κανονικές συνθήκες και ως απόκριση σε στρες, οι παράγοντες αυτοί παραμένουν ασαφείς.

Στόχος της παρούσας διατριβής είναι η διαλεύκανση αυτών των παραγόντων χρησιμοποιώντας ως πρότυπο οργανισμό το *C. elegans*. Στα πλαίσια αυτή, αποκαλύπτουμε ότι κυτταροπλασματικοί παράγοντες που σχετίζονται με το μονοπάτι 5'-3' αποικοδόμησης των αγγελιοφόρων RNA (mRNA), αποτελούν νέους, βασικούς ρυθμιστές του αριθμού και της λειτουργίας των μιτοχονδρίων στο νηματώδη. Πιο συγκεκριμένα, δείχνουμε ότι το πρωτεϊνικό σύμπλοκο που πραγματοποιεί την αφαίρεση του καλύμματος των mRNA και το σύμπλοκο αποαδενυλίωσης (CCR-4 / NOT) εμπεριέχονται σε

ξεχωριστούς σχηματισμούς που έχουν φυσική αλληλεπίδραση με τα μιτοχόνδρια και ρυθμίζουν αντίθετα τον αριθμό τους κατά τη διάρκεια της γήρανσης. Ο μηχανισμός μέσω του οποίου επιτυγχάνουν κάτι τέτοιο βασίζεται στη μετα-μεταγραφική ρύθμιση των NEMTTs που πραγματοποιείται κοντά στο οργανίδιο. Η ισορροπημένη αποικοδόμηση και αποθήκευση των NEMTTs-στόχων είναι αναγκαία για τη ρύθμιση του αριθμού και της λειτουργίας των μιτοχονδρίων. Η επίτευξη μιας τέτοιας ισορροπίας τελικά προάγει την απόκριση σε στρες και τη μακροβιότητα ατόμων *C. elegans*. Τα ευρήματά μας αποκαλύπτουν ένα νέο ρόλο των παραγόντων μεταβολισμού των mRNAs στη βιογένεση των οργανιδίων και με αυτό τον τρόπο οδηγούν στην ταυτοποίηση των κυτταροπλασματικών συστατικών που συντονίζουν την τοπική μετάφραση κατά τη διάρκεια της γήρανσης και υπό συνθήκες στρες στο *C. elegans*.

Abstract

Mitochondrial abundance and function are essential regulators of healthspan and lifespan in organisms as diverse as the nematode *Caenorhabditis elegans* and humans. Importantly, their perturbation has been associated with various pathological conditions, including lysosomal storage disease, cardiovascular disease, neurodegeneration and type 2 diabetes mellitus, among others. Mitochondrial abundance is tightly regulated by the two opposing processes of mitochondrial biogenesis and mitophagy. While mitophagy has been extensively studied, mitochondrial biogenesis remains largely unexplored. This is a complex, multi-step process coordinated by retrograde and anterograde responses. Local translation of nuclear-encoded and mitochondrial-targeted transcripts (NEMTTs) in the vicinity of mitochondria is crucial for the organelle biogenesis. Although cytoplasmic factors are expected to principally regulate local translation under normal conditions and in response to stress, the identity of such factors remain elusive. Here, we uncover a pivotal role for cytoplasmic components known to participate in the 5'-3' mRNA degradation pathway, in regulating mitochondrial abundance and function in *C. elegans*. Specifically, we show that the mRNA decapping and the CCR-4/NOT complexes form distinct foci that physically associate with mitochondria and oppositely regulate mitochondrial abundance during ageing. The underlying mechanism relies on the post-transcriptional regulation of NEMTTs in the vicinity of the organelle. Balanced mRNA degradation and storage of target NEMTTs is required for the regulation of mitochondrial abundance and function, ultimately promoting stress resistance and longevity in *C. elegans*. Our findings uncover a novel role for mRNA metabolism components in mitochondrial biogenesis and identify the cytoplasmic constituents that fine-tune local translation during ageing and under conditions of stress in *C. elegans*.

Contents

CHAPTER 1
INTRODUCTION

1.1 *C. elegans* as a model organism

Caenorhabditis elegans (*C. elegans*) is a species which belongs to the superphylum of *Ecdysozoa*, the phylum of *Nematoda* and the family of *Rhadbitidae*. It is a free-living, nonparasitic microscopic roundworm which, in nature, is found in the soil. In its natural habitat, it feeds on bacteria grown on rotting matter (usually decomposing plant or fruit matter) while in the laboratory it feeds on bacterial *E. coli* strains grown either on solid or in liquid growth media (Riddle et al., 1997). In nature, *C. elegans* lives worldwide, but the strain most commonly used among the scientific society was isolated from mushroom compost in the area of Bristol in the UK, and so it was named, N2 Bristol (or just N2)(Nicholas W L, 1959). *C. elegans* is tiny enough to make its observation by naked eye impossible. In respect to that, the length of an adult animal is about 1mm and its width around 50μm. Dissecting microscopes assist animal study and handling in the laboratory. Sydney Brenner in 1974 first established *C. elegans* as a model organism, and since then it has become the model for studies in the field of apoptosis, ageing and neurodegeneration, among others (Brenner, 1974).

One of its notable advantages is its short life cycle. It can reach adulthood in just ~2.5 days when grown at 20^{o}C (**Figure 1**). Temperature plays a vital role in numerous metabolic processes as well as the time interval needed for the organism to reach adulthood. Temperatures higher than 20^{o}C and within an accepted temperature window for animal survival, accelerate development, whereas lower temperatures reduce developmental rates (Byerly et al., 1976).

Even though a *C. elegans* population comprises two different sexes, the hermaphrodites (XX) and the males (XO), males naturally occur quite infrequently (0,1% of the total population) while they rise in number upon heat stress or *him* mutation (Hodgkin and

Doniach, 1997; Hodgkin et al., 1979; Ward and Carrel, 1979). We implement very frequently such means of enhanced male production in the laboratory for crossing *C. elegans* transgenic or mutant strains. In this manner, we can create animals with the required genetic backgrounds needed for specific applications in genetic analyses studies. Hermaphrodites produce sperm, and at some point during late larval development, they subsequently shift from sperm to oocyte generation. The spermatheca contains the sperm. There, unfertilized oocytes are fertilized and continue to develop into the developing embryo (WormAtlas, Introduction to *C. elegans* anatomy). Part of embryogenesis takes place in utero while it finalizes ex utero. During ex utero embryonic development, the embryos within the laid eggs continue to develop and grow until they hatch. The newly hatched animals are larvae of developmental stage 1 (L1). The L1 larvae grow in size and proceed through four larval stages until they reach adulthood (L1-L4) (Ref: https://www.wormatlas.org/hermaphrodite/introduction/mainframe.htm).

When conditions become unfavorable, for example, food scarcity, overpopulation or high temperature, then stage 2 *C. elegans* larvae may enter an alternative developmental pathway. This alternative pathway is called the dauer stage. *C. elegans* dauer larvae are phenotypically distinct from wild type larvae as they are longer, thinner, with a relatively impermeable cuticle as compared to the non-dauer cuticle and are super-resistant to chemicals and other stressors (Klass and Hirsh, 1976). The dauer larva does not feed, although it contains more body fat when compared to wild type larvae. Besides, the dauer larva continually moves quickly around the petri dish, while seeking for a favorable environment for growth. It is remarkable, though, that in this stage, it can survive up to about five months without food (Cassada and Russell, 1975; Frezal and Felix, 2015). When conditions become favorable again, dauer larvae can rapidly enter normal development and directly transform into an L4 larva (**Figure 1**).

The L1 larvae can also be frozen in a solution with glycerol and stored at -80^{o}C. This feature enables researchers to maintain thousands of diverse transgenic lines or mutant strains, and use them even years later. The number of progeny any wild type adult hermaphrodite can produce during the first three-four days of adulthood, is around 300. This feature enables researchers the utilization of a large number of animals in each experimental process.

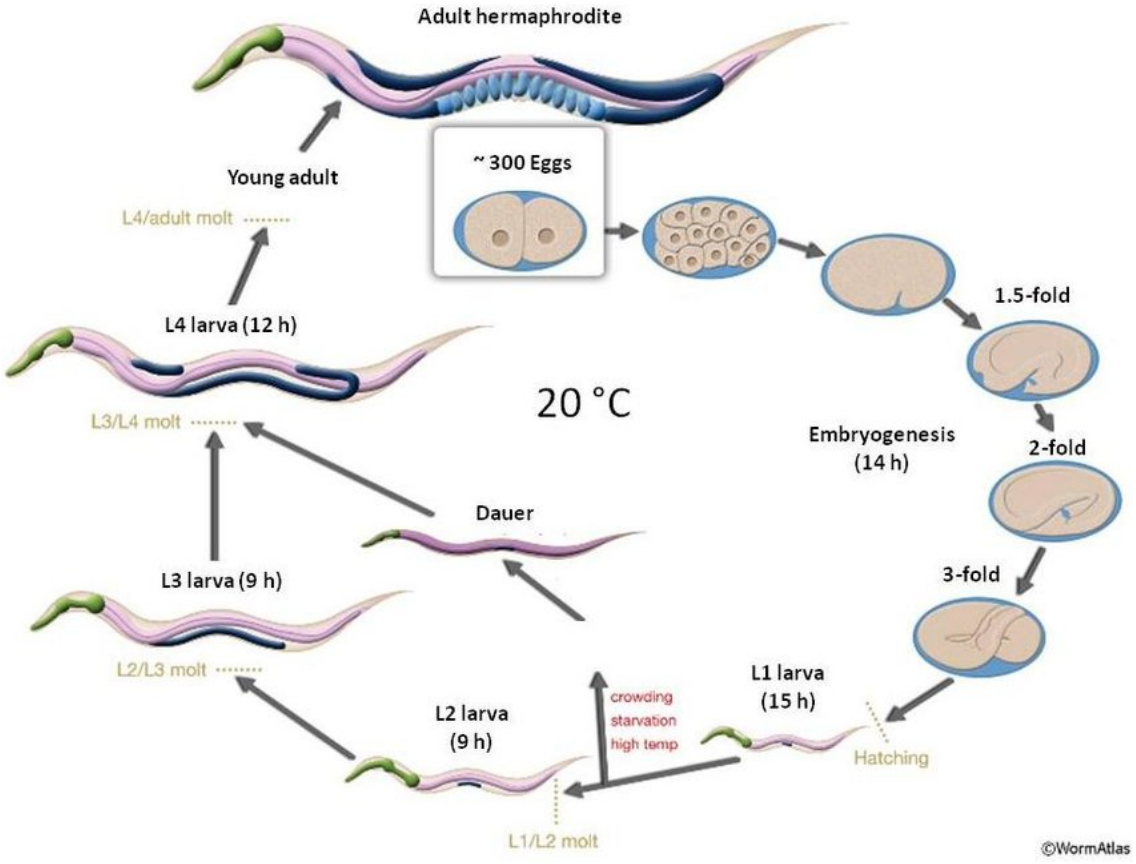

Figure 1. The life cycle of *C. elegans* at 20^{o}C.

Another essential trait of *C. elegans* is that it is a transparent organism. This trait facilitates the study of cell differentiation and the tracking of the developmental fate of each of its cells (Corsi et al., 2015). Furthermore, it enables the *in vivo* imaging of whole organelles or single, fluorescent-tagged molecules, among others.

Indispensable for genetic studies is the fact that the progeny of *C. elegans* adults are genetic clones of their parents and have an invariable cell lineage since the organism is self-fertile. Hermaphrodites have 959 somatic cells, while males have 1031 somatic cells. Additionally, the *C. elegans* genome consists of about 21.000 genes, a number pretty close to the human genome, which consists of approximately 25000 genes (Hillier et al., 2005). *C. elegans* was the first multicellular organism to have its genome sequenced in 1998 (Consortium, 1998).

Moreover, physical maps of the genome based on the use of cosmids and artificial chromosomes (YACs) have been constructed (Coulson et al., 1991). *C. elegans* genome is quite compact and organizes in five pairs of autosomal chromosomes and one pair of sex chromosomes (Hodgkin, 2005). Interestingly, 60-80% of human genes have an orthologue in the *C. elegans* genome (Aboobaker and Blaxter, 2000). This finding reinforces the evolutionary conservation of many cellular functions from *C. elegans* to humans. All the above make the organism highly amenable to genetic analysis since they enable the implementation of double-stranded RNA mediated interference (dsRNAi) techniques for targeted silencing of genes of interest even in genome-wide scale (Mello and Conte, 2004).

Another trait that encourages the notion that *C. elegans* is an excellent genetic model is the fact that viable mutants for genes of interest can be easily generated (Kutscher and Shaham, 2014). Moreover, transgenesis is also applicable and accessible in *C. elegans*. Microinjection or microparticle bombardment are techniques implemented for the generation of transgenic strains that overexpress genes of interest with fluorescent or non-fluorescent tags (Isik and Berezikov, 2013; Rieckher and Tavernarakis, 2017). Notably, through microparticle bombardment, it is possible to even get the integration of the genetic cassette of interest in the *C. elegans* genome. A more controlled way to

create *C. elegans* strains that have single genetic integration at the desired locus is through CRISPR/Cas9 (Dickinson and Goldstein, 2016). This technique is not only utilized for the generation of transgenics but also mutant strains bearing the type of mutation of interest.

What is more, the organism's neuronal system is quite simple as it consists of 302 neurons (Hobert, 2010). The system simplicity, the transparency of the organism as well as the well-characterized cell lineages, allowed the full characterization of the organism's connectome in 1996. In this study, they found that the organism's connectome consists of 5000 chemical synapses, 600 gap junctions and 2000 neuromuscular junctions (Mulcahy et al., 2018; White et al., 1986). Despite the relatively simple neuronal system, it displays numerous primitive and complicated behaviors such as feeding, locomotion and reproduction or learning, mating and social behaviors respectively. The animal's behavior can be representative of neuronal function, making it an exceptional model for studying compounds and molecular mechanisms that regulate neurons or for investigating how ageing influences the neuronal system (Mori, 1999).

Last but not least, *C. elegans* mean lifespan is about fifteen days, and the maximal lifespan is around thirty days. Interestingly, adults who have reached the last third of their lifespan display significantly lower locomotion and pumping rates, muscle deterioration and an overall decline of healthspan as witnessed in aged humans too (Collins et al., 2008). These features, in combination with its short lifespan, make it a perfect model for ageing studies.

1.2 Regulation of ageing in *C. elegans*

Ageing is the gradual accumulation of damage to molecules, cells and tissues. In a living organism, this accumulation drives physical and functional deterioration. It is a multifaceted and complex, time-dependent process which is encountered by the vast majority of all living organisms. Ageing entirely correlates with an enhanced probability of disease onset and neurodegeneration (Lopez-Otin et al., 2013; Tosato et al., 2007). Lately, considerable effort has been invested in understanding the genetic regulation behind the ageing process. The intention of this effort is the identification of single genes, the molecular pathways, chemical compounds or environmental factors that modify lifespan in model organisms such as *C. elegans* (Olsen et al., 2006). Development of intervention strategies that would slow down the ageing process and would improve healthspan is currently the heart of the ageing studies.

C. elegans, for all reasons, as mentioned earlier, is an ideal model for such studies. The most robust output we get from ageing studies in *C. elegans* is the analysis of the animal's mean and maximal lifespan. Importantly, the first evidence supporting that the ageing process is genetically regulated emanated from *C. elegans* studies (Kenyon, 2010). The high conservation between the *C. elegans* and the human genomes facilitates the successful conduction of such complex studies. Lifespan analysis studies would be time-consuming or even impossible if not conducted in the simple, short-lived nematode. In most cases, findings apply to higher, complex eukaryotes such as humans due to genome conservation. Currently, there is a significant advancement in the field of ageing. To date, among the most critical genetic regulators of ageing are the Insulin/IGF-1 signaling cascade, AMP-activated kinase activity, TOR signaling, the JNK-1 pathway, signaling from the reproductive system of *C. elegans* and signaling from mitochondria (**Figure 2**).

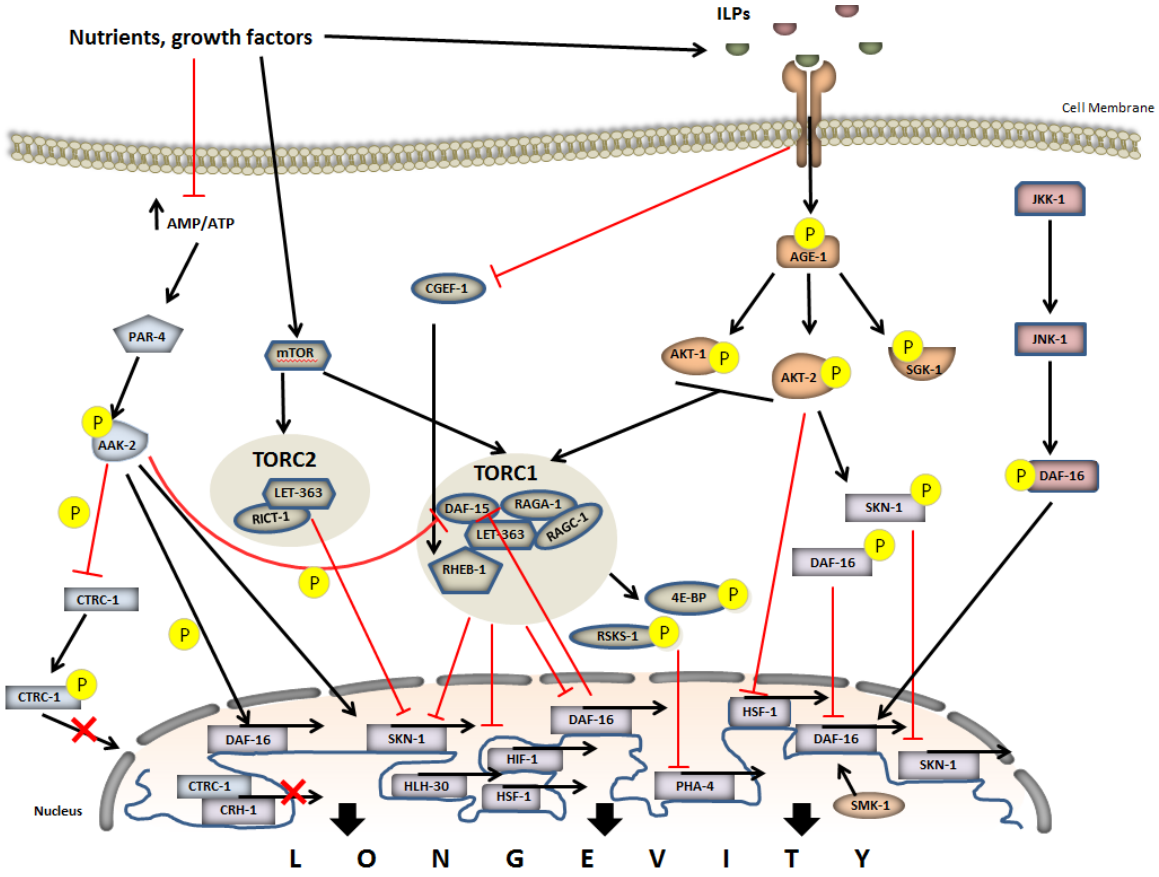

Figure 2. **Genetic regulation of lifespan**.
The insulin/IGF- (IGF-1), the target of rapamycin (TOR), and the AMPK signaling pathways act both in parallel and synergistically to affect lifespan. Phosphorylation events and pathway crosstalk fine-tune transcription factor activation in the nucleus and determine longevity.

In addition to genetic regulation, ageing is also subjected to non-genetic regulation. Non-genetic regulation comprises of epigenetic mechanisms such as chromatin modifications and environmental stimuli. Furthermore, stress insults such as heat stress, oxidative stress or hypoxia and pharmacological interventions, are robust, non-genetic ways to intervene with the function of transcription factors and molecular processes to influence longevity as displayed in **Figure 3 (A & B,** respectively**)** (Daskalaki et al., 2020).

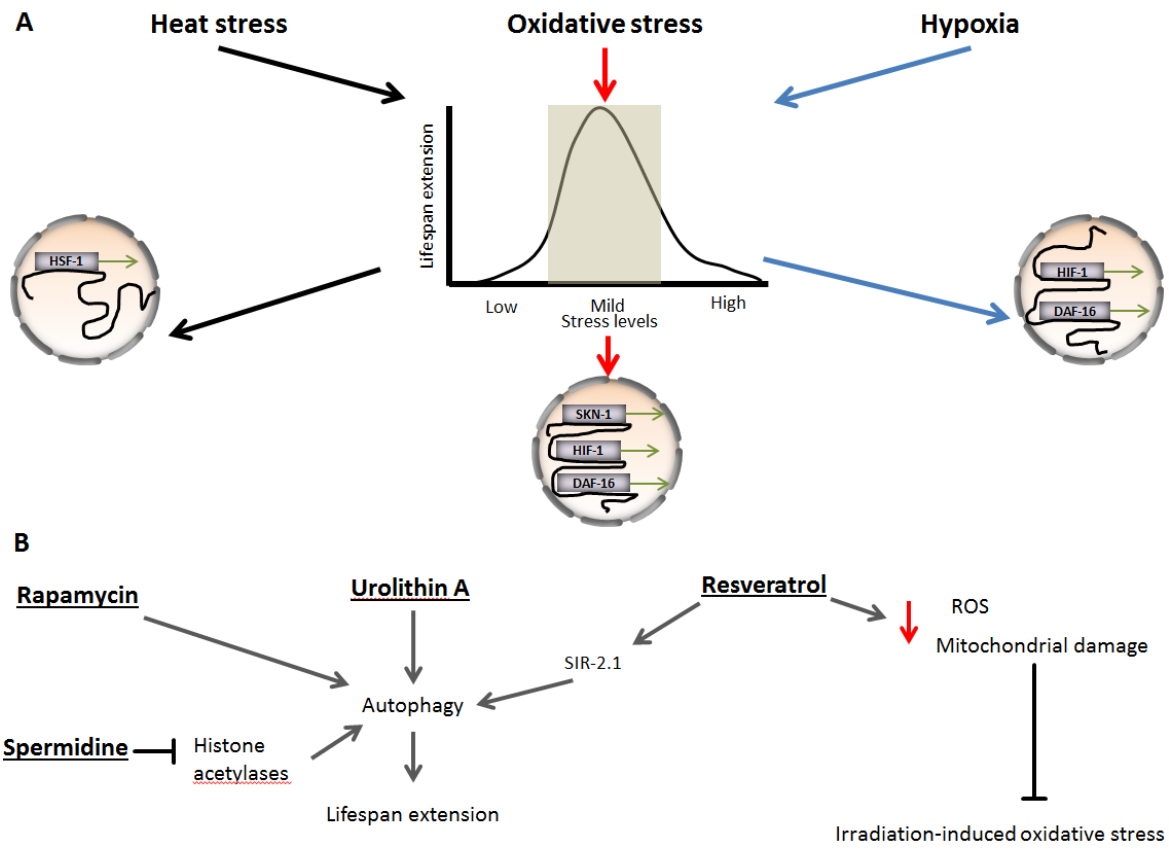

Figure 3. Environmental and pharmacological factors that modulate lifespan. (A) Animals exposed to mild heat, oxidative, and hypoxic stress display lifespan extension, which is mediated by the activation of distinct transcriptional programs (black arrows are representative of heat stress-related responses, red arrows of oxidative stress, and blue arrows of hypoxic stress); (B) treatment with rapamycin, resveratrol, urolithin A, and spermidine confer lifespan extension by inducing autophagy-related mechanisms.

1.3 P bodies: composition and function

Processing bodies (P-bodies) were first discovered in 1997 by Bashkirov et al. (Bashkirov et al., 1997). They are conserved across eukaryotes, non-membranous cytoplasmic granules that consist of untranslated mRNAs and RNA binding proteins. P-bodies coordinate mRNA metabolism post-transcriptionally and are ubiquitous, in all somatic tissues. They are mobile and travel on microtubules in a dynein-dependent manner (Aizer

et al., 2008). Their formation is dynamic and displays remarkable modification during ageing and under stress (Rieckher et al., 2018). While our understanding of their formation and composition is yet limited, only recently, progress emerged regarding both.

Notably, the fundamental notion that non-translating mRNAs are a pre-requisite for P-body formation is presently improved by the finding that the process depends on the liquid-liquid phase transition. Concerning this theory of P-body formation, when stalled mRNAs and RNA binding proteins (RBPs) reach a critical concentration, protein-protein or protein-RNA associations urge the assembly of the mRNP granules. These initial condensates mainly comprise of scaffold molecules required for the foci assembly. These initial associations, most likely, trigger an alteration in the conformation of the primary components that subsequently triggers new associations with adjacent proteins or mRNAs. These additional components that bind on the scaffold proteins most possibly designate the function of the formed P-body. Interestingly, this suggests that foci with diverse protein constituents may exert distinct functions.

Moreover, P-body isolation and subsequent characterization of its proteins and mRNA cargoes would improve understanding of their physiology and function. Nonetheless, this is pretty laborious, considering P-bodies are highly dynamic and membrane-less. Lately, Arnaud Hubstenberger et al. sought to isolate P-bodies by developing a fluorescence-activated particle sorting (FAPS) method. By applying this technique, the authors discovered more than one hundred new P-body components. In the same study, they showed that around the one-fifth of the cytoplasmic transcripts could be located in P-bodies. It was surprising though, that these transcripts encoded only regulatory molecules, while transcripts that encode housekeeping components were not present in the formations (Hubstenberger et al., 2017). While the analyzed sample in this study was extracted from human epithelial cells, it is more than expected that much of this cargo

would vary among the different cell-types. We speculate that P-body composition and cargo would differ if cells are primary or cultured (cell lines), especially in the case that P-bodies are regulated cell non-autonomously. Other factors that could remodel P-body composition are the developmental stage, the type of tissue and stress, among others.

Owing to their function, P-bodies govern mRNA metabolism and the regulation of mRNA storage, degradation and translation of target mRNAs. Notwithstanding, although the P-body component repository has expanded lately, still their role in mRNA metabolism is not questioned. The dispute is arising pertinent to whether P-bodies are sites for both mRNA degradation and storage. Indeed, depletion of P-bodies did not affect mRNA degradation in yeast and mammalian cells (Decker and Parker, 2012; Eulalio et al., 2007b). Initial studies suggested that both processes operate inside P-bodies while contemporary data corroborate the notion that P-bodies serve as mRNA storage sites, though this needs further validation.

P-bodies insulate mRNAs for storage and 5'-3' exonucleolytic decay, while a subset of their bound mRNAs is released for translation when conditions become permissive (Aizer et al., 2014; Luo et al., 2018; Temme et al., 2014). Like yeast, flies and mammals, 5'-3' exonucleolytic decay entails shortening of the poly-A tail by the CCR-4/NOT deadenylase complex in the nematode *C. elegans* (Nousch et al., 2013).

Of note, the poly-A tail length positively correlates with the translation competence of each transcript. Long poly-A tails are associated with high translation efficiency, mild shortening associated with mRNA storage and complete shortening with mRNA degradation. As a result, the CCR-4/NOT complex dominantly controls mRNA storage apart from the translation and degradation of target transcripts (Gotic and Schibler, 2012). CNOT6/CCR-4 and CAF1/CCF-1 are the two main deadenylase enzymes with complementary functions while CNOT2, the NTL-2 homologue in *C. elegans,* positively

regulates the formation of the complex and the deadenylation efficiency of the enzymes (Ito et al., 2011; Zheng et al., 2008). After complete shortening of the poly-A tail, target mRNAs are driven for decapping by the decapping complex DCAP-1/DCAP-2/EDC-3 and subsequent exonucleolytic degradation by the 5'-3' exonuclease, XRN-1(Eulalio et al., 2007a; Garneau et al., 2007; Nishimura et al., 2015). Rarely though, following deadenylation, mRNAs are degraded in a 3' to 5' direction by the exosome (**Figure 4**).

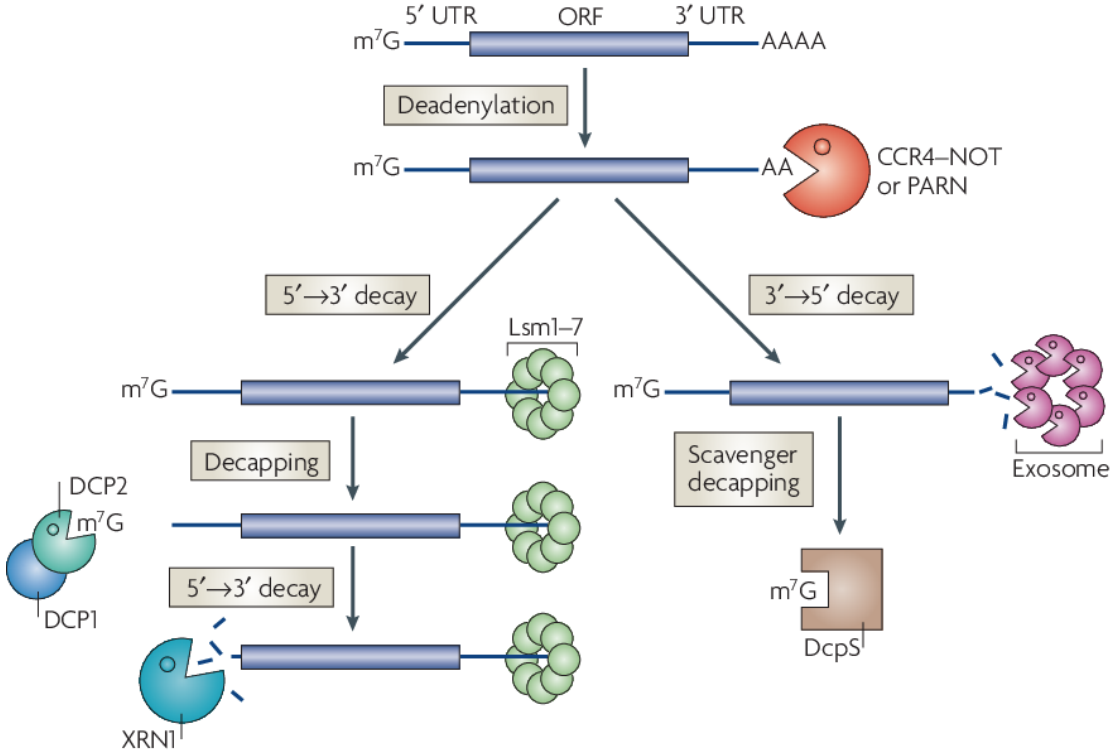

Figure 4. **mRNA degradation pathways at a glance.** The left branch of the Figure shows the 5' to 3' mRNA degradation pathway that functions inside P- bodies and the right branch the 3'-5'degradation by the exosome.

1.4 P-bodies and control of protein synthesis

Protein synthesis is an energy-consuming process which tightly regulates the majority of cellular processes. It modulates organismal homeostasis through fine-tuning gene

expression in response to a great variety of stimuli such as development, stress and ageing. It was initially observed, *in vivo*, that global translation levels drop with age in various model organisms; this finding was reproduced *in vitro* (Gems et al., 2002; Partridge and Gems, 2002; Tavernarakis and Driscoll, 2002). The age-dependent drop in translation rates occurs presumably because both the efficiency of translation factors' activity and their abundance significantly decrease during ageing in several model organisms (Kimball et al., 1992; Makrides, 1983; Moldave et al., 1979; Partridge and Gems, 2002; Rattan, 1996; Takahashi et al., 1985; Vargas and Castaneda, 1981, 1983; Webster and Webster, 1983). Supplementary studies provided evidence indicating that not only translation initiation factors but also ribosome and translation elongation factors are affected (Gonskikh and Polacek, 2017; Janssens and Veenhoff, 2016; Rattan, 1996). Still, it was hard to answer, whether this was the result of the global decline of cell function regulated by the ageing process itself or if translation rates govern ageing. Recent studies in yeast, *C. elegans*, flies and mice unveiled that either genetic or pharmacological interventions that lower translation rates, extend lifespan, thus regulate ageing (Hansen et al., 2007; Kaeberlein and Kennedy, 2008; Steffen et al., 2008; Syntichaki et al., 2007).

Protein synthesis consists of three fundamental stages: initiation, elongation and termination. Importantly, inhibition at the first steps of the process is critical for lifespan extension. Even though blocking the initiation step of translation is very crucial; still, inhibition of translation at the elongation step confers lifespan extension too (Leprivier et al., 2013). The translation initiation factor eIF4E, which binds on the 5' cap of mRNAs and recruits the ribosomes, holds an executive role at the initiation step (Gingras et al., 1999). In *C. elegans*, eIf4E has five isoforms: IFE-1, IFE-2, IFE-3, IFE-4 and IFE-5. While IFE-1, IFE-3 and IFE-5 are specifically expressed in the gonad of the nematode, IFE-2 and IFE-4 are expressed in somatic cells (Tavernarakis, 2007). Concerning the control of the

ageing process, only IFE-1 has a moderate effect when blocked post-developmentally while the most prominent effect, was observed upon IFE-2 depletion (Syntichaki et al., 2007). Considering that the rest of the translation initiation factors did not have any effect on lifespan and that *ife-2* lifespan extension was observed even in the absence of a gonad, we conclude that reduction of protein synthesis drives lifespan extension acting principally through the somatic tissues. Further, post-developmental downregulation of several additional factors from the eIF complex and the ribosome can significantly extend lifespan (Chen et al., 2007; Curran and Ruvkun, 2007; Hansen et al., 2007; Pan et al., 2007).

At the genetic level, numerous pathways modulate protein synthesis. The kinase target of rapamycin (TOR and more specifically the mTORC1 branch) pathway, the insulin/IGF-1 pathway, the integrated stress response (ISR) and the p38 mitogen-activated protein kinase (MAPK) pathway are among the most critical signal transduction cascades that modulate protein synthesis and ageing (Gingras et al., 2004; Proud, 2007; Tavernarakis, 2008). Nevertheless, not every aspect of this regulation is entirely understandable to date, since they and eIF4E, do not seem to control lifespan through the same genetic pathway (Tavernarakis, 2007).

Decreased global translation rates are not only beneficial for lifespan but also for stress resistance. Why animals that have lower translation rates become long-lived and more stress-resistant, is a fascinating field to study. It is becoming apparent that the beneficial effects of protein synthesis inhibition are due to two different etiologies. First, since ageing positively correlates with the aggregation of dysfunctional or misfolded proteins, it is expected that diminished protein synthesis would alleviate toxicity induced by the accumulation of such malfunctioning products. Lower protein synthesis rates could correlate with higher accuracy and less toxic byproducts, although the fidelity of the translation processes does not seem to significantly decline during ageing (Filion and

Laughrea, 1985; von der Haar et al., 2017). Second, since as mentioned before, protein synthesis is an incredibly energy-consuming process, its downregulation is expected to save much of the cell energy. In that case, the cell can invest the extra energy for cell maintenance, repairing and surveillance processes. The latter is supported by findings showing that animals displaying low protein synthesis rates are more resistant to several stresses such as oxidative stress (Syntichaki et al., 2007). Evidence points that although global translation attenuates, the translation of stress response factors is selectively induced, through yet not well-understood mechanisms (Clemens, 2001; Holcik and Sonenberg, 2005; Rogers et al., 2011). It is possible, though, that P-bodies control the selective gene expression witnessed under conditions similar to the previously discussed. As explained earlier, P-bodies can encapsulate, conditionally and occasionally, up to the one-third of the transcriptome. Besides, their formation capability and composition may vary in a stress- and age-specific manner (Borbolis and Syntichaki, 2015; Lechler and David, 2017; Rieckher et al., 2018; Rousakis et al., 2014). Under the above-mentioned conditions, although specific components may exit or appear inside P-bodies, the prevailing idea is that the core P-body components aggregate more and form larger and more numerous foci per cell upon stress. Since P-bodies are sites of mRNA degradation and storage, their rise during ageing and in response to stress positively correlates with a dip in global translation rates noted under the same conditions. Nevertheless, considerable effort is still required to interpret if the translational regulation is transcript-specific, or equal for all bound mRNAs.

In respect to transcript-specific regulation, it is possible that confined associations with select RNA binding proteins, regulate the fate of each mRNA differently, even compared to adjacent mRNAs. The ability of P-bodies to control the fate of these mRNAs renders them translation regulatory hubs of target transcripts. Recent work further established their role in translation. Specifically, P-bodies marked by either EDC-3 or DCAP-1 have

been shown to sequester and entrap a principal mRNA translation regulator, eIF4E/IFE-2 during ageing and upon stress, making it unavailable for translation initiation. Interestingly, this phenomenon was further induced by EDC-3 deficiency (Rieckher et al., 2018). EDC-3-depleted animals are long-lived and more resistant to stressors due to cytoplasmic translation inhibition (Rieckher et al., 2018; Syntichaki et al., 2007). Although further research is still needed to advance our understanding of P-body physiology and function, the upcoming role of these foci as dynamic translation regulators of target transcripts highlights their significance towards improving healthspan and stress resistance. Of note, perturbation of P-body components has been associated to severe human pathologies, corroborating their significance for organismal physiology (Singh et al., 2008; Vicente et al., 2018; Yoshimi and Abdel-Wahab, 2018; Zhang and Rabouille, 2019).

1. 5 Mitochondria and ageing

Mitochondria are cytoplasmic organelles of prokaryotic origin. They contain their genome which encodes just about the 1%-2% of their protein content while the nuclear genome encodes the rest. Therefore, they are semi-autonomous organelles. Mitochondria serve conserved functions among model organisms. They primarily regulate ATP production, the primary cellular source of energy, through the electron transport chain (ETC)-mediated oxidative phosphorylation.

Moreover, they regulate lipid metabolism, copper and calcium homeostasis, cell cycle, apoptosis, amino acid production and maintenance of heme and iron/Sulphur cluster homeostasis among others (Alaynick, 2008; Antico Arciuch et al., 2012; Duchen, 2000; Guda et al., 2007; Horn and Barrientos, 2008; Lill et al., 2012; Wang and Youle, 2009). Taking into account the significance of these processes, one can appreciate the

significance of mitochondria for the regulation of organismal physiology and their influence on healthspan and lifespan. Lately, scientific interest for understanding the mechanisms that coordinate the organelle abundance and function has increased. Although mitochondria are present in every tissue, their abundance may range depending on the cell type, developmental stage or stress status of the organism. Interestingly, mitochondrial dysfunction correlates with severe human pathologies such as cancer, neurodegeneration, diabetes, cardiomyopathy and premature ageing, among others.

To date, we hold the perception that mild perturbation of the mitochondrial function, either genetically or pharmacologically, confers increased lifespan and stress resistance. The condition when a moderate intervention benefits organismal physiology by any means is called mitohormesis. Of note, the effect on lifespan is gene-specific as even the mutation or genetic inhibition of the same ETC component can produce significant yet varying results on the lifespan of *C. elegans* or other model organisms. For example, genetic inhibition of *atp-3*, *nuo-6*, *clk-1*, *cco-1*, *nuo-1*, *isp-1* and *frh-1* significantly extends lifespan, contrary to *mev-1* or *gas-1* genetic interference which shortens lifespan. Adding higher complexity, even the mutation versus downregulation of the same gene target may differently influence the animal's lifespan. As a result, the effect on lifespan is gene-dose- and component targeted- dependent.

Interestingly, such perturbations show their full effect on lifespan only when implemented through development, irrespectively of the targeted component. While in most cases, post-developmental interventions have no noticeable effect. Moreover, the beneficial effects on lifespan, observed following perturbation of the mitochondrial function, are primarily attributed to the altered production of metabolites such as ATP and ROS, which are oxidative phosphorylation derivatives. For instance, a drop in respiration and ATP levels has a beneficial effect on lifespan. The beneficial effect is mostly assigned to

reduced metabolic rates and suits the “rate of living theory of ageing” first established by R. Pearl in 1928. Considering ROS levels and how do they modulate lifespan, at least to some extent; still remarkable controversy exists. While the prevailing notion today is that a slight increase in ROS levels triggers longevity acting through mitohormesis mechanisms, it was until recently accepted that increased ROS is detrimental for survival. Back then, the established theory supported that elevated ROS levels cause gradual accumulation of mtDNA damage and protein oxidation. By that time, the "free radical or oxidative damage theory of ageing" was built. Later, it was displaced by the "mitohormesis" theory of ageing as discussed earlier. More recent evidence revealed that O_2^- is uncoupled from ageing, and even that, mild paraquat treatment, a chemical oxidative stress-inducing agent can extend lifespan in *C. elegans*. The explanation to this is apparently that ROS, in this case, acts as a signaling molecule which stimulates stress responses and transcription factors which ultimately confer the aforementioned beneficial effects on lifespan.

Interestingly, for all mitochondrial perturbations that trigger lifespan extension, the identification of the molecular players that drive these beneficial effects is of great interest. Towards this direction, several pathways play a role, among the most critical of which are: the mitochondrial unfolded protein response (mtUPR), the intrinsic apoptosis pathway, selective mitochondrial autophagy (mitophagy), mitochondrial biogenesis, activation of the detoxification response, fatty acid oxidation, activation of the AMPK/AAK-2 pathway and extensive metabolic reprogramming. Notably, among the transcription factors or the transcription regulators that interfere with these responses are ATFS-1, DVE-1, SKN-1, HIF-1, CHE-23, FSTR-1/2, CEP-1 and the TAF-4/TFIID complex in *C. elegans*. Distinct perturbations can differentially activate one or more of the pathways mentioned above to confer lifespan extension.

Interestingly, evidence confirms that not only mitochondria influence the ageing process but also that ageing itself reshapes mitochondrial features. Representative features are the altered function, morphology, density and subcellular localization/organization of the organelles in aged versus young animals. Besides, alterations in most of them have been correlated with ageing and age-related pathologies even though their appearance does not always meet cellular senescence. It is becoming apparent that during ageing, dysfunctional organelles tend to accumulate. Studies in our laboratory recently elucidated the mechanism via which this occurs. There, it was revealed that while in young animals, the balancing actions of mitophagy and mitochondrial biogenesis sustain a stable and healthy mitochondrial population, in aged animals such mechanisms fail. Following the deterioration of the mitophagy machinery and the accumulation of dysfunctional organelles, thus cellular damage, the lifespan of long-lived *C. elegans* mutants dramatically declines (Palikaras et al., 2015).

1.6 The mechanism of mitochondrial biogenesis

Mitochondrial abundance and function are regulated by the tight coordination of mitochondrial biogenesis and mitophagy. Mitochondrial biogenesis propagates a healthy mitochondrial population in contrast to mitophagy which selectively eliminates the dysfunctional or superfluous organelles. While mitophagy mechanisms have been extensively studied in complex eukaryotes *in vivo*, the molecular underpinnings of mitochondrial biogenesis remain obscure.

Mitochondrial biogenesis is required under normal conditions, during development, cell division, renewal and differentiation as well as under stress conditions, such as oxidative and heat stress or upon exercise (Islam et al., 2018; Jornayvaz and Shulman, 2010). It is

a process tightly regulated by both anterograde and retrograde signals due to the semi-autonomous nature of mitochondria (Quiros et al., 2016). The significance of this binary regulation becomes apparent when considering, among others, that electron transport chain complexes consist both of nuclear- and mitochondrial- encoded components and mtDNA replication and expression is dependent on nuclear-encoded factors (Isaac et al., 2018; Scarpulla, 2012). Hence, mitonuclear communication and synchronization of mitochondrial and nuclear gene expression are considered critical for a healthy mitochondrial population both under normal conditions and upon stress (Couvillion et al., 2016). Although abnormalities in mitochondrial content and function have been directly linked to ageing and severe human pathologies, the mechanisms controlling mitochondrial biogenesis and its physiologic relevance are poorly understood (Kim et al., 2010; Lamb et al., 2015; Lien et al., 2017; Pyle et al., 2016; Short et al., 2005).

1.6.1 Transcriptional control of mitochondrial biogenesis

Mitochondrial biogenesis initiates with the transcription of the nuclear-encoded mitochondrial-targeted transcripts (NEMTTs) followed by translocation of NEMMTs in the vicinity of mitochondria, their local translation, import and eventually sorting into the organelle. The main transcription factor that positively regulates the expression of NEMTTs is the nuclear factor-erythroid 2-related factor 2 (Nrf2/NFE2L2), the mammalian homologue of SKN-1 (SKiNhead-1) in *C. elegans.* NFE2L2 together with nuclear respiratory factor 1 (NRF1) and nuclear respiratory factor 2 (NRF2), additional NRFs and the GA-binding protein transcription factor (GABP) are the most well-characterized transcriptional regulators of mitochondrial biogenesis (Ploumi et al., 2017). Additional factors may play a role in mitochondrial biogenesis depending on the triggering conditions or the stress status of the cell (Bouchez and Devin, 2019).

Under conditions where mitochondrial biogenesis is triggered, the presumption that the transcription of select NEMTTs is imperative exists. Recruitment of the transcription regulators discussed earlier under these conditions, activates transcription of genes encoding mitochondrial components implicated in ETC function, Krebs cycle, mitochondrial genome expression as well as core constituents such as mitochondrial import complex components among others (Bouchez and Devin, 2019). The function of NRF2 is regulated in mammals by a co-regulator of transcription, Peroxisome proliferator-activated receptor gamma coactivator 1-alpha (PGC1α), which does not have a *C. elegans* homologue. Moreover, AMP-activated protein kinase (AMPK), the AAK-2 homologue in *C. elegans*, is crucial for mitochondrial biogenesis under conditions of energy shortage, such as caloric restriction or exercise (Jornayvaz and Shulman, 2010). The elevation in the ratio of adenosite monophosphate (AMP) to adenosine triphospahte (ATP) triggers AAK-2. AAK-2 promotes mitochondrial biogenesis through phosphorylation of its targets and activation of transcription of nuclear-encoded mitochondrial genes or via other pathways downstream AMPK (Hardie, 2011). Importantly, AMPK regulates mitochondrial biogenesis through direct phosphorylation PGC-1α and Nrf2, which activates them (Jager et al., 2007; Joo et al., 2016). Furthermore, evidence exists that Nrf2 positively regulates PGC1α expression, thus forming a positive feedback loop (Baldelli et al., 2013).

Further, transcription of mtDNA is also needed for mitochondrial biogenesis to take place. Tight control of mtDNA expression is crucial for proper respiration and ETC function. The primary regulator of mitochondrial DNA transcription is the mitochondrial transcription factor A (TFAM), which is nuclear-encoded. Apart from mtDNA regulators, most of the respiratory chain complexes are composed of both nuclear and mitochondrial encoded components. Additionally, their stoichiometry within the complex is of compelling importance. Therefore, it is becoming possible that the nuclear and mitochondrial

transcriptional programs are tightly coordinated for correct organelle biogenesis to take place. Notably, of the more than seventy components of the respiratory chain complexes, only twelve are mitochondrially encoded in *C. elegans*, pretty comparable to what also happens in mammals (**Figure 5**). Findings point that, the imbalance between the nuclear and mitochondrial encoded components within the respiratory complexes, causes proteotoxic stress and triggers the mitochondrial unfolded protein response (mtUPR) or even mitophagy if damage persists.

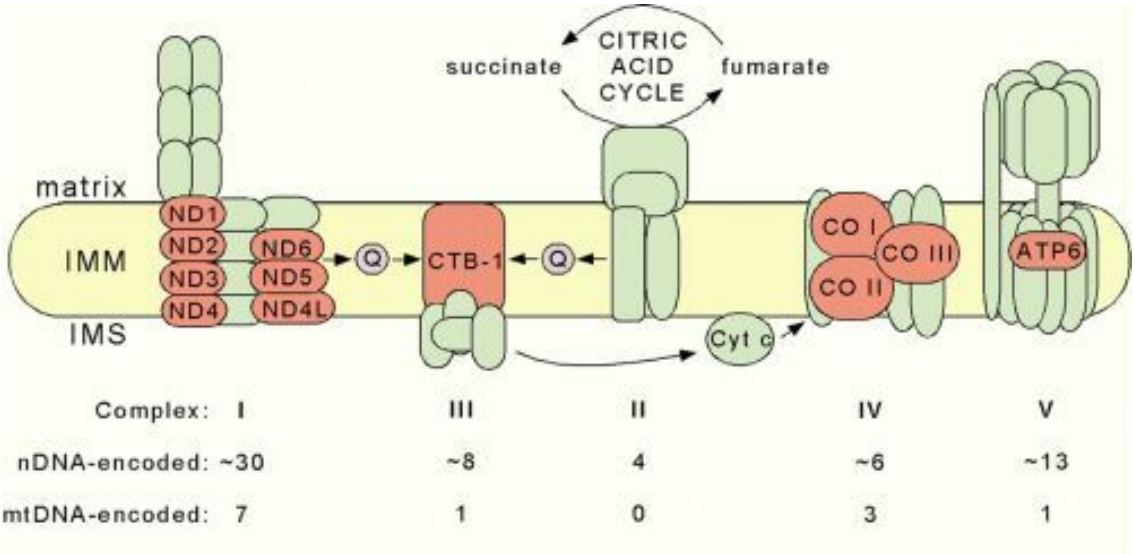

Figure 5. The organization of the mitochondrial respiratory complexes in *C. elegans*. Mitochondrial-encoded subunits are shown in red while nuclear-encoded ones in green.

1.6.2 Post-transcriptional control of mitochondrial biogenesis

The first step concerning post-transcriptional control of mitochondrial biogenesis is the delivery of NEMTTs in the vicinity of mitochondria. Evidence exists that RNA binding proteins accomplish this transport but the exact list of these components and the regulatory mechanism that drives this process are not well understood yet. For example, evidence shows that Puf3 localizes select mRNAs on the mitochondrial surface in yeast, although current data indicate that this trait is not conserved in higher eukaryotes

(Galgano et al., 2008; Gerber et al., 2004; Hafner et al., 2010; Morris et al., 2008). Sequence analysis of NEMTTs has unveiled though, that many of them carry a mitochondrial targeting signal within their nucleotide sequence that drives their targeting to mitochondria. Although some of the NEMTTs may not contain the canonical mitochondrial targeting signals, they contain instead, noncanonical sequences that are currently not well characterized, yet can still successfully mediate NEMTT translocation to the organelle (Chacinska et al., 2009; Garcia et al., 2010).

Apart from the MTS signal, the 3'-UTRs of NEMTTs can also drive their specific translocation to the organelles (Eliyahu et al., 2010). Interestingly, implementation of electron microscopy and *in situ* hybridization assays helped in the initial detection of NEMTTs on the outer mitochondrial membrane (OMM). Lately, unconventional methodologies can distinguish the specifically expressed transcripts by OMM bound ribosomes (Egea et al., 1997; Garcia et al., 2007; Marc et al., 2002; Ricart et al., 1997; Sylvestre et al., 2003; Williams et al., 2014).

NEMTT anchoring on the OMM is facilitated by the OMM proteins MDI (the homologue of *C. elegans* AKAP-1), as shown in *Drosophila* ovaries *ex vivo*, and TOM20 as shown in yeast, mammalian cells and *Drosophila* muscle cells (Eliyahu et al., 2010; Gehrke et al., 2015; Zhang et al., 2016). Notably, evidence shows that these proteins bind select NEMTTs like ETC subunit components, mitochondrial ribosome components and mtDNA replication factors through yet not well-understood mechanisms. Interestingly, tom20 binds the MTS of NEMTTs, and *tom20*Δ mutants exhibit decreased but not a null association of NEMTTs with mitochondria. Simultaneous mutation of *Puf3*, which binds the 3'-UTRs of NEMTTs to drive their localization, displays additive effects, promoting the notion that the two mechanisms act synergistically to regulate local translation in yeast (Eliyahu et al., 2010; Garcia-Rodriguez et al., 2007). It also becomes apparent that the function of Tom20 is most possibly complementary to other OMM anchoring components

(Eliyahu et al., 2010). Notably, the effect of systemic perturbation of these factors in multicellular eukaryotic organisms has not been studied yet in vivo. These OMM proteins anchor NEMTTs and promote their local translation which is mediated by OMM bound ribosomes or by free cytoplasmic ribosomes found in the mitochondrial vicinity, as revealed by proximity-specific ribosome profiling in yeast (Gold et al., 2017; Margeot et al., 2005; Williams et al., 2014). The first evidence for the presence of ribosomes associated with mitochondria emerged in 2007 (Haim et al., 2007). Since then, serious progress to the direction of accurate and comprehensive visualization and mapping of cytoplasmic ribosomes on the outer mitochondrial membrane (OMM) came into view. In particular, cryo-tomography visualization has revealed that they interact with the translocase of the outer membrane (TOM) complex (Gold et al., 2017). This interaction matches the idea that while NEMTTs are locally translated they are co-translationally imported into the organelles through the TOM and translocase of the inner membrane (TIM) complexes (Fujiki and Verner, 1991, 1993). After their import and folding inside the organelle, they are distributed in the various sub-organelle compartments, named the OMM, the mitochondrial intermembrane space (IMS), the IMM and the mitochondrial matrix.

Like for transcription, here again, evidence shows that cytosolic translation of NEMTTs should synchronize with the mitochondrial translation of mtDNA. As discussed earlier, the assembly of most of the OXPHOS complexes requires both nuclear and mitochondrial encoded components. Since mtDNA encodes OXPHOS complex components, synchronization of the two programs would facilitate the flawless assembly of OXPHOS complexes. To this extent, it was discovered in yeast cells, that a switch from fermentable to a non-fermentable carbon source, which triggers respiration and so the generation of new OXPHOS complexes, does not concomitantly trigger the upregulation of both nuclear and mitochondrial-encoded respiratory transcripts. Mainly, nuclear-encoded transcripts

propagate first while an increase of the mitochondrial ones belatedly follows. Also, it appears that the coordination of the two translation programs is not occurring through bidirectional communication between the cytoplasmic and the mitochondrial ribosomes, but only from the cytoplasm to mitochondria through yet not well-understood mechanisms (Couvillion et al., 2016). Also, whether this is a conserved phenomenon in more complex eukaryotes or not, needs to be investigated in the future.

This growing body of evidence shows that local translation in the vicinity of mitochondria occurs, but the underlying molecular mechanism and how it is regulated during ageing or upon stress, how it affects organelle and organismal homeostasis and which is the physiologic relevance and physiological significance of this process in higher eukaryotes are not yet understood.

The dependence of translation inside mitochondria from the local translation of NEMTTs in the cytoplasm raises, even more, the significance of tight regulation of local translation events. The translation of NEMMTs locally, in the proximity of mitochondria expedites accuracy and credibility that would ensure error-free mitochondrial biogenesis upon triggering conditions and would circumvent mitochondrial dysfunction and ectopic mitochondrial protein deposition.

While there is mechanistic understanding at the transcriptional level, mitochondrial biogenesis regulation remains a mystery at the post-transcriptional and pre-translational level. It is possible that mitochondrial biogenesis continuously occurs at basal levels, but rises under triggering conditions. Especially in response to either acute or chronic stress, the cell must rapidly increase mitochondrial abundance and function to adapt successfully. This response should be quick enough, as prolonged stress exposure often leads to cell death and homeostatic collapse. Availability of the necessitated transcript just at stress onset should be of imperative importance. It is conceivable that transcript availability would permit active mitochondrial biogenesis or its rapid onset, and so the

execution of a successful stress response. Especially upon acute stress induction, how cells respond rapidly, remains a puzzle. We assume that a successful stress response would occur if a mechanism existed by which the mRNAs encoding critical components for mitochondrial biogenesis would be stored-be ready for translation- and released upon biogenesis-inducing conditions. Such a mechanism would enable the cell bypass, the time-consuming step of transcription.

However, it is also likely that when conditions become inhibitive, local translation rates drop or the process halts or even ceases. In the latter case, a mechanism should exist to either store or degrade those locally pre-deposited mRNAs. Post-transcriptional RNA processing could, among others, offer a precise way of co-regulation of the two genomes. The field of post-transcriptional RNA processing in the mitochondrial vicinity and its effect on local translation events and organelle homeostasis remain obscure to date. Investigating whether such a mechanism exists and whether it affects mitochondrial biogenesis is what attracted our interest in the current study.

1.7 P-bodies and mitochondria

The best well-characterized and organized subcellular compartment devoted to performing post-transcriptional regulation of target mRNAs is the earlier introduced mRNP aggregates, the processing bodies (P-bodies). P-bodies dynamically interact with various subcellular formations and organelles depending on cell status. For example, they form either transient or stable associations with stress granules, the nucleus, neuronal granules or late endosomes among others (Kedersha et al., 2005; Lee et al., 2009; Zeitelhofer et al., 2009). Notably, a specific P-body component, p54, localizes to the vicinity of mitochondria in HUVEC (**Figure 6**) and HeLa cells while is not found near the endoplasmic reticulum (ER) or endosomes. Nevertheless, any additional mechanistic

insight concerning this association was missing (Huang et al., 2011). In the same study, they perceived that inhibition of P-body formation did not alter mitochondria. Furthermore, loss of mitochondrial membrane potential (Δψ) followed by CCCP treatment could not disrupt the associations of the P-body marker with mitochondria but triggered the removal of the RISC component Ago2 from P-bodies and a subsequent reduction in miRNA silencing. Analysis of the kinetics of p54 association with mitochondria exhibited that the associations are close and long enough to permit the exchange of biological material either way between the two subcellular compartments (Huang et al., 2011).

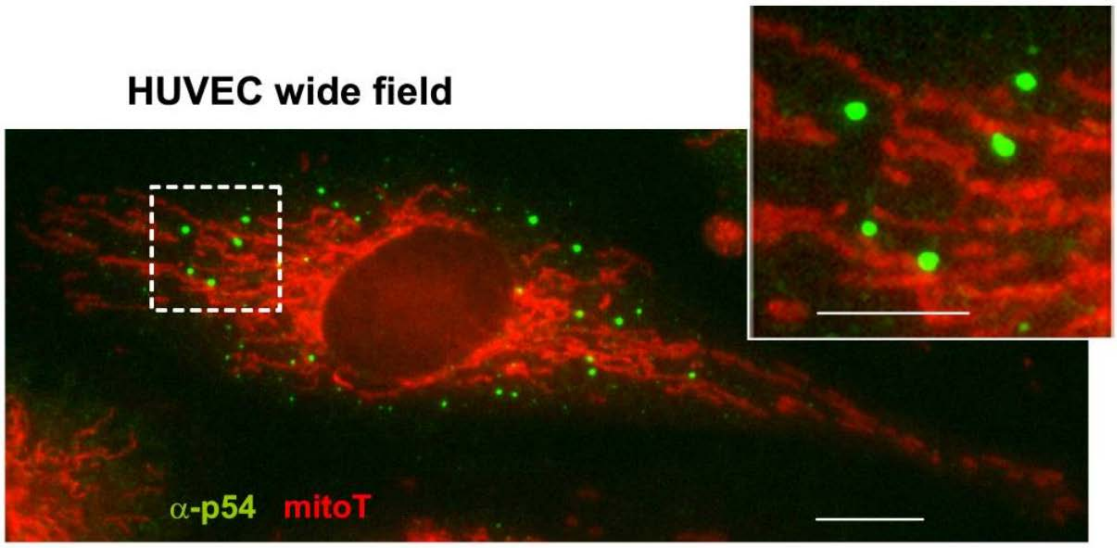

Figure 6. **P bodies (green) associate with mitochondria (red) in HUVEC cells.**

To this extent, Ago2 was detected inside the matrix of mitochondria in C2C12 cells upon myogenesis inducing conditions. There, in complex with miR-1, it positively regulates the translation of endogenously expressed mitochondrial proteins (Zhang et al., 2014). Whether this function of Ago2 is conserved among model organisms or in other cell types and under normal conditions, waits to be shown. However, our data show that ALG-1, the Ago2 *C. elegans* orthologue, does not localize inside mitochondria in *C. elegans* under

control conditions (**Figure 7**). Also, like miR-1, several additional miRNA species have been found inside mitochondria with some of them even being mitochondrial-specific (Barrey et al., 2011; Bian et al., 2010; Kren et al., 2009). Even though in several studies, mitochondria carry these molecules, yet we do not know whether the exchange of such material is the reason for their association. Identification of the exchanged material and the purpose of this association anticipate for coming studies.

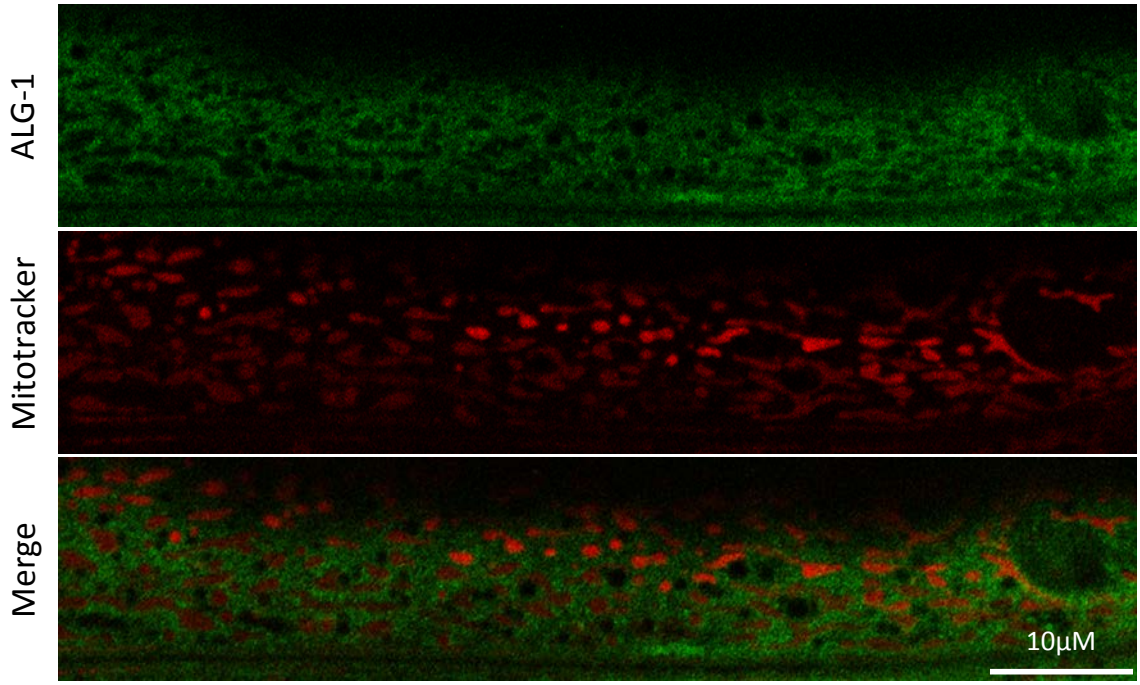

Figure 7. **The subcellular localization of ALG-1 relative to mitochondrial in hypodermal cells in *C. elegans*.**

Besides, it was lately demonstrated by Wang *et al.* in 2018 that P-bodies store mitochondrial encoding mRNAs specifically upon glucose deprivation conditions in yeast. Their storage prevents them from degrading and therefore triggers elevated protein levels (Wang et al., 2018b). Nevertheless, in this study, whether a physical association between the two subcellular compartments exists, is not considered. Also, targeting of

mitochondrial encoding transcripts to P-bodies occurs solely upon conditions of glucose deprivation. On the other hand, P-body purification by FAPS in human epithelial cells in unstressed conditions showed exclusion of mitochondrial mRNAs from the P-body isolates (Hubstenberger et al., 2017) raising controversy in the field.

In the current study, we hypothesize that P-bodies associate with mitochondria to regulate local expression of NEMTTs. We speculate that P-bodies regulate protein synthesis for mitochondrial biogenesis and organelle quality control, both under physiologic conditions and upon stress. We hold the belief that post-transcriptional processing of NEMTTs is the missing regulatory node of local translation and that its understanding will shed light in this complicated procedure. We suggest that P-bodies in the mitochondrial vicinity act as hubs of NEMTT processing, either for their storage or degradation. To date, cytoplasmic factors that regulate NEMTTs post-transcriptionally and pre-translationally remain obscure. We envisage improving understanding of mitochondrial biogenesis and quality control mechanisms. In parallel, we aim to provide a mechanistic understanding of the association of P-bodies and mitochondria, which seems to be conserved, according to our findings.

1.8 Mitochondrial biogenesis and disease

Mitochondrial biogenesis is an actively regulated process, sensitive to environmental and stress factors, including physiologic conditions such as development and ageing. Through this process, which coordinates with mitophagy (the mitochondrial-specific elimination of dysfunctional organelles) under physiologic conditions, organisms respond to external demands by modulating their mitochondrial content and functionality whenever needed. Towards this direction, mitochondria act as core regulators of ageing and disease onset (Gureev et al., 2019). Mitochondrial mutations can extensively alter organismal lifespan,

while many of them profoundly correlate to severe human pathologies (**Figure 8**) (Bishop et al., 2019).

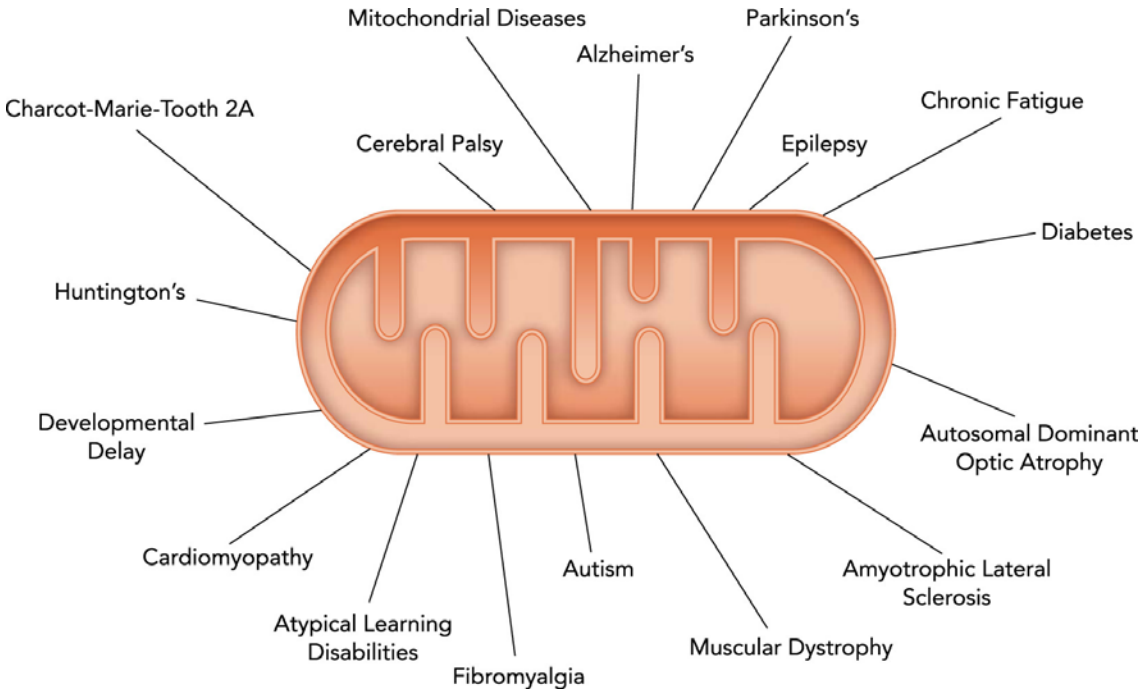

Figure 8. **Human syndromes and pathologies associated with mitochondrial dysfunction.**

Furthermore, mitochondrial impairment is not only the consequence of disease onset but in numerous cases is itself the trigger for disease onset. Several studies prove that depletion or mutation of a single mitochondrial component can trigger severe acute or chronic human pathologies. On top of that, deregulation of mitochondrial biogenesis is likely to trigger global mitochondrial dysfunction and be the etiology of various diseases. The fact that mitochondrial biogenesis drops in aged animals compared to younger isogenics represents substantial evidence concerning the importance of studying mitochondrial biogenesis, for organismal healthspan and lifespan. Likewise, tight control of the rate of mitochondrial biogenesis is crucial, since a decrease or an increase in

mitochondrial biogenesis, associates with pathological conditions. Notably, in the neurodegenerative Huntington's disease (HD) mitochondrial biogenesis is diminished owing to PGC-1α dysfunction. Interestingly, NRFs and TFAM, that act downstream PGC-1α, are also studied with the aim to reverse the consequences of PGC-1α dysregulation in HD (Rona-Voros and Weydt, 2010; Taherzadeh-Fard et al., 2011; Weydt et al., 2009). Furthermore, mitochondria are essential regulators of cardiac function and PGC1-1a, a highly expressed molecule which positively affects the function of cardiomyocytes (Arany et al., 2005). Importantly, PGC-1a loss in these cells results in severe energy deficiency among other scarcities in different mitochondrial metabolism byproducts ending up in heart failure and hypertrophy (Arany et al., 2005; Dorn et al., 2015; Sun et al., 2007). PGC-1a insufficiency, as in other cases, triggers a cascade of events including reduced NRF and TFAM function and suppression of their transcriptional targets. These consequences of PGC-1a loss occur owing to its reported role as a coactivator of transcription and its assertive regulatory role on several transcription factors involved in mitochondrial biogenesis. While PGC-1a acts in the first steps in the mitochondrial biogenesis program, inactivation of downstream molecules should have the same results in pathology.

Another age-related neurological disorder, Alzheimer's disease, has also been associated with mitochondrial biogenesis. In this case, it is appreciated that AD is coupled with defective mitochondrial biogenesis. Furthermore, strategies that trigger enhanced mitochondrial biogenesis are implemented to fight AD. Such strategies include caloric restriction and exercise among others, while the underlying molecular mechanism for AD-induced mitochondrial dysfunction plus the role of mitochondrial biogenesis in AD is not yet understood (Cabezas-Opazo et al., 2015; Onyango, 2018). Also, evidence exists that enhanced mitochondrial biogenesis, principally through Nrf2 activation, becomes a promising approach for therapy or delay of neurodegenerative disease progression such

as depression, Parkinson's disease and multiple sclerosis (Hayashi et al., 2017; Hesham A El-Beshbishy, 2019; Van Laar et al., 2018; Youdim and Oh, 2013; Zheng et al., 2010). Likewise, reduced mitochondrial content accompanied by decreased PGC-1a has been associated with obesity and type 2 diabetes. Interestingly, strategies that result in mitochondrial biogenesis activation such as exercise or activation of AMPK and its downstream target, SIRT1, can alleviate from diabetic defects and abate insulin resistance and obesity (Baur et al., 2006; Benton et al., 2008; Guarente, 2006; Liang et al., 2009; Nisoli et al., 2007; Zhang et al., 2009). Additional diseases which are coupled with decreased mitochondrial biogenesis are acute kidney injury (AKI) and folic acid nephropathy, among others (Funk and Schnellmann, 2012; Stallons et al., 2014).

Last but not least, mitochondrial biogenesis obtains an upcoming role in the regulation of cancer progression. Clear evidence about the role of mitochondrial biogenesis is still missing, as evidence up to know is controversial (Lamb et al., 2015; LeBleu et al., 2014; Scatena et al., 2018; Torrens-Mas et al., 2019; Yoshida et al., 2011). While the current notion supports that the effect of mitochondrial biogenesis in cancer progression is cancer-cell-type-specific, its complex role in disease needs further elucidation in the future (Vyas et al., 2016).

Currently, there is much effort to define mitochondrial biogenesis-associated diseases and discover compounds or possible molecular targets to reverse malignant phenotypes. Nowadays, complete elucidation of the molecular partners that regulate mitochondrial biogenesis is imperative since many diseases have been associated with mitochondrial biogenesis defects, while efficient therapy is still missing. Intervening with mitochondrial biogenesis regulatory mechanisms is expected to offer significant benefits against diseases such as the ones mentioned above.

Aim of the PhD thesis

This PhD thesis aims to delineate the cellular and molecular mechanisms that underlie mitochondrial biogenesis and investigate their impact on cellular and organismal homeostasis, lifespan and stress resistance. To achieve our goal, we use *C. elegans*.as a model system.

CHAPTER 2
MATERIALS AND METHODS

2.1 Strains and transgenic lines

We followed standard procedures for *C. elegans* maintenance, crosses and other genetic manipulations (Brenner, 1974). Nematode rearing temperature was kept at 20^{o}C unless noted otherwise. The following strains, available at CGC, were used for this study: N2: Wild type Bristol isolate, SJ4103: N2;*Is*[p_{myo-3}mtGFP] to monitor mitochondrial matrix of body wall muscle cells, SJ4143: N2;*Is*[p_{ges-1}mtGFP] to monitor mitochondrial matrix of intestinal cells, OP178: *wgIs178*[skn-1::TY1::EGFP::3xFLAG;unc-119(+)], CL2166: N2;*Is*[p_{gst-4}GFP] to measure SKN-1 protein levels, MQ887: *isp-1(qm150)IV*, PS6187: *syEx1155* [p_{myo-3}TOMM-20::mRFP::3xMyc;unc-119(+)] to monitor the mitochondria in body wall muscle cells.

To investigate the localization and abundance of degradation body components we used the N2;*Ex*[p_{edc-3}EDC-3::DsRed;pRF4] (Rieckher et al., 2018) and the N2;*Ex*[p_{dcap-2}DCAP-2::mcherry;unc-119(+)] (generated for this study) transgenic animals. To investigate the localization and abundance of storage body components we used the N2;*Ex*[p_{ntl-2}NTL-2::GFP;unc-119(+)] and the N2;*Ex*[p_{ccf-1}CCF-1::GFP;unc-119(+)] transgenic animals both generated for this study. To investigate the localization of ALG-1 relative to mitochondria we used CT20: *zaIs5*[p_{alg-1}GFP::ALG-1; rol-6(su1006)] provided by CGC.

For FRAP analysis were we measure global protein synthesis levels we used the N2;*Ex*[p_{ife-2}IFE-2::GFP;pRF4] transgenic animals (Syntichaki et al., 2007).

To study the localization of degradation bodies relative to mitochondria in body wall muscle cells we established: N2;*Is*[p_{myo-3}mtGFP];*Ex*[p_{edc-3}EDC-3::DsRed;pRF4]. To study the relative positions of storage bodies and mitochondria in body wall muscle cells we established: N2;*Ex*[p_{ntl-2}NTL-2::GFP;unc-119(+)];s*yEx1155*[p_{myo-3}TOMM-20::mRFP::3xMyc;unc-119(+)].

To monitor mitophagy we used the following strains and transgenic animals: IR1284: N2;*Is*[p_{myo-3}mtGFP];*Ex011*[p_{lgg-1}DsRed::LGG-1] (Palikaras et al., 2015) and N2; *Ex*[p_{myo-3} TOMM-20 :: Rosella; unc-119(+)].

To measure *gst-4* expression levels in an inducing genetic background we used the *daf-2(e1370)*;*Is*[p_{gst-4}GFP] strain generated by cross and the SPC167: P_{gst-4}GFP;*skn-1(lax120)* which is available in CGC.

To measure AAK-2 abundance we used AGD383: *uthIs202*[aak-2 (intron 1)::aak-2(aa1-aa321)::Tomato::unc-54 3'UTR;pRF4] available from CGC.

2.2 Molecular cloning

To generate the p_{ntl-2}NTL-2::GFP reporter construct, we amplified the coding region of the gene from *C. elegans* genomic DNA using the primers "*ntl-2* coding forward" (which contains the BamHI restriction enzyme sequence) and "*ntl-2* coding reverse" (which contains the AgeI restriction enzyme sequence). This amplified region was inserted in the TOPO-pCRII vector. In parallel, a ~2000bp region upstream *ntl-2* gene coding sequence was amplified using the primers "*ntl-2* promoter forward" and "*ntl-2* promoter reverse" which was also inserted in the TOPO-pCRII vector. Subsequently, *ntl-2* coding region was extracted from TOPO-pCRII vector with BamH/AgeI and inserted in frame at the amino (N) terminus of GFP, in the pPD95.77 plasmid vector. This genetic cassette was linearized using BamHI restriction enzyme and dephosphorylated using CIP. The promoter region was extracted from TOPO-pCRII vector with BamHI and inserted into the dephosphorylated genetic cassette described previously. The construct was checked for correct promoter orientation with several diagnostic restriction digestions.

To generate the p_{dcap-2}DCAP-2::mcherry reporter construct we amplified the coding region of the gene from *C. elegans* genomic DNA in two steps owing to the big size of the sequence (~7000bp) using the primers "*dcap-2* coding part 1 forward" (which contains the NotI restriction enzyme sequence) and "*dcap-2* coding part 1 reverse" (which contains the XbaI restriction enzyme sequence) and "*dcap-2* coding part 2 forward" (which contains the XbaI restriction enzyme sequence) and "*dcap-2* coding part 2 reverse" (which contains the XmaI restriction enzyme sequence). Both amplified regions were separately inserted in the TOPO-pCRII vector. In parallel a ~1700bp region of the operon promoter was amplified using the primers "*dcap-2* promoter forward" and "*dcap-2* promoter reverse" also inserted in the TOPO-pCRII vector. In the last genetic cassette, which contains the operon promoter in the TOPO-pCRII vector we ligated the first fragment of *dcap-2* coding region cut by NotI/XbaI. Following, the TOPO-pCRII vector containing the operon promoter and *dcap-2* fragment 1 was cut with XbaI and dephosphorylated by CIP. Subsequently, *dcap-2* coding region fragment 2 was inserted and the correct orientation of this fragment insertion was verified. Next, the operon promoter and the full *dcap-2* coding sequence were extracted from TOPO-pCRII vector as one fragment in a single step with BamHI/XmaI and ligated in frame at the amino (N) terminus of mCherry, in the pPD95.77 plasmid vector which was cut with BamHI/AgeI taking advantage of the AgeI compatibility to XmaI.

To generate the p_{ccf-1}CCF-1::GFP reporter construct we amplified the coding region of the gene from *C. elegans* genomic DNA using the primers "*ccf-1* coding forward" and "*ccf-1* coding reverse" (which contains the AgeI restriction enzyme sequence). To amplify the operon promoter in which *ccf-1* belongs we used the primers "*ccf-1* promoter forward" and "*ccf-1* promoter reverse". Both amplified regions were separately inserted in the TOPO-pCRII vector. Next, *ccf-1* coding region was extracted from TOPO-pCRII vector

and inserted in frame at the amino (N) terminus of GFP, in the pPD95.77 plasmid vector. Following, the pPD95.77-containing the *ccf-1* coding region- genetic cassette was linearized with HindIII and dephoshorylated by CIP. *ccf-1* promoter region was extracted from the TOPO-pCRII vector with HindIII digest and ligated to the linearized vector. The correct orientation of the promoter was verified with additional diagnostic digests.

To generate the RNAi constructs, gene-specific fragments of interest were obtained by PCR amplification directly from the *C. elegans* genomic DNA using appropriate primer sets. The PCR-generated fragments were initially inserted into the TOPO-pCRII vector and then sub-cloned in the pL4440 plasmid vector. The final constructs were transformed into HT115 (DE3) *E. coli* bacteria. For *ntl-2(RNAi)* we amplified a 1549bp region by using the primers "*ntl-2* RNAi forward" and "*ntl-2* RNAi reverse". For *atp-3(RNAi)* we amplified a 694bp region by using the primers "*atp-3* RNAi forward" and "*atp-3* RNAi reverse". For *mrps-5(RNAi)* a 2150bp region was amplified by using the primers "*mrps-5* RNAi forward" and "*mrps-5* RNAi reverse". For *tomm-20(RNAi)* a 984bp region was amplified by using the primers "*tomm-20* RNAi forward" and "*tomm-20* RNAi reverse". For *akap-1(RNAi)* a 1997bp region was amplified by using the primers "*akap-1* RNAi forward" and "*akap-1* RNAi reverse".

The sequences of all primers are listed in the Key Resource Table.

2.3 mRNA isolation and quantification

Total RNA was extracted as follows: 1. Collect around 50 worms in M9 in a RNase-free Eppendorf tube, 2. Pellet worms by spinning at 14.000rpm (x3), 3. In the hood add 250µl Trizol, 4. Vortex by hand for about 30sec and then 20 minutes vortes at 4^{o}C, 5a. put the samples at -80^{o}C for 10minutes, 5b. put the samples at 65^{o}C for 5 minutes (perform 5a and 5b twice-optional-), 6. In the hood, add 50µl od chloroform, 7. Vortex for 15 sec and

then let at room temperature for 3min, 8. Centrifuge at 12.000rpm for 15min at 4^{o}C, 9. Transfer the clear layer in to a new Eppendorf tube, 10. Repeat steps 6-9, 11. Add 125μl 2-propanol and invert to mix, 12. Let it at room temperature for several minutes (around 3 minutes), 13. Spin down at 12.000rpm for 10 minutes at 4^{o}C, 14. Keep the pellet and leave a few μls at the bottom so as not to disturb the pellet, 15. Add 500μl 70% ethanol, 16. Spin down at 14.000rpm for 5minutes at 4^{o}C, 17. Remove as much supernatant and air dry the pellet (in the hood), 18. Dissolve the pellet in 20μl of RNAse-free ddH_2O, 19. Heat at 60^{o}C for 10minutes (optional), 20. Quantification (OD_{260}/OD_{280}:2 for pure RNA) For cDNA synthesis, we used the iScriptTM cDNA Synthesis Kit (BioRad). Quantitative PCR was performed as previously described.

2.4 FRAP

To determine the role of mRNA degradation and storage body components in protein synthesis control, we performed FRAP analysis as described in (Kourtis and Tavernarakis, 2017). Specifically, we measured global translation rates using the N2;*Ex*[$p_{ife\text{-}2}$GFP;pRF4] strain which expresses the GFP protein under the *ife-2* gene promoter which is ubiquitously expressed in somatic tissues. We performed the assay on the agar plates, seeded with the wanted bacteria without the use of any anesthetics (step B1a described in the aforementioned study). We bleached whole animals for 6 minutes at the 10x lens using the Zeiss AxioImager Z2 epifluorescence microscope. Time zero is the time point following photobleaching. Fluorescent recovery of each animal was measured every one hour for at least 6 hours. For each and every measurement one photo per animal was acquired and this was used to measure the mean fluorescence at each time point. Cycloheximide which is an inhibitor of global protein synthesis was used as a control in a final concentration of 500μg/ml. At least 20 animals were bleached in each experiment and each condition tested. Animals with signs of damage after

photobleaching were excluded from the final analysis. Fluorescence intensity quantification was performed using Image J.

2.5 Degradation and storage body monitoring

Quantification of storage and degradation body components was performed either tissue-specifically or in whole animals. In the first case, we acquired images using the Zeiss LSM 710 confocal microscope. We acquired thin, single confocal slices and subsequently measured the number of particles using the volocity software.

In the second case, we used the Zeiss AxioImager Z2 epifluorescence microscope and acquired images of whole animals using a 5x lens. Then, we quantified the mean fluorescence intensity of each animal using the Image J software.

The colocalization analysis of storage and degradation bodies was performed by acquiring 2μm slices in Zeiss LSM 710 confocal microscope using the 63x lens. The 2μm thickness of the stack is small enough to enable us capture several foci in more than one slices. Colocalization analysis and Pearson's correlation coefficient were measured with the volocity software.

The distances of storage/degradation bodies from mitochondria were acquired in the Zeiss LSM 710 confocal microscope using a 63x lens. Single slices were acquired and distances between each foci from adjacent mitochondria was measured with the volocity software.

For confocal microscopy experiments we immobilized animals on 5% agarose pads with Nanobeads in M9 to avoid the use of anesthetics. For epifluorescence microscopy we anesthetized animals using levamisole.

2.6 Mitochondrial imaging

To monitor the mitochondrial network formation we acquired single slices in the 40x lens of a confocal microscope using the SJ4103 strain which expresses GFP in the matrix of body wall cell mitochondria.

To monitor the relative positions of mitochondria and storage/degradation bodies we either used the SJ4103 strain (crossed with the N2;*Ex*[p_{edc-3}EDC-3::DsRed;pRF4] strain) or stained mitochondria with specific dyes. In these experiments we acquired images of single slices using a 63x lens of the confocal microscope.

To measure mitochondrial mass we used several approaches: 1. we measured the mean fluorescence intensity in whole animals expressing GFP in the matrix of intestinal mitochondria with the strain SJ4143. Since the intestine is the most abundant tissue in *C. elegans* measuring mitochondrial mass in this tissue would be representative for the global mitochondrial mass. Mean fluorescence intensity was quantified using the Image J software. 2. Using the same strain we acquired single confocal slices of defined size and measured fluorescence intensity in a certain number of slices using the volocity software.3. We used the same approach as in “2” but this time we stained animals with mitotracker Green and measured fluorescence in the hypodermis as Mitotracker staining stains more efficiently in that tissue.

2.7 Stress assays

2.7.1 Heat stress

We performed a heat shock assay to measure thermotolerance of *dcap-2(RNAi)* and *ntl-2(RNAi)* treated animals versus control. We bleached animals and put the isolated eggs

on seeded plates with HT115 cells expressing the desired RNAi. We transferred animals on fresh seeded plates every two days and at day 5 we performed the heat stress assay. We first incubated seeded plates without worms at 37^{o}C for 1,5 hours to pre-warm them. Afterwards, we placed the animals on the pre-warmed plates (we placed around 40 animals in each plate and used at least 3 plates per condition in each experiment). Next, we placed the plates containing the animals in the incubator at 37^{o}C for 5 hours. Afterwards, we put the animals in a 20^{o}C incubator and let them recover for at least 12 hours. The next day (after 12hours) we scored for deaths and we continued scoring every 24 hours until all animals died.

2.7.2 Paraquat stress

For the oxidative stress resistance assay we placed 5-day old adult animals on paraquat-containing plates (we placed paraquat at the top of pre-seeded plates) at a final concentration of 8mM. We placed 40 animals per plate and at least three plates for every condition tested. Every three days we placed animals on fresh plates and measured death events every day until all animals died.

2.7.3 CCCP stress

For the CCCP stress resistance assay we diluted CCCP of an initial concentration 49mM in M9 and placed it on the top of pre-seeded plates at a final concentration of 15μM. Since CCCP is dissolved in DMSO we used DMSO containing plates in the same concentration (15μM) as a control. Fourty 5-day-old adult animals were placed in each plate and at least three plates were used per condition tested. Death events were monitored every day until all animals died.

2.8 Western blotting

Protein samples were analyzed by Tricine-SDS–polyacrylamide gel electrophoresis (SDS–PAGE) and transferred on nitrocellulose membrane. They were blotted against antibodies listed in the Key Resource Table. For total worm protein extraction, worm pellets were diluted in RIPA buffer 1:5 containing complete mini proteinase inhibitor cocktail and then they were sonicated. In the total protein extracts we put the same volume of 2x Laemmle sample buffer containing b-mercaptoethanol and boil at 95^{o}C form 5min. Boiled samples are stored in -20^{o}C or directly run in a gel.

2.9 Mitochondria isolation

For total mitochondrial isolation from *C. elegans* adults, we performed the following steps: 1. We gather worms from 7 big plates with M9 + 0,01% Triton, 2. Centrifuge at 50g form 1minute at 4^{o}C, 3. Resuspend in 5ml M9, 4. Centrifuge at 50g form 1minute at 4^{o}C (perform steps 3 and 4 twice), 5. Resuspend in 1ml M9, 6. Transfer the worms with the M9 with a glass pipette (Pasteur) in an Eppendorf, 7. Add 10μl 1M DTT (10mM final concentration), 8.cincubate in cold room 30minutes rotating, 8. Transfer the solution in 15ml falcon, 9. Dilute it up to 5ml with M9, 10. Centrifuge at 200g for 1minute at 4^{o}C, 11. Resuspend in 5ml M9, 12. Centrifuge at 200g for 1minute at 4^{o}C, 13. Resuspend in 1m Incubation Buffer plus Proteinase Inhibitors plus PMSF (final concentration 1mM), 13. Transfer in a homogenizer, 14. Homogenize with 100 strokes, 15. Transfer the homogenate in 15ml falcon and dilute it up to 7ml with Incubation Buffer containing Proteinase Inhibitors and PMSF, 16. Centrifuge at 300g for 1minute at 4^{o}C, 17. Keep supernatant in a different falcon (it contains the mitochondria), 18. Add 1ml of Incubation Buffer plus Proteinase Inhibitors plus PMSF to the pellet and transfer in dounce, 19. Add 5ml Incubation Buffer to wash the Pasteur pipette and the tube, 20. Homogenize with 100 strokes, 21. Transfer the homogenate in 15ml falcon tube, 22. Centrifuge at 300g for 1minute at 4^{o}C, 23. Keep the supernatant and combine with previous, 24. Centrifuge at

300g for 1minute at 4^{o}C (throw the remaining pellet), 25. Aliquot in 1,5ml Eppendorf, 26. Centrifuge for 5 minutes max speed (16.000g), 27. Keep the pellet (mitochondria-containing fraction) and the supernatant in a different Eppendorf (post-mitochondrial fraction).

2.10 Proteinase K treatment

We added 1/10 of the final volume Prokeinase K (100mg/ml, Signa-Aldrich) in the samples at step 25 of the previous protocol. We incubated the samples for 1 hour at 37^{o}C and continued with the rest of the steps.

2.11 RNA Immunoprecipitation

To identify possible NEMTTs as cargo of storage bodies we performed RNA immunoprecipitation as follows: first we incubated in two different 1.5ml Eppendorf tubes (one for the NTL-2::GFP sample and one for the control no GFP sample) 40µl of magnetic beads with a-GFP diluted in PBST overnight at 4^{o}C rotating. Next we used a magnetic stand and washed the beads bound with a-GFP twice in wash buffer (50mM Hepes, 150mM Nacl, 1mM EDTA, 1mM EGTA, 10% Glycerol, Proteinase Inhibitor and 1/100 PMSF). We removed wash buffer and added our whole worm protein extracts (diluted in 50mM Hepes, 2M Nacl, 1mM EDTA, 1mM EGTA, 10% Glycerol, Proteinase Inhibitor and 1/100 PMSF, 0,1% NP-40 and 1/1000 Protector RNase Inhibitor) in the antibody bound magnetic beads pellet. We incubate 5hr in the coldroom rotating. After 5hr the Eppendorfs were placed on a magnetic stand and supernatant was removed. Beads were washed twice with wash buffer plus NP-40 0, 1%. Wash buffer was removed and 2x Laemmle sample buffer containing b-mercaptoethanol was added and boiled at 95^{o}C form 5min. Eppendorfs were placed on a magnetic stand and supernatant was

collected in new eppendorfs. 1ml Trizol was added to the isolated supernatant and then we continued with the RNA extraction protocol as described previously. The only addition is that before the step with the addition of isopropanol we added glycoblue. Whole worm protein extracts where prepared by gridding flash-freezed in liquid nitrogen worms (worms pellets were diluted in 50mM Hepes, 150mM Nacl, 1mM EDTA, 1mM EGTA, 10% Glycerol, 1mM DTT, Proteinase Inhibitor and 1/100 PMSF, 1% NP-40) . When a fine powder was produced we stopped gridding and added the powder in a 15ml Eppendorf and let it melt in ice. We centrifuged at 10.000rpm at 4^{o}C and kept supernatant for the rest of the protocol described above.

2.12 Lifespan assays

Lifespan assays were performed at 20^{o}C unless noted otherwise. Synchronous animal populations were generated by hypochlorite treatment of gravid adults to obtain tightly synchronized embryos that were allowed to develop into adulthood under appropriate, defined conditions. When they reach the L4 stage, 20-25 worms were placed on NGM plates containing 2mM IPTG and seeded with HT115(DE3) bacteria transformed with either the pL4440 vector or the test RNAi construct. At least a total of 150-200 animals were tested per condition in each experiment. The day of egg collection and initiation of RNAi is t=0. Animals were transferred to newly seeded plates every 2 days thereafter and examined every day for touch-provoked movement and pharyngeal pumping, until death. Worms that died owing to internally hatched eggs, an extruded gonad or desiccation due to crawling on the plate edges were scored as censored and incorporated as such into the data set. Each survival assay was repeated at least twice and figures represent typical assays. Survival curves were created using the product-limit method of Kaplan and Meier. We used the log-rank (Mantel–Cox) test to evaluate differences between survivals and determine P values. We used the Prism software package (GraphPad

Software) for statistical analysis and to determine lifespan values. Full lifespan statistics are summarized in Table 1.

2.13 Mitotracker staining

For staining of the animals with Mitotracker Green FM, Mitotracker Red CM-H2X ROS, Mitotracker Deep Red FM and TMRE we diluted the stain in M9 and placed it at the top of pre-seeded plates in a final concentration of 0,28μM. We let the worms feed overnight and the next day we measured parameters of interest as described previously

2.14 Microparticle Bombardment

The Biolistic PDS-1000/He system (BioRad) was used for biolistic transformation. For generating transgenic strains we linearized 10-15μg plasmid DNA which was bombarded onto unc-119(ed3) mutant L4/adult hermaphrodites. Animals were grown on NGM plates seeded with Na22 bacteria and the rest of the procedure was done according to (Isik and Berezikov, 2013) as follows: 1. Grow unc-119 animals on 5 big plates seeded with Na22 bacteria, 2. When the plates are full of worms, bleach them, separate the eggs on 10 big plates seeded with Na22 bacteria and let them grow until they they become L4/young adults, 3. Wash off the worms from the plates with M9 and remove bacteria, 4. Spread about 1.5ml of worms to the surface (so as the worms cover the whole surface equally) of a dried plate (left 1 day before at 37^{o}C or at the day of Bombardment for 1hr at 65^{o}C and then put on ice), 5. Leave the plate with the worms on ice with the cover off until the liquid evaporates, 6. With a continuous and careful suspendation put 20μl-20μl from the DNA (specifically prepared for this protocol and bound on gold particles) into the middle of all macrocarrier, 7. After the gold granules get dry assemble the macrocarrier holder and the stopping screen, 8. Meantime put one rupture disc (1350psi) into isopropanol and then immerdiately place into its holder, pipett 20μl isopropanol to the rupture disc surface that

it can form a ring and twist the rupture disc holder into its place and tighten, 9. Set up the hepta adaptor, 10. Place the macrocarrier holder the closest under the hepta adaptor, 11. Adjust the macrocarriers to the hepta adaptor holes, 12. Fix the full of animals plate into the tray(without cover) and put it under the closest place to the macrocarrier holder and lock the door, 13. Open the He source, 14. Set the redactor behind the gene gun to 4.1, 15. Turm on the gene gun, 16. Turn on the vacuum pump, 17. Make vacuum into the chamber (28inHg), 18. Turn the vacuum button into the “hold” position, 18. Push the “fire” button until the rupture disc will make a sound, 19. Then dissolve the vacuum, disassemble the system, throw away the rupture disc and the macrocarriers, 20. Close the chamber’s door, 21.close the He source, 21. Make vacuum (25 inHg), 22. Hold the “fire” button until the pressure goes down from the system, 23. Dissolve the vacuum, 24. Turm off the vacuum pump, 25. Turm off the gene gun, 26. Then leave the animals to rest for 0.5-1 hour and then wash with M9 into 15ml falcon, 27. Centrifure for 1minute at 2000rpm and discart the supernatant, 28. Wash with M9, centrifuge for 1 minute at 2000rpm and discard the supernatant until 3ml, 29. Resuspend and then put 100μl into each small plate, 30. Wait until the plates dry and then store the anomals on the proper temperatutre, 31. 4 days after search the plates for the first transgenics.

2.15 Quantification and statistical analysis

Quantification was performed using the Image J software (NIH, http://imagej.nih.gov/ij/) and the Volocity 6.3 software as specified in the Figure legends.

Statistical analyses were carried out using the Prism software package (GraphPad Software Inc., San Diego, USA) and the Microsoft Office 2010 Excel software package (Microsoft Corporation, Redmond, WA, USA). The statistical tests applied for each experiment are specified in the Figure legends.

Key Resource Table		
Reagent or Reasource	**Source**	**Identifier**
Chemicals		
Mitotracker Green FM	Molecular Probes, Invitrogen	M7514
TMRE	Molecular Probes, Invitrogen	T669
Mitotracker Red CM-H2X ROS	Molecular Probes, Invitrogen	M7513
Cycloheximide	Sigma Aldrich	C7698
Mitotracker Deep Red FM	Molecular Probes, Invitrogen	M22426
Paraquat	Sigma Aldrich	856177
CCCP	Sigma-Aldrich	857815
Magnetic Beads	Merc, Millipore	LSKMAGAG 02
Levamisole	Sigma-Aldrich	196142
RNAse inhibitor	Roche	3335399001
Nanobeads 100nm	Polysciences	6401015
DMSO	AppliChem	A3672,0250
Glycoblue	Invitrogen, ThermoFisher Scientific	AM9515
CIP enzyme	NEB	M0290
Completemini Proteinase inhibitor coctail	Roche	1183615300 1
Protector RNase Inhibitor	Roche	3335399001
Antibodies		
anti-GFP	Minotech	
anti-MTCOI	Abcam	ab14705
anti-alpha tubulin	DSHB	AA4.3 (concentrate)
a-flag	Sigma-Aldrich	F3165
Experimental models: Organisms/Strains		
C. elegans: Strain N2: Wild Type	Caenorhabditis Genetics Center	
C. elegans: Strain SJ4103: N2;*ls*[p_{myo-3}mtGFP]	Caenorhabditis Genetics Center	
C. elegans: Strain SJ4143: N2;*ls*[p_{ges-}	Caenorhabditis Genetics Center	

$_{1}$mtGFP]		
C. elegans: Strain CL2166: N2;*Is*[p$_{gst-4}$GFP]	Caenorhabditis Genetics Center	
C. elegans: Strain OP168: *unc-119(ed3) III*;[skn-1::TY1::EGFP::3xFLAG;unc-119(+)]	Caenorhabditis Genetics Center	
C. elegans: Strain AGD383: *uthIs202* [*aak-2 (intron 1)*::*aak-2(aa1-aa321)*::Tomato::unc-54 3'UTR;pRF4]	Caenorhabditis Genetics Center	
C. elegans: Strain CB1370: *daf-2(e1370)III*	Caenorhabditis Genetics Center	
C. elegans: Strain MQ887: *isp-1(qm150)*	Caenorhabditis Genetics Center	
C. elegans: Strain TJ1052: *age-1(hx546)*	Caenorhabditis Genetics Center	
C. elegans: Strain RB759: *akt-1(ok525)*	Caenorhabditis Genetics Center	
C. elegans: Strain MQ133: *nuo-6(qm200)*	Caenorhabditis Genetics Center	
C. elegans: Strain TK22: *mev-1(kn1)III*	Caenorhabditis Genetics Center	
C. elegans: Strain IR1284: N2;*Is*[p$_{myo-3}$mtGFP];*Ex011*[p$_{lgg-1}$DsRed::LGG-1]	Palikaras et al.,2015	
C. elegans: Strain SPC167: *skn-1(lax120)IV*;P$_{gst-4}$GFP	Caenorhabditis Genetics Center	
C. elegans: *daf-2(e1370)*;*Is*[p$_{gst-4}$GFP]	This paper	
C. elegans: N2;*EX*[p$_{edc-3}$EDC-3::DsRed;pRF4]	Rieckher et al., 2018	
C. elegans: *unc-119 (ed3)III*;*EX*[p$_{ntl-2}$NTL-2::GFP;unc-119(+)]	This paper	

C. elegans: N2;*Ex*[p_{edc-3}EDC-3::DsRed;pRF4];*unc-119 (ed3)III*;*Ex*[p_{ntl-2}NTL-2::GFP;unc-119(+)]	This paper	
C. elegans: *unc-119 (ed3)III*;*EX*[p_{dcap-2}DCAP-2::mcherry;unc-119(+)]	This paper	
C. elegans: *unc-119 (ed3)III*;*Ex*[p_{ccf-1}CCF-1::GFP;unc-119(+)]	This paper	
C. elegans: N2;*Ex*[p_{ife-2}GFP;pRF4]	Syntichaki et al., 2007	
C. elegans: *unc-119 (ed3)III*;*Ex*[p_{ntl-2}NTL-2::GFP;unc-119(+)];*syEx1155* [p_{myo-3}TOMM-20::mRFP::3xMyc;unc-119(+)]	This paper	
C. elegans: SJ4103; N2;*Ex*[p_{edc-3}EDC-3::DsRed; pRF4]	This paper	
C. elegans: *unc-119 (ed3)III*;*Ex*[p_{edc-3}EDC-3::GFP;unc-119(+]	This paper	
C. elegans: *unc-119 (ed3)III*;*Ex003*[p $_{myo-3}$TOMM-20::Rosella;unc-119(+)]	This paper	
Oligonucleotides		
Name	**Sequence**	
Primer: *ntl-2* promoter Forward:	ACACGACGGATCATTTCACGAG	
Primer: *ntl-2* promoter Reverse	GGATCCCTGAAAGAAAATCGATTT	
Primer: *ntl-2* coding Forward	GGATCCATTTATGAGTAGAACGTAGCCA T	
Primer: *ntl-2* coding Reverese	ACCGGTGGGTTTGGAGTAGCTCG	
Primer: *dcap-2* promoter Forward	ACATTGCACTATACCCCTCTTATTGC	
Primer: *dcap-2* promoter Reverse	ACGAGAGATTCAAGCAAGTGGTGTC	

Primer: *dcap-2* coding part 1 Forward	GCGGCCGCATGCAGCAACA	
Primer: *dcap-2* coding part 1 Reverse	TCTAGACGTTTCAGCGAGTAATGAAACTTTTG	
Primer: *dcap-2* coding part 2 Forward	TCTAGAGATAGTGAAGCCCTTTCTCTTTT	
Primer: *dcap-2* coding part 2 Reverse	CCCGGGTGGTAATTGTGGTC	
Primer: *ccf-1* promoter Forward	TTCGTGTTTTGAAGAATTATCTTGTAAAATGAG	
Primer: *ccf-1* promoter Reverse	AAGCTTCTAGAATTTTCGTTTTAGAGTGAACG	
Primer: *ccf-1* coding Forward	TTCCAGATATCATAAAAATGGCTTCTAGTAGC	
Primer: *ccf-1* coding Reverese	ACCGGTGGGGCTTGTTGTGGAACT	
Primer: *ntl-2* RNAi Forward	ATGTTAGCAGACGACCATCAAGTCG	
Primer: *ntl-2* RNAi Reverse	TTAGTTTGGAGTAGCTCGCGCC	
Primer: *atp-3* RNAi Forward	AGAACAAGCTCGACCAGATTTC	
Primer: *atp-3* RNAi Reverse	GGGCATCCTTGTATTTCTTGAC	
Primer: *mrps-5* RNAi Forward	ATGGCATCACTTTTGCCATTTGTC	
Primer: *mrps-5* RNAi Reverse	ACCGGTCTTTTTGGGAACCACATGCGA	
Primer: *tomm-20* RNAi Forward	ATGTCGGACACAATTCTTGGTTTCAAC	
Primer: *tomm-20* RNAi Reverse	CTCCAAGTCGTCGGTGTCATCGA	
Primer: *akap-1* RNAi Forward	ACCGGTGAACATTTTCTCACTTACTG	
Primer: *akap-1* RNAi Reverse	TTTGCGACGAGAATGATGGTC	

CHAPTER 3
RESULTS

3.1 P-body components physically and functionally associate with mitochondria

Former studies in human cell lines designated that the mRNA metabolism component Rck/p54/DDX6, the homologue of CGH-1 in *C. elegans*, localizes to the vicinity of mitochondria. Notably, measurement of the frequency and duration of this event excludes stochasticity (Huang et al., 2011). To gain deeper insight into whether P-bodies also associate with mitochondria in *C. elegans*, we generated *in vivo* monitoring systems for tracking their localization relative to mitochondria in body wall muscle cells. The mitochondrial network in these cells, in contrast to other cell types, is well-organized and mitochondrial morphology well-defined, enabling us to succinctly distinguish and visualize even single organelles (Regmi et al., 2014). We found that the CCR-4/NOT complex component NTL-2 localizes close to mitochondria as shown by staining of animals with TMRE (**Figure 9A**) or by co-expressing NTL-2::GFP with the OMM protein TOMM-20::RFP (**Figure 9B**). We further verified this result by using an additional mitochondrial specific dye, Mitotracker Deep Red (**Figure 9C**). Again, in this case, NTL-2 bodies were closely associated with mitochondria.

To test whether this effect is limited to a specific protein or not, we also examined EDC-3 localization. We found that the decapping complex component EDC-3 also localizes in the proximity of mitochondria as tested both by genetic and staining methods (**Figure 9D, 9E**). To exclude the possibility that the results we observed are due to DsRed aggregation, we created transgenic animals that express EDC-3 fused with GFP, which is a less stable fluorophore (Verkhusha et al., 2003). Again, we observed that EDC-3-foci localize next to mitochondria (**Figure 9F**). Then, we measured the distances between NTL-2- or EDC-3-foci and mitochondria under physiological conditions and found that, in both cases, approximately 60% of the foci obtained zero distances from mitochondria, while the bulk majority (a percentage higher than 80% of the total bodies quantified)

where found in less than 1µm away from mitochondria (**Figure 9G**). To further validate this result, we performed mitochondrial fractionation analysis. To this end, we separated the mitochondrial from the cytoplasmic fractions from extracts of transgenic animals that express mRNA metabolism components fused with GFP. mRNA metabolism components that physically associate with mitochondria should be detected in both fractions by using an anti-GFP antibody (antibodies specific to the endogenous C. elegans proteins of interest are not available). Indeed, EDC-3 and NTL-2 were detected in both the cytoplasmic and the mitochondrial fractions. Moreover, we found that RNase A treatment did not abolish this association, in contrast to proteinase K treatment (data not shown) (**Figure 9H**). Together, these findings suggest that both P- body components physically associate with mitochondria in an RNA-independent manner.

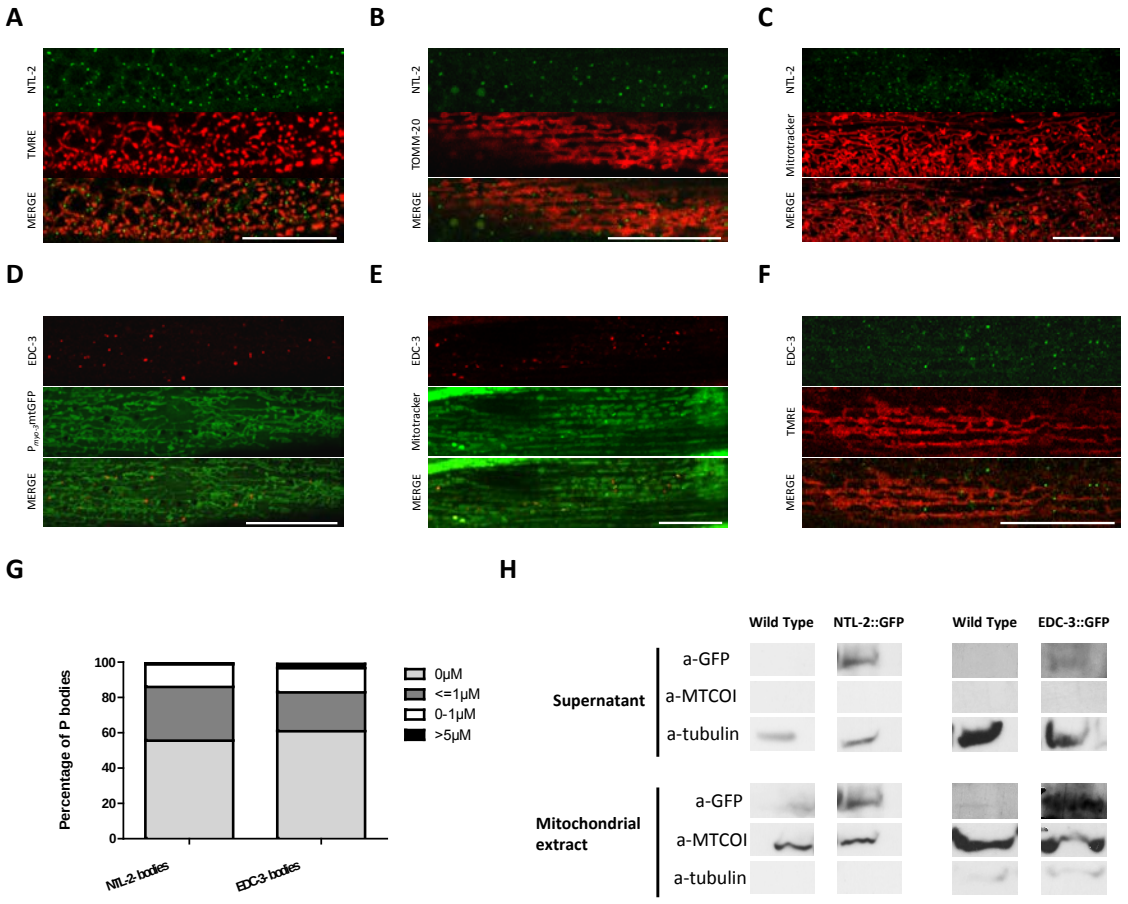

Figure 9. P-body components physically associate with mitochondria. (A) NTL-2/storage bodies localize in close proximity to mitochondria in young adult animals (green: NTL-2, red: TMRE, a mitochondrial membrane potential-dependent dye), (B) Additional evidence for the localization of NTL-2/storage bodies relative to the mitochondria in young adult animals (green: NTL-2, red: TOMM-20, an OMM protein-marker of mitochondria), (C) Representative images showing the localization of NTL-2/storage bodies relative to mitochondria (green: NTL-2, red: mitochondria stained with mitotracker deep red FM, a mitochondrial-specific dye) under control conditions. Scale bars, 20μm. Images were acquired using the ×63 objective lens, (D) EDC-3/degradation bodies localize in the close vicinity of mitochondria in young adult animals (red: EDC-3, green: mitochondrial matrix targeted by GFP), (E) Staining method showing the localization of EDC-3/degradation bodies relative to mitochondria in young adult animals (red: EDC-3, green: mitotracker deep red FM, a mitochondrial-specific dye), (F) Representative images showing the localization of EDC-3/degradation bodies relative to mitochondria (green: EDC-3, red: TMRE, a mitochondrial membrane potential-dependent dye) under control conditions. Scale bars, 20μm. Images were acquired using the ×63 objective lens, (G) Quantification of the percentage of NTL-2/storage bodies and EDC-3/degradation bodies that obtained the depicted distances from mitochondria, (H) Immunoblot analysis of a cytoplasmic and a mitochondria-containing fraction showing that both storage and degradation body components are detected in the mitochondrial fraction apart from the cytoplasmic one.

The physical association between the two P-body components and mitochondria suggests a functional association between them. To test further this possibility, we examined whether these associations change during ageing. We found that the abundance of NTL-2-bodies markedly drops during ageing in unstressed animals and the NTL-2::GFP fusion protein obtains a diffused, cytoplasmic pattern (**Figure 10A**) recommending that the associations between NTL-2-bodies and mitochondria significantly weaken during ageing. Also, even though EDC-3-body formation is sustained, or even enhanced in aged animals, their association with mitochondria is significantly lost as compared with their young counterparts (**Figure 10B, 10C**). To exclude the possibility that mitochondrial network fragmentation that occurs in aged animals leads to the destruction of EDC-3-body with mitochondria associations, we mimicked the effects of age-dependent mitochondrial network disruption in young animals

by knocking down *atp-3*, which encodes the nematode homologue of mitochondrial ATP synthase (complex V). ATP-3 depletion results in mitochondrial fragmentation even from the first day of adulthood. We measured the distances of EDC-3-bodies from mitochondria under these conditions and found that despite the severe fragmentation of the mitochondrial network, EDC-3-bodies maintained their associations with mitochondria (**Figure 10D**). Precise quantification of the EDC-3/degradation bodies that obtain zero distances from mitochondria validated this observation (**Figure 10E**). Together, these findings corroborate that the associations of P-body components with mitochondria are not random, but associated with the age-dependent deterioration of cell function.

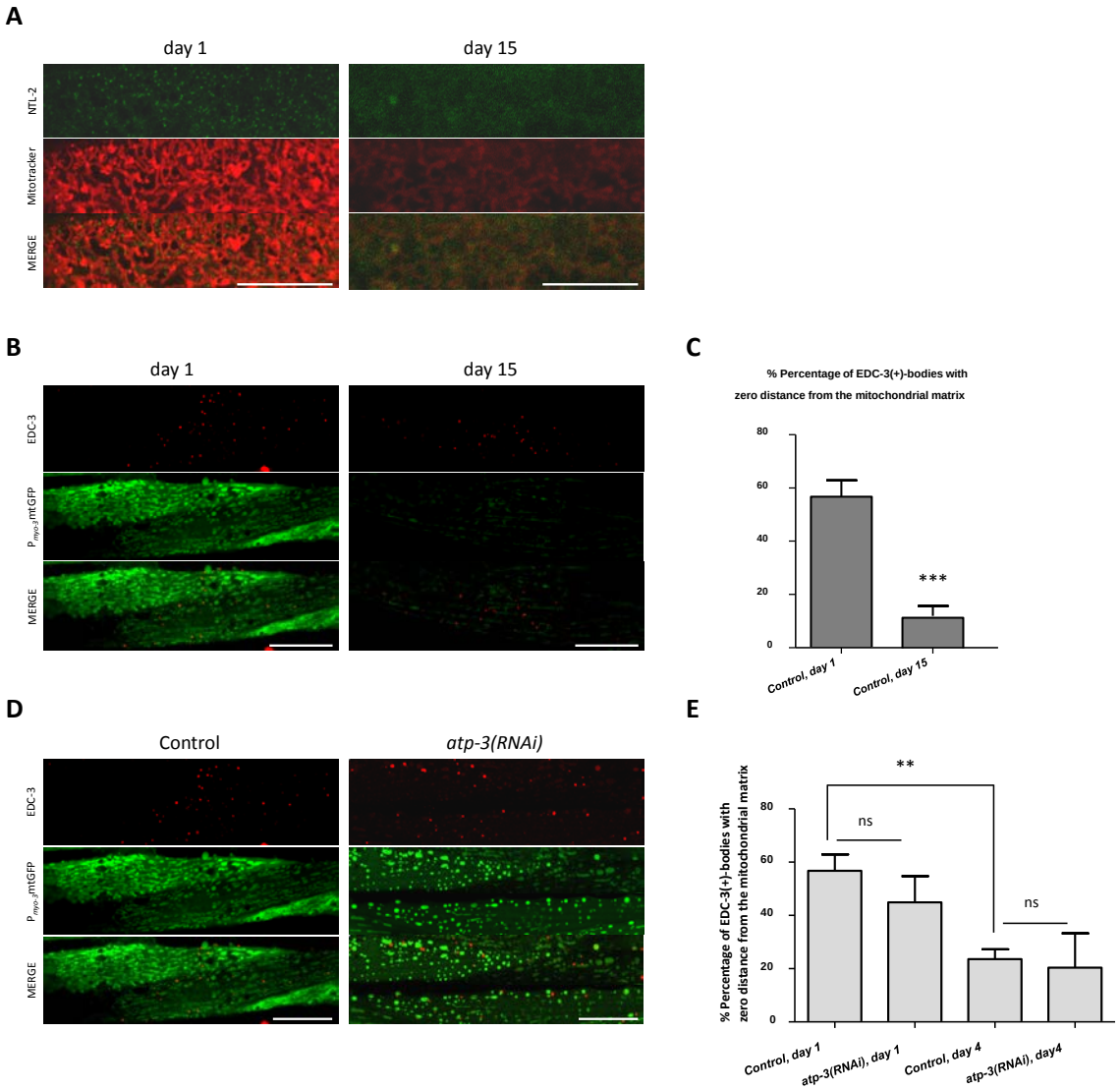

Figure 10. The physical associations of P-body components with mitochondria are age-dependent. (A) Representative images showing the localization of NTL-2- bodies relative to mitochondria in young versus old animals (green: NTL-2, red: mitotracker deep red FM, a mitochondrial-specific dye), (B) Representative images showing the localization of EDC-3- bodies relative to mitochondria in young versus old animals (red: EDC-3, green: mitochondrial matrix targeted by GFP), (C) Quantification of the percentage of EDC-3- bodies that obtain zero distance from mitochondria in young and old animals (n=90 ***P<0.001; unpaired t-test). Error bars denote s.e.m., (D) Representative images showing the localization of EDC-3- bodies relative to mitochondria in young adult animals upon genetic inhibition of *atp-3* (red: EDC-3, green: mitochondrial matrix targeted by GFP). Scale bars, 20μm. Images were acquired using the ×63 objective lens, (E) Quantification of the percentage of EDC-3- bodies with zero distance from mitochondria under control conditions and following genetic inhibition of *atp-3* in young adults and 4-

day-old animals (n=40; ***P < 0.001; one-way analysis of variance (ANOVA)). Error bars denote s.e.m.

We have seen previously that perturbation of mRNA metabolism components severely affects mitochondrial physiology. To strengthen our hypothesis that a direct functional association between mitochondria and P-bodies exists, we impaired mitochondrial function suspecting that the localization pattern, the formation of P-bodies or both phenotypes would change. Indeed, perturbation of mitochondrial function either pharmacologically, by treatment with the oxidative stress inducer paraquat, or genetically, by genetic inhibition of *mrps-5*, encoding a protein subunit of the mitochondrial ribosome (Castello et al., 2007; Houtkooper et al., 2013), extensively and differentially affected the abundance of the two P-body components. Notably, we observed that both treatments significantly increased EDC-3-body formation, while eliminated NTL-2-bodies (**Figure 11A, 11B, 11C**). The distance between EDC-3-bodies and mitochondria indicated that their association was weakened upon perturbation of mitochondrial function, even though the frequency of colocalization events increased (**Figure 11D, 11E, 11B**).

Besides, NTL-2 body formation was abolished upon mitochondrial dysfunction, and consequently, the association between the two structures was lost (**Figure 11A, 11B**), similarly to what observed in aged animals (**Figure 10A**). These findings indicate that the dynamic nature of cytoplasmic P-bodies is affected by mitochondrial dysfunction. Collectively, our results recommend that P-body components form RNA-independent physical and functional contacts with mitochondria that change with age.

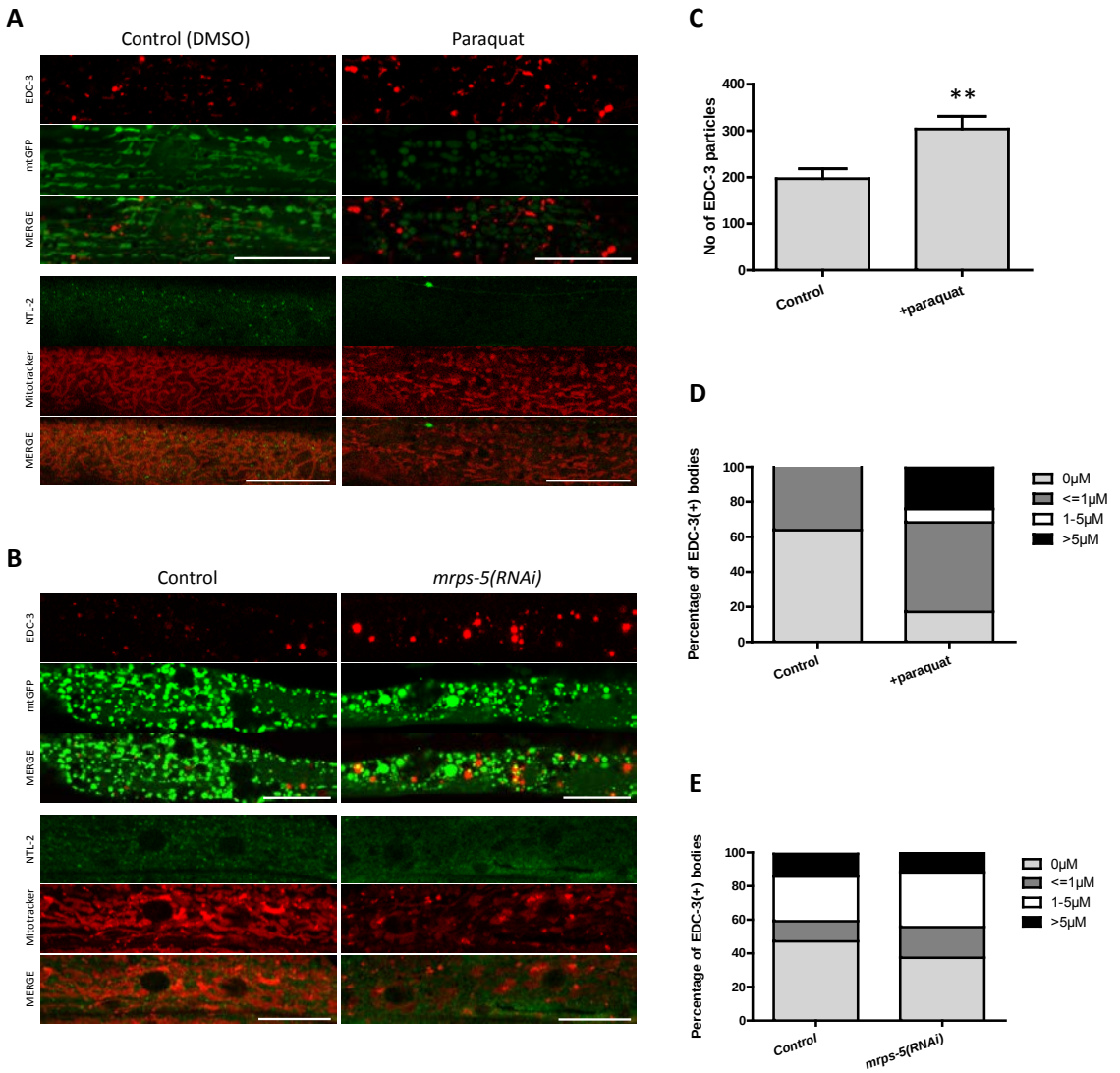

Figure 11. Mitochondrial dysfunction impairs the association of P-body components with mitochondria. (A) Representative images showing the formation and localization of EDC-3- and NTL-2- bodies relative to mitochondria under control conditions and upon paraquat treatment, top: EDC-3- bodies, bottom: NTL-2-bodies, (B) Representative images showing the formation and localization of EDC-3- and NTL-2-bodies relative to mitochondria under control conditions and upon genetic inhibition of *mrps-5*, top: EDC-3-bodies, bottom: NTL-2-bodies. Scale bars, 20μm. Images were acquired using the x63 objective lens, (C) Quantification of EDC-3 foci in control conditions and upon paraquat treatment. (n=30 ***P<0.001; unpaired t-test). Error bars denote s.e.m., (D) Measurement of the distances between EDC-3 foci and mitochondria under paraquat treatment as compared with their control counterparts, (E) Measurement of the distances between EDC-3 foci and mitochondria upon genetic inhibition of *mrps-5* as compared to control.

3.2 mRNA metabolism components control mitochondrial abundance and function

The observation that mitochondrial perturbations profoundly and differentially influence P-body components provided us with the first evidence that P-bodies and mitochondria associate also functionally apart from physically. Based on that, we hypothesized that perturbation of the mRNA turnover components affects mitochondrial physiology. To examine this, we tested the effects of cytosolic mRNA metabolism components on mitochondrial abundance, network formation and function. To this end, we downregulated components of the CCR-4/NOT and the decapping complexes by feeding reporter strains that express GFP in the mitochondrial matrix of body wall muscle or intestinal cells with bacteria producing the desired dsRNA. We observed that genetic inhibition of *dcap-2* disrupted the mitochondrial network, triggered mitochondrial fragmentation and increased mitochondrial abundance in body wall muscle cells compared to control animals (**Figure 12A**).

Moreover, genetic inhibition of *ntl-2* disrupted the mitochondrial network and triggered mitochondrial globularization, swelling and a total drop in the number of the organelles (**Figure 12A**). To test whether this effect is tissue-specific or not, we additionally examined intestinal mitochondria. Mitochondrial abundance in the intestine is representative of the total mitochondrial population in the entire animal since the intestine is the primary somatic and the central metabolic organ of *C. elegans.* Again, in this case, genetic inhibition of *dcap-2* increased the abundance of intestinal mitochondria in contrast to *ntl-2* genetic inhibition (**Figure 12B, 12C**). The effect of these treatments on mitochondria sustained or even propagated when wild type animals were chronically subjected to RNAi against these genes (**Figure 12D, 12E**). Complementary to measuring mitochondria-targeted GFP in the intestine, we examined the effects of either *dcap-2* or *ntl-2* knockdown by staining animals with Mitotracker (**Figure 12F**).

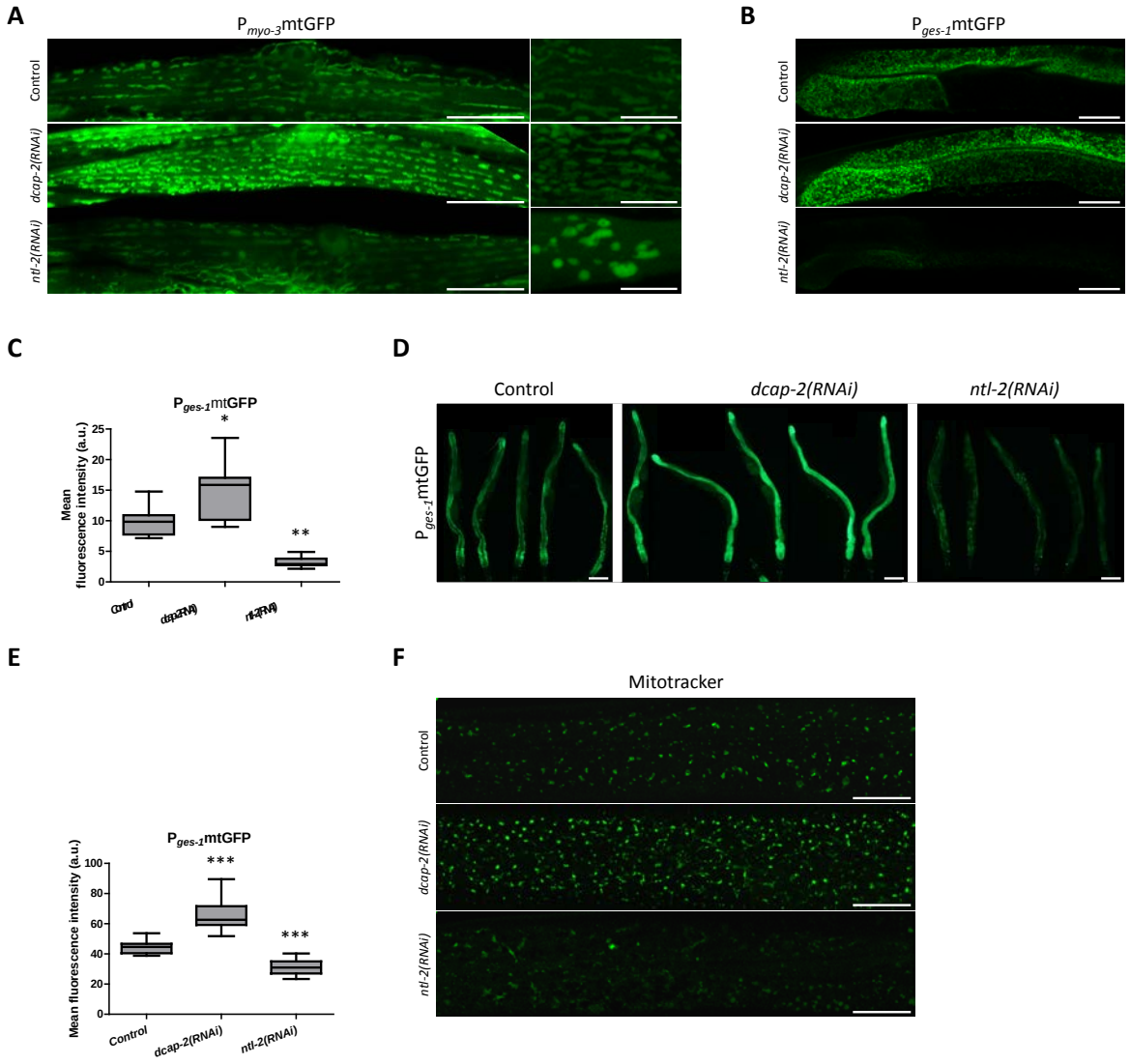

Figure 12. Perturbation of P-body components significantly and differentially influences mitochondrial abundance. (A) Confocal images of young adult animals expressing mitochondria-targeted GFP in body wall muscle cells upon *dcap-2* or *ntl-2* RNAi treatment. Scale bars, 20μm (Figure 1A right panel scale bar, 5μm). Images were acquired using the ×40 objective lens, (B) Confocal images of young adult animals that express mitochondria-targeted GFP in the intestine upon *dcap-2* or *ntl-2* knockdown. Scale bars, 20μm. Images were acquired using the ×40 objective lens, (C) Quantification of intestinal mitochondrial mass upon knockdown of either *dcap-2* or *ntl-2* of animals shown in Figure 1B. (n=27; ***P < 0.001; one-way analysis of variance (ANOVA)). Error bars denote s.e.m., (D) Representative images showing the effect of *dcap-2* and *ntl-2* genetic inhibition on the intestinal cell mitochondria in 7-day-old nematodes. Scale bars, 20μm. Images were acquired using the ×5 objective lens, (E) Quantification of the mean GFP fluorescence intensity in the matrix of intestinal mitochondria of whole animals as shown in Figure S1B (n=62; ***P < 0.001; one-way analysis of variance (ANOVA)). Error

bars denote s.e.m., (F) Confocal images of young adult animals stained with Mitotracker Green in the hypodermis. Scale bars, 20μm. Images were acquired using the ×40 objective lens.

Since knockdown of *dcap-2* or *ntl-2* affects not only mitochondrial abundance but also mitochondrial network and shape, we tested whether genetic inhibition of these mRNA metabolism components could also alter mitochondrial function. Two key indicators of mitochondrial function are mitochondrial membrane potential (Δψ) and ROS production (Joshi and Bakowska, 2011). To measure these parameters *in vivo*, we utilised feeding staining methods. We observed that both *dcap-2* and *ntl-2* knockdown increased total mitochondrial ROS production and mitochondrial membrane potential (**Figure 13A, 13B**). Collectively, these results indicate that perturbation of the decapping complex through *dcap-2* genetic inhibition increases the functional mitochondrial population, whereas perturbation of the CCR-4/NOT complex through *ntl-2* genetic inhibition results in less yet hyper-functional mitochondria compared to control animals. All in all, these data suggest that components of the decapping and the CCR-4/NOT complexes can specifically and differentially regulate mitochondrial abundance and function.

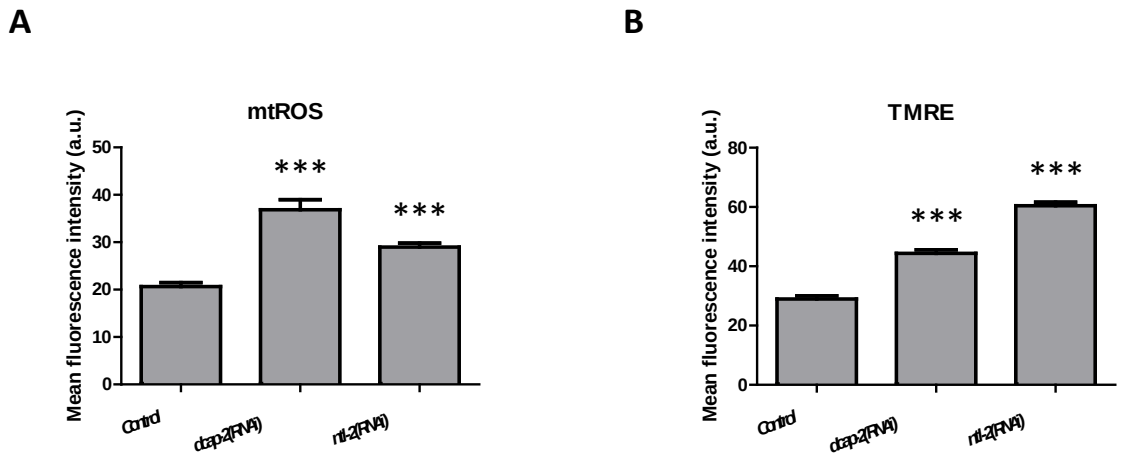

Figure 13. Genetic inhibition of P-body components enhances mitochondrial function. (A) Quantification of mitochondrial ROS production in animals subjected to

either *dcap-2* or *ntl-2* RNAi (n=114 ; ***P < 0.001; one-way analysis of variance (ANOVA)). Error bars denote s.e.m., (B) Quantification of mitochondrial membrane potential (Δψ) in animals subjected to RNAi with either *dcap-2* or *ntl-2* (n=144; ***P < 0.001; one-way analysis of variance (ANOVA)). Error bars denote s.e.m.

3.3 Components of the decapping and the CCR-4/NOT complexes are located in distinct foci that form independently from one another and obtain opposing functional properties

Having observed previously that the P-body components EDC-3 and NTL-2 are oppositely regulated upon mitochondrial dysfunction, in combination with the observation that the decapping and the CCR-4/NOT components oppositely regulate mitochondrial abundance, we hypothesized that they belong to two types of bodies serving different functions. To test this hypothesis, we generated transgenic animals that co-express the two mRNA metabolism components, NTL-2 fused with GFP and EDC-3 fused with DsRed on their C' terminus under the control of their endogenous promoters. We initially sought to examine whether these components colocalize. Interestingly, we found that they formed distinct foci, although they were co-expressed in the same tissues (**Figure 14A**). These foci most often obtained different positions inside the cell, while they were infrequently colocalized and occasionally detected in very close proximity to each other (**Figure 14A**). To confirm this result, we calculated Pearson's correlation coefficient that describes the degree of correlation between the two types of foci. The correlation coefficient values ranged between -0,5 and 0,5, with an average of 0,08 (r=0,08), validating our initial observations and suggesting that the two proteins are indeed components of distinct foci (**Figure 14B, 14C**). Although localization of the CCR-4/NOT and the decapping complex components in distinct foci has never been reported *in vivo*, recent evidence from *in vitro* analyses (Ozgur et al., 2015; Youn et al., 2018) are in line

with our findings, supporting the idea that the decapping and the CCR-4/NOT complexes are parts of two distinct foci. Taking into account the functional properties of their constituents, we will refer hereafter to the decapping complex (DCAP-1/DCAP-2/EDC-3)-containing foci as degradation bodies and to the CCR-4/NOT-containing ones as storage bodies (**Figure 14D**).

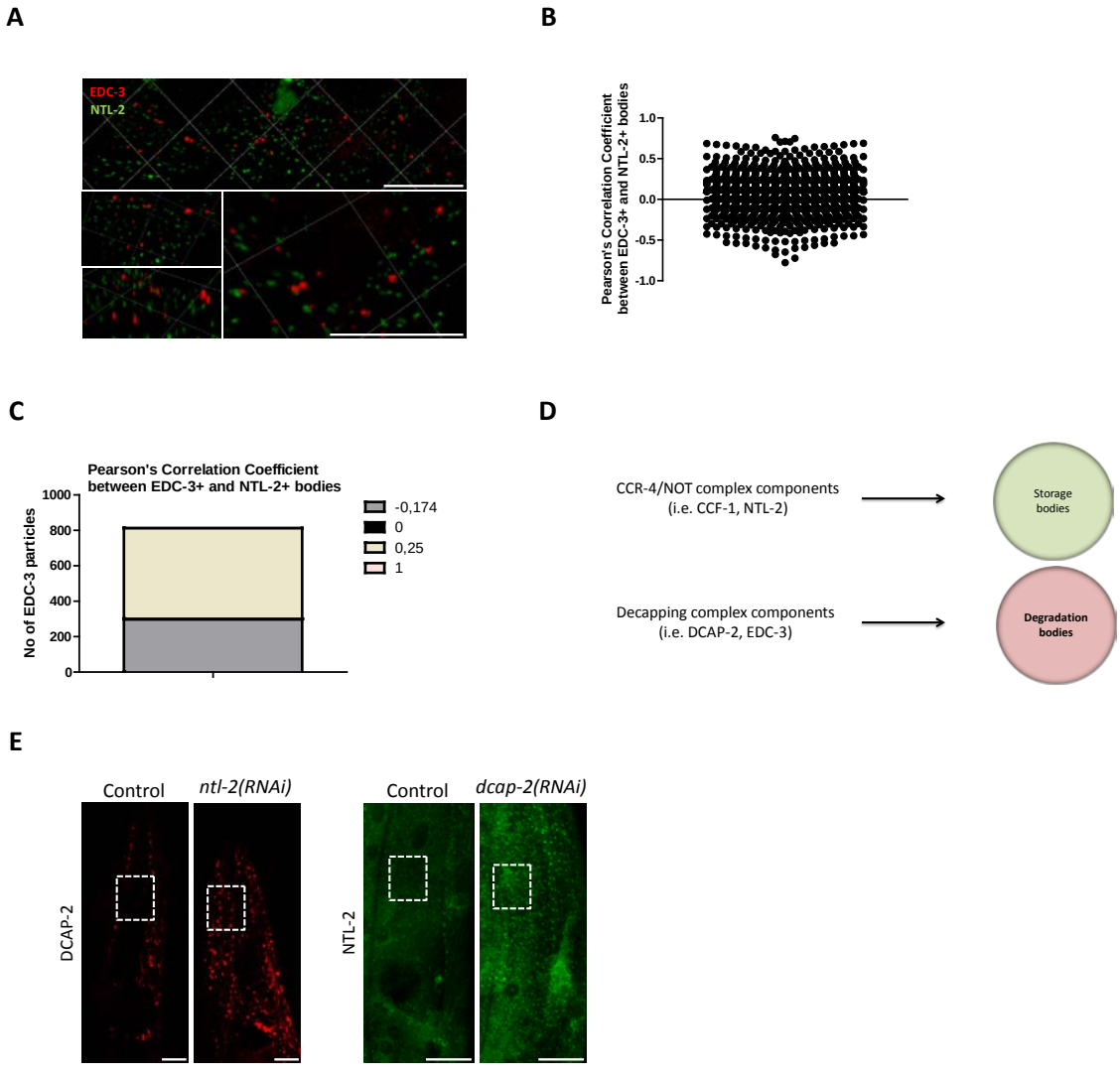

Figure 14. Components of the decapping and the CCR-4/NOT complexes form distinct foci. (A) Volocity software 3D representation of the subcellular localization of EDC-3 (red) and NTL-2 (green) (lower panels are higher magnification and rotation images of the top panel image). Scale bars, 20µm. Images were acquired using the x63

objective lens, (B) Diagram showing the Pearson's correlation coefficient values after measuring the correlation between EDC-3- and NTL-2-bodies as shown in Figure 14A, (C) Diagram showing the number of EDC-3-bodies that obtained the depicted Pearson's correlation values when their relative association with NTL-2-bodies was calculated, (D) Schematic representation showing the components of storage and degradation bodies referred in our study, (E) Representative images showing the increase of DCAP-2-foci following *ntl-2* genetic inhibition (left panel) and elevation of NTL-2-foci following *dcap-2* genetic inhibition (right panel) (white boxes include representative areas of interest for comparison). Scale bars, 20μm. Images were acquired using the x40 objective lens.

To further establish that the two types of bodies are indeed distinct, we hypothesized that they form independently from one another. To test this, we initially blocked a core component from each type of body and tested whether the formation of the other type is affected. For storage body perturbation, we downregulated *ntl*-2 and monitored the abundance of degradation bodies in vivo by tracking DCAP-2 (**Figure 14E**). Oppositely, we downregulated *dcap-2* and monitored storage bodies through NTL-2::GFP fusion protein (**Figure 14E**). We found that knockdown of storage body components increases the number of degradation bodies and oppositely, downregulation of degradation body components positively influences storage body abundance (**Figure 14E**). We conclude that the two types of bodies form independently and antagonistically of each other.

To understand their physiology thoroughly, we measured the abundance of degradation and storage bodies during ageing *in vivo* in *C. elegans*. In line with our earlier work (Rieckher et al., 2018), we found that degradation body components such as EDC-3 and DCAP-2 accumulate during ageing, indicating that the formation of degradation bodies rises with age (**Figure 15A**). By contrast, storage body components such as NTL-2 and CCF-1 were significantly less abundant or almost lost in aged animals under control conditions (**Figure 15B**). Their opposite regulation during ageing, besides confirming that the two types of bodies accumulate independently from one another, additionally

suggests that they may exert different, age-dependent functions. Our previous study showing that the P-body component EDC-3 modulates protein synthesis by controlling eIF4E availability to the translation machinery (Rieckher et al., 2018) together with the fact that translation is an age-dependent process (Gonskikh and Polacek, 2017), prompted us to test whether the two types of foci oppositely affect global translation rates. To monitor global translation rates upon genetic inhibition of *ntl-2* or *dcap-2*, we performed FRAP analysis and measured fluorescence recovery in animals expressing GFP throughout somatic tissues under the control of the *ife-2* gene promoter (Kourtis and Tavernarakis, 2009, 2017; Syntichaki et al., 2007). We found that knockdown of *dcap-2* reduced global protein synthesis rates, while *ntl-2* genetic inhibition had the opposite effect (**Figure 15C, 15D**). To confirm the efficiency of our method, we concomitantly assessed protein synthesis rates in animals subjected to mTOR/*let-363* RNAi or treated with 500μg/ml cycloheximide (**Figure 15C, 15D, 15E**). Together, these results indicate that the CCR-4/NOT and the decapping complexes are parts of distinct foci which form independently, mutually antagonize each other and oppositely influence mRNA translation.

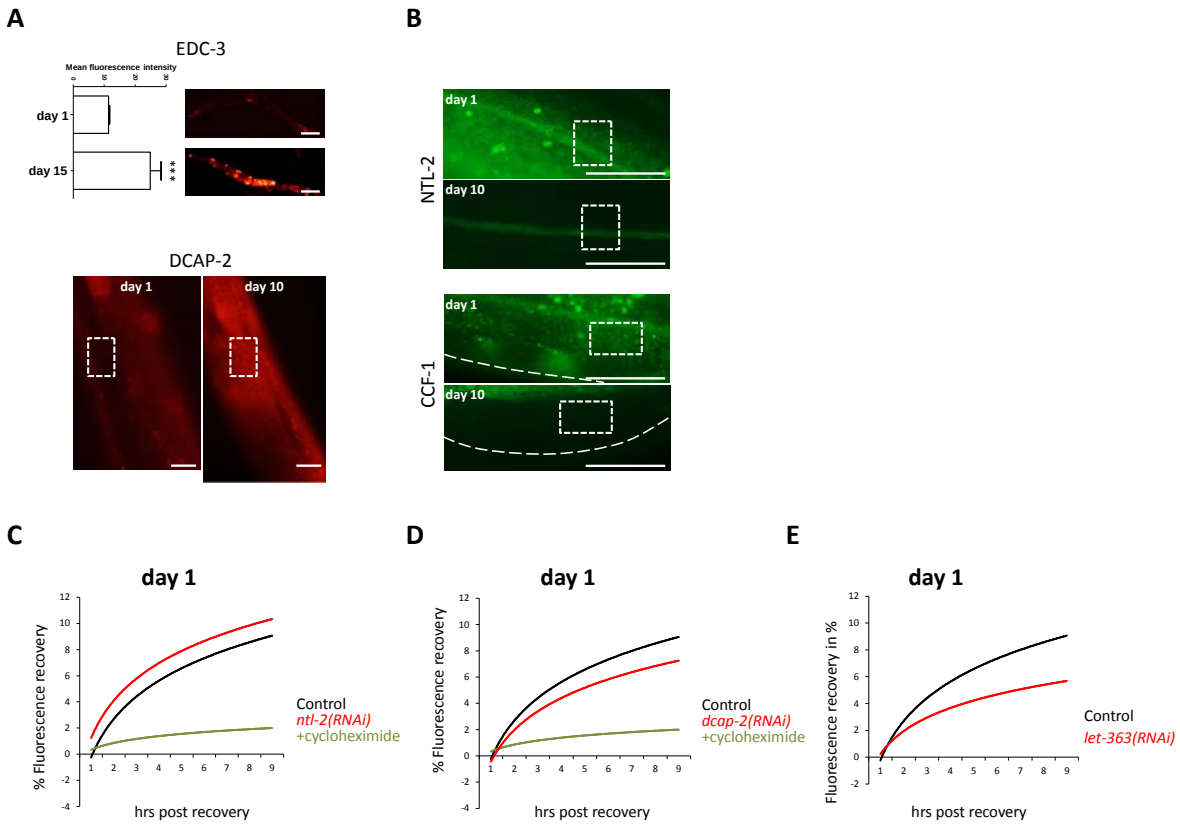

Figure 15. Storage and degradation bodies differentially expressed during ageing and oppositely regulate global translation rates. (A) Quantification of EDC-3 levels in young versus old animals (n=60 ***P<0.001; unpaired t-test), (top) and representative images showing DCAP-2 expression levels in young versus old animals (bottom) (white boxes include representative areas of interest for comparison). Error bars denote s.e.m. Images were acquired using the ×5 (top panel) and the x40 (bottom panel) objective lenses, (B) Representative images showing NTL-2 expression levels in young versus old animals (top) and CCF-1 expression levels in young versus old animals (bottom) (white boxes include representative areas of interest for comparison). Scale bars, 20μm. Images were acquired using the x40 objective lens, (C) Fluorescent recovery after photobleaching (FRAP) to measure the rates of *de novo* protein synthesis upon genetic inhibition of *ntl-2* in young adult animals; the protein synthesis inhibitor cycloheximide (500μM) was used as a positive control; time 0 is the time just after photobleaching and the recovery of the fluorescence was measured every one hour, (D) Fluorescent recovery after photobleaching (FRAP) to measure the rates of *de novo* protein synthesis upon genetic inhibition of *dcap-2* in young adult animals; cycloheximide (500μM) was used as a positive control; time 0 is the time just after photobleaching and the recovery of the fluorescence was measured every one hour, (E) Fluorescent recovery after photobleaching (FRAP) to measure the rates of *de novo* protein synthesis upon genetic inhibition of *let-363* in young adult animals; used as an additional positive control.

3.4 Storage and degradation body components regulate mitochondrial biogenesis in a SKN-1 and AAK-2-dependent manner

Since our data point towards the existence of a strong and direct functional association between mitochondria and storage/degradation bodies, we turned our interest in identifying the mechanism that mediates this association. We have previously found that mitochondrial abundance is oppositely regulated by storage and degradation bodies. Mitochondrial biogenesis and mitophagy are the two opposing cellular processes that coordinately regulate mitochondrial content in order to meet cellular metabolic needs in response to various intracellular or environmental stimuli. To test the potential involvement of mitophagy, we initially used the pH-sensitive Rosella Biosensor (Palikaras et al., 2015). We observed that genetic inhibition of either *ntl-2* or *dcap-2* does not affect mitophagy under normal conditions and instead blocks mitophagy upon paraquat exposure (**Figure 16A**). To further confirm this result, we used transgenic animals that co-express a GFP targeted to the mitochondrial matrix of body wall muscle cells and DsRed fused with LGG-1 under the control of the endogenous *lgg-1* gene promoter and examined the colocalization of the two fluorescent proteins. In this case, we did not detect mitophagy events under control conditions; however, after paraquat treatment, mitophagy was highly induced as expected (**Figure 16B**). On the other hand, both *ntl-2* and *dcap-2* genetic inhibition blocked mitophagy induction even after paraquat treatment (**Figure 16B**), despite their differential effect on mitochondrial mass (**Figure 12A, 12B, 12F**). Together, these findings suggest that storage and degradation bodies regulate mitochondrial mass through mitophagy-independent mechanisms.

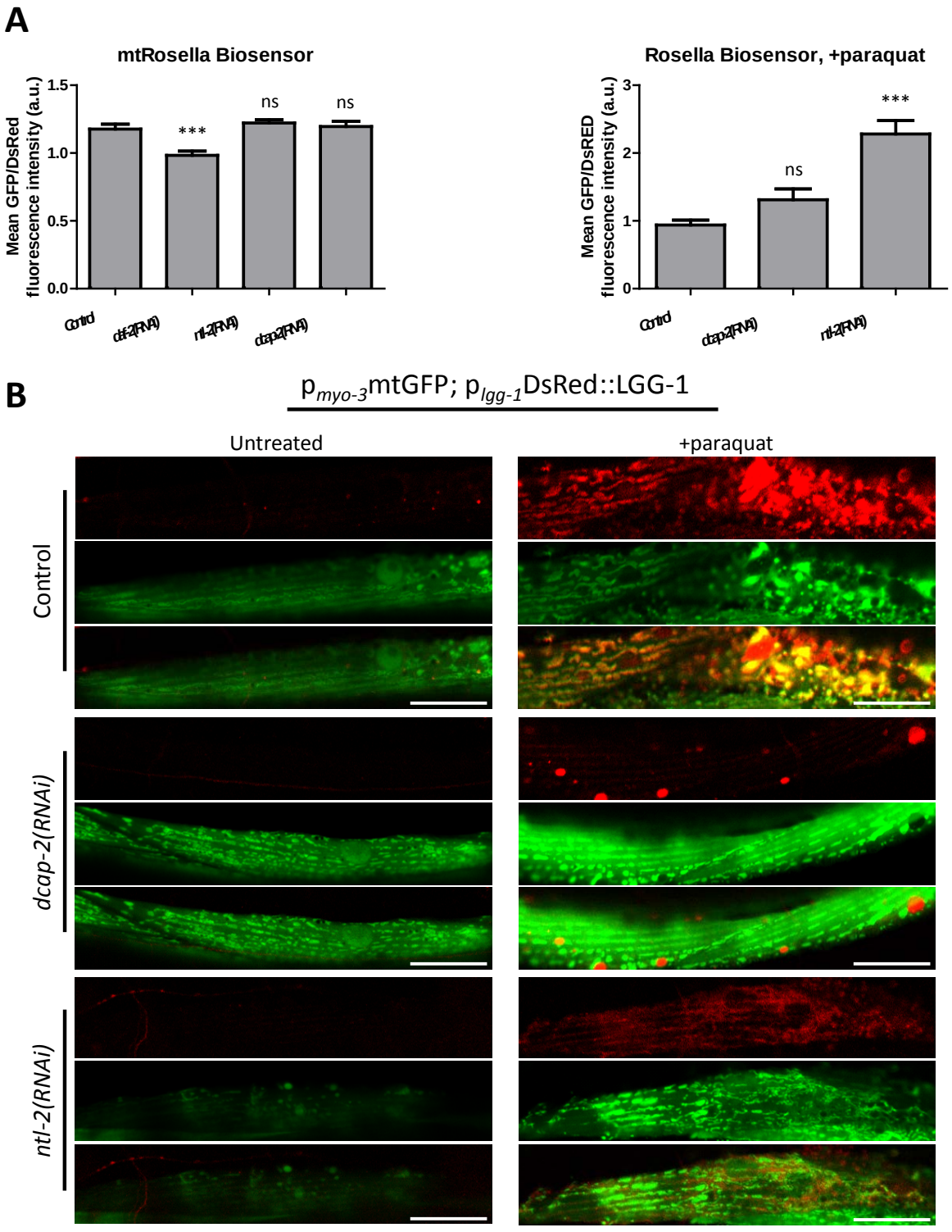

Figure 16. Mitophagy is blocked upon both storage and degradation body perturbation. (A) Mitophagy assessment by using the mitochondria-targeted Rosella

(mtRosella) Biosensor upon genetic inhibition of either *ntl-2* or *dcap-2* under control conditions (left) and upon paraquat exposure (right); *daf-2* genetic inhibition is used as a positive control (n=115; ***P < 0.001; one-way analysis of variance (ANOVA)). Error bars denote s.e.m., (B) Representative images showing mitophagy events under control and paraquat treatment in animals subjected to either *dcap-2* or *ntl-2* RNAi. Scale bars, 20μm.

Having excluded that mitophagy mediates the effects of storage and degradation body components on mitochondrial abundance, we examined whether mRNA metabolism components interfere with mitochondrial biogenesis mechanisms. We focused on SKN-1 and AAK-2, two key regulators of mitochondrial biogenesis. To this end, we examined whether storage and degradation bodies could influence SKN-1 levels and activity. We discovered that genetic inhibition of *dcap-2* significantly increased both the protein levels and the transcriptional activity of SKN-1 as measured by its target gene *gst-4*, while genetic inhibition of *ntl-2* had the opposite effect (**Figure 17A, 17B**). Notably, we observed the same effects when SKN-1 activity is pre-induced such as in a *daf-2* mutant background, in a mutant background (*skn-1(lax120)*), where SKN-1 is constitutively active or under paraquat treatment (**Figure 17B, 17C**). Subsequently, we checked whether the transcript levels of *skn-1* are affected by our treatments and found that neither *dcap-2* nor *ntl-2* genetic inhibition affected *skn-1* transcription (**Figure 17D**). These results indicate that both *dcap-2* and *ntl-2* oppositely regulate SKN-1 abundance and activity post-transcriptionally.

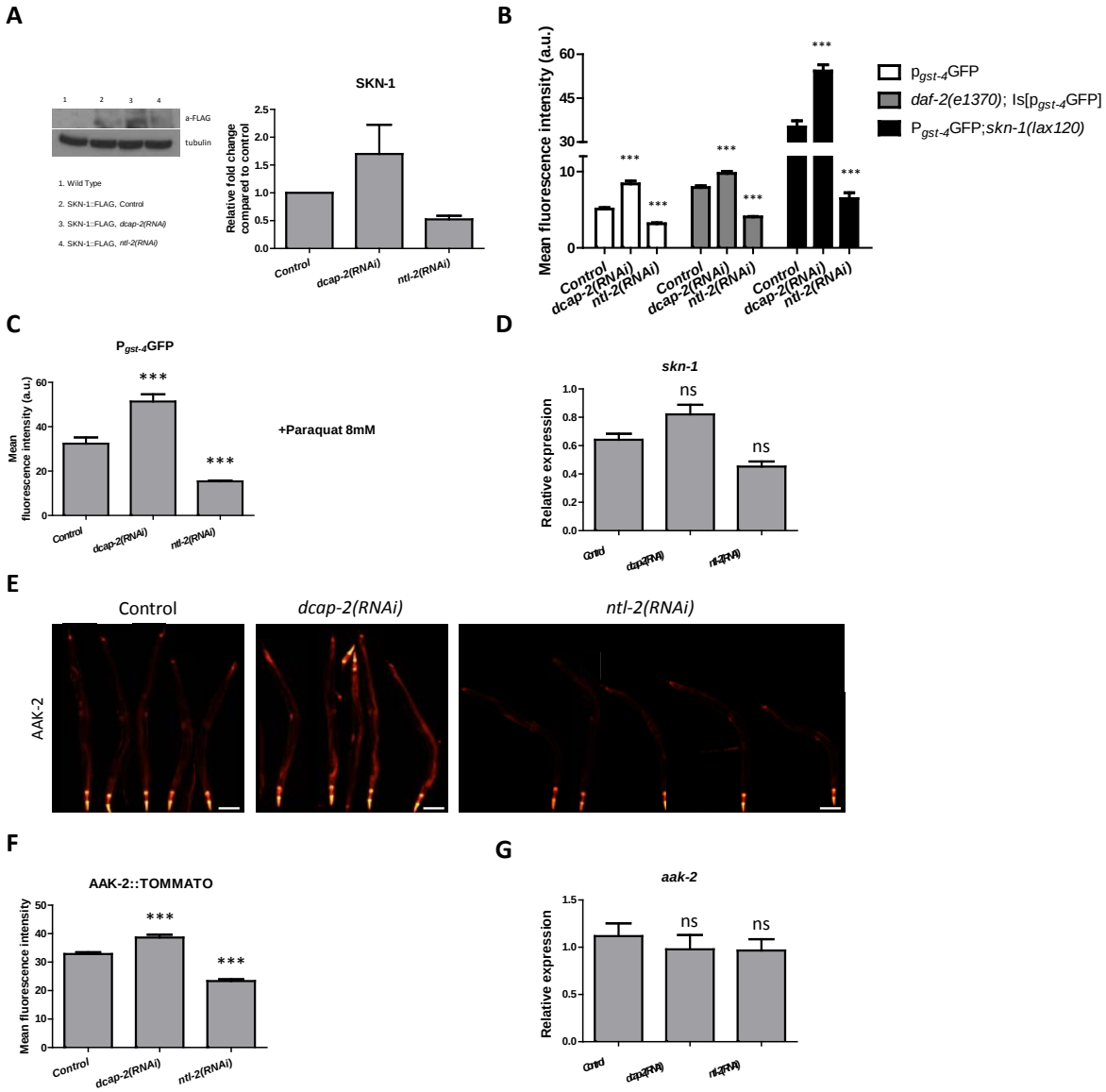

Figure 17. AAK-2 and SKN-1 are oppositely regulated by storage and degradation bodies. (A) Immunoblot analysis of SKN-1 protein levels upon *dcap-2* or *ntl-2* genetic inhibition (n=3), (B) Measurement of the promoter activity of the SKN-1 target gene *gst-4* upon genetic inhibition of either *dcap-2* or *ntl-2* in wild type background (white columns), in *daf-2* mutant background (grey columns) and in a mutant background (*skn-1(lax120)*) where SKN-1 is constitutively active (black columns), (n=270; ***P < 0.001; one-way analysis of variance (ANOVA)). Error bars denote s.e.m., (C) Measurement of the promoter activity of the SKN-1 target gene *gst-4* upon genetic inhibition of either *dcap-2* or *ntl-2* in wild type conditions and upon paraquat treatment (n=90; ***P < 0.001; one-way analysis of variance (ANOVA)). Error bars denote s.e.m., (D) Relative normalized expression of *skn-1* mRNA in wild type, DCAP-2 and NTL-2 depleted animals. Error bars denote s.e.m., (E) Representative images showing AAK-2 protein levels in animals fed bacteria expressing control and *dcap-2* or *ntl-2* RNAi. Scale bars, 100μm. Images were acquired using the ×5 objective lens, (F) Quantification of AAK-2 protein levels in whole

animals under control conditions and upon genetic inhibition of *dcap-2* or *ntl-2* (n=120; ***P < 0.001; one-way analysis of variance (ANOVA)). Error bars, denote s.e.m., (G) Relative normalized expression of *aak-2* mRNA in wild type, DCAP-2 and NTL-2 depleted animals. Error bars denote s.e.m.

Next, we tested whether the mRNA metabolism components *dcap-2* and *ntl-2* influence AAK-2 levels. To our surprise, we found that *dcap-2* genetic inhibition increased AAK-2 abundance in contrast to *ntl-2* downregulation which significantly decreases it (**Figure 17E, 17F**). Again, in this case, *aak-2* mRNA levels were not affected by our treatments, indicating that both *dcap-2* and *ntl-2* genetic inhibition post-transcriptionally regulate *aak-2* (**Figure 17G**).

Given that SKN-1 and AAK-2 are both master regulators of mitochondrial biogenesis, we hypothesized that *dcap-2* and *ntl-2* oppositely regulate mitochondrial content through these factors. To confirm this, we measured mitochondrial abundance in animals subjected to RNAi against *skn-1* or *aak-2* combined with *dcap-2* or *ntl-2* by staining mitochondria with Mitotracker Green. As expected, both *aak-2* and *skn-1* knockdown caused a significant drop in mitochondrial mass (**Figure 18A, 18B**). Moreover, the increased mitochondrial mass triggered by *dcap-2* genetic inhibition was reversed by either *skn-1* or *aak-2* genetic inhibition, while the lower mitochondrial mass observed after *ntl-2* depletion remained equal by the combined depletion of either *skn-1* or *aak-2* with *ntl-2* (**Figure 18A, 18B**). Collectively, these findings indicate that both DCAP-2 and NTL-2 exert their opposing effects on mitochondrial biogenesis acting through SKN-1 and AAK-2.

A

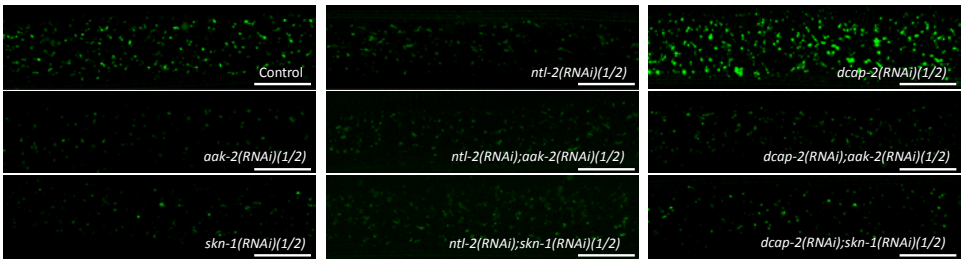

B

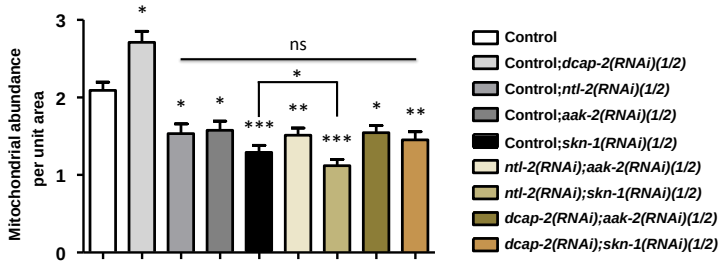

Figure 18. Storage and degradation bodies regulate mitochondrial abundance in a SKN-1- and AAK-2-dependent manner. (A) Representative images showing the effect of the depicted genetic inhibitions on the mitochondrial mass of young adult animals. Scale bars, 20μm (B) Quantification of the mitochondrial mass in the conditions shown in Figure 4SD. (n=84; ***P < 0.001; one-way analysis of variance (ANOVA)). Error bars denote s.e.m.)

3.5 Storage components bind NEMTTs and associate with mitochondria in a local translation-dependent manner

Transcription of NEMTTs followed by their local translation in the mitochondrial vicinity is crucial for mitochondrial biogenesis. We envisage that storage and degradation bodies regulate local translation of NEMTTs in the mitochondrial vicinity based on two findings: first, that mRNA storage and degradation body components can regulate mitochondrial abundance by interfering with mechanisms that regulate the organelle biogenesis. Second, these components physically interact with mitochondria and serve as translation regulators in the cytoplasm, supported by our findings up to now. If this happens, we

would be able to detect NEMTTs bound to storage body components as we expect them to form more stable associations with them than with degradation body components, which probably associate with mRNAs transiently to degrade them. To test this, we performed RNA immunoprecipitation and subsequent real-time PCR analysis for selected NEMTTs. Using an anti-GFP antibody, we isolated the NTL-2-bound material (associated proteins and mRNAs) from whole animal extracts, and then we purified the bound mRNAs to test whether select NEMTTs were solely present in the NTL-2::GFP-containing isolate and not in the control that lacks the GFP protein fusion or the one that has the GFP protein fusion tagged with HIS-72, to exclude unspecific binding of NEMTTs on GFP. Surprisingly, we found that the NTL-2-precipitated sample was enriched with NEMTTs and the *skn-1* transcript itself (**Figure 19**). Interestingly, NTL-2 does not bind *spcs-1* transcript, which encodes a core ER protein, indicating that NTL-2 binds preferentially to mitochondrially targeted transcripts under control conditions (**Figure 19**).

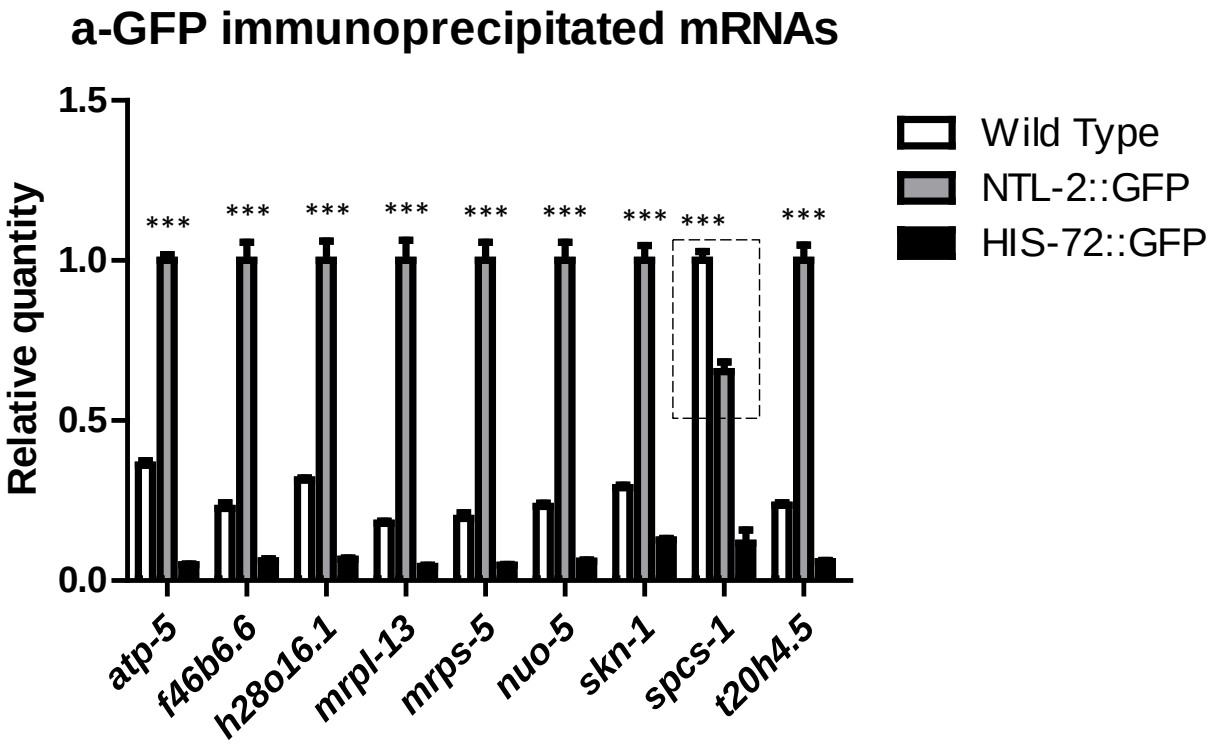

Figure 19. The storage body component NTL-2 is co-immunoprecipitated specifically with mitochondrial mRNAs and not the ER-protein encoding transcript *spcs-1*.

Then, we hypothesized that storage and degradation bodies perform post-transcriptional processing of NEMTTs to regulate their local translation in the vicinity of mitochondria. To test whether the associations of storage bodies with mitochondria are local-translation dependent, we downregulated the OMM local translation regulators TOMM-20 and AKAP-1, expecting that we would observe an alteration in the localization pattern of storage body components relative to mitochondria. Indeed, we measured the distances between storage bodies and mitochondria and found that knockdown of either *tomm-20* or *akap-1* severely impaired their associations, despite the increased abundance of storage bodies (**Figure 20A, 20B**). We validated this result by isolating mitochondria from

whole animal extracts and performing immunoblot analysis to detect NTL-2 protein, bound explicitly to mitochondria. We found that the amount of NTL-2 tethered to mitochondria was significantly decreased upon either *tomm-20* or *akap-1* genetic inhibition, as compared to their untreated control counterparts (**Figure 20C, 20D**).

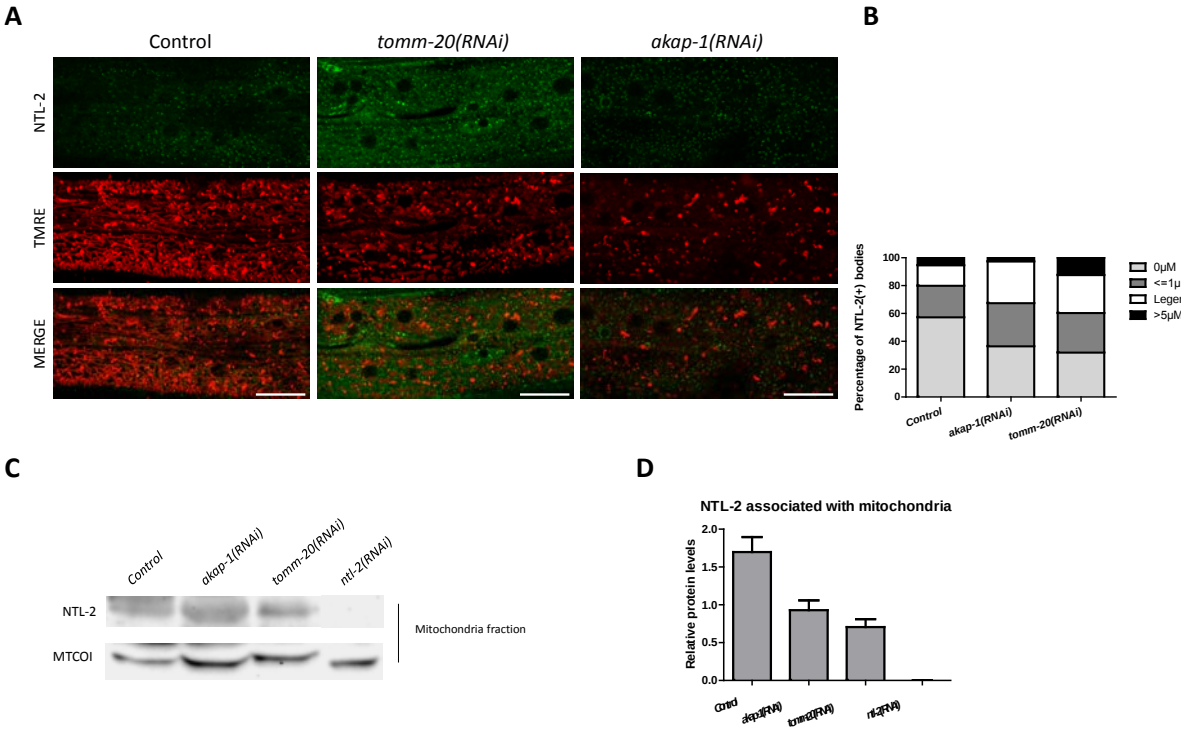

Figure 20. Storage bodies associate with mitochondria in a local translation-dependent manner. (A) Representative images showing the localization of NTL-2/storage bodies relative to mitochondria upon genetic inhibition of either *tomm-20* or *akap-1* (green: NTL-2, red: TMRE, a mitochondrial-membrane potential-dependent dye). Scale bars, 20 μm. Images were acquired using an x63 objective lens, (B) Quantification of the percentage of NTL-2/storage bodies that obtain the depicted distances from mitochondria upon genetic inhibition of either *tomm-20* or *akap-1*, (C) Immunoblot analysis in mitochondria-containing isolates of whole animal extracts showing the protein levels of NTL-2 bound to mitochondria in wild type conditions and upon genetic inhibition of *akap-1* or *tomm-20*; genetic inhibition of *ntl-2* is used as a positive control and NTL-2 protein is detected by an anti-GFP antibody in transgenic animals that contain the NTL-2::GFP protein fusion, (D) Quantification of NTL-2 protein bound to mitochondria under wild type conditions and upon genetic inhibition of *akap-1* or *tomm-20*; genetic inhibition of *ntl-2* is used as a positive control. Error bars denote s.e.m.

To exclude the possibility that the perturbed mitochondrial network caused by *akap-1* and *tomm-20* knockdown is responsible for the weakened associations, we assessed the effects of *atp-3* knockdown, which is known to cause severe mitochondrial network fragmentation. Surprisingly, we found that the associations between storage bodies and mitochondria are preserved or even strengthened in ATP-3-depleted animals despite mitochondrial fragmentation (**Figure 21A, 21B**). This was also confirmed by immunoblot analysis, as previously described (**Figure 21C, 21D**). Therefore, we conclude that the associations of storage bodies with mitochondria are local-translation-dependent.

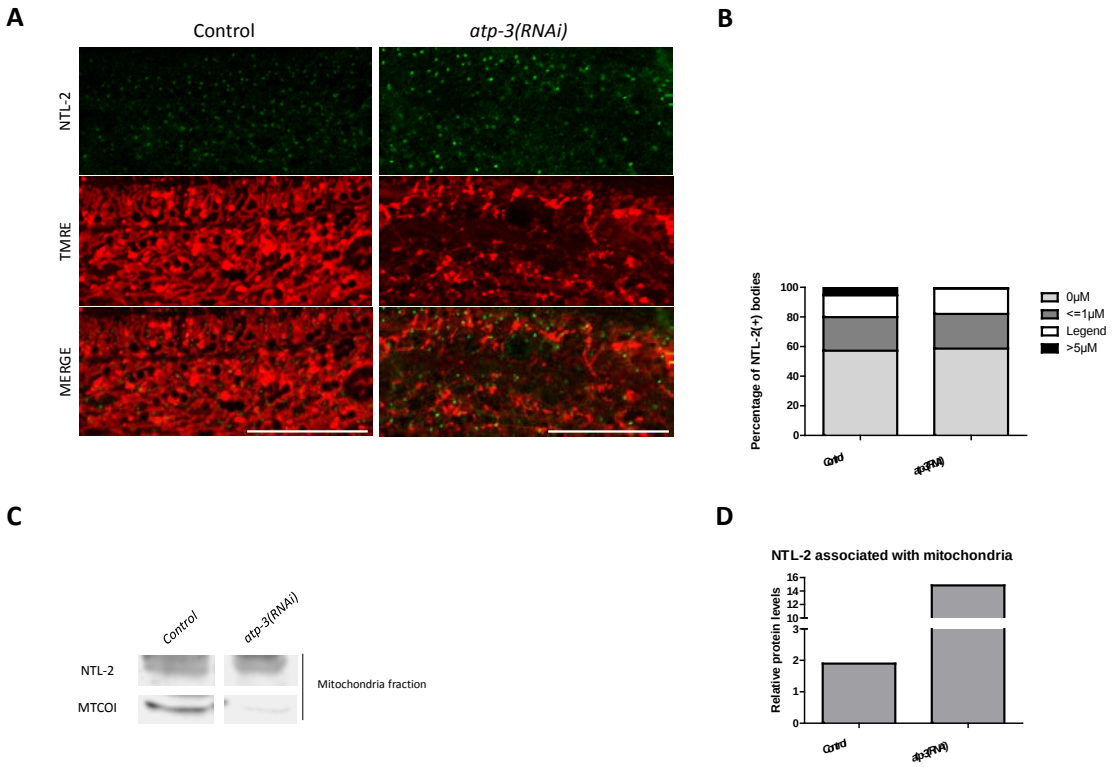

Figure 21. The associations of storage bodies with mitochondria form independent of the mitochondrial network integrity. (A) Representative images showing the localization of NTL-2/storage bodies relative to mitochondria in wild type conditions and upon genetic inhibition of *atp-3* (green: NTL-2, red: TMRE, a mitochondrial membrane potential-dependent dye). Scale bar, 20 µm. Images were acquired using the x63 objective lens, (B) Quantification of the percentage of NTL-2/storage bodies that obtain the depicted distances from mitochondria in control conditions and upon genetic inhibition of *atp-3*, (C) Immunoblot analysis in mitochondria-containing isolates of whole animals extracts showing the protein levels of NTL-2 bound to mitochondria in wild type conditions

and upon genetic inhibition of *atp-3*; NTL-2 protein is detected by an anti-GFP antibody in transgenic animals that contain the NTL-2::GFP protein fusion, (D) Quantification of NTL-2 protein bound on mitochondria under wild type conditions and upon genetic inhibition of *atp-3*.

3.6 mRNA metabolism components regulate lifespan and stress resistance by altering mitochondrial physiology

Our findings dictate that mRNA metabolism components alter mitochondrial function and oppositely affect mitochondrial biogenesis. Taking into account the importance of mitochondria for stress resistance and lifespan, we hypothesized that mRNA metabolism components also oppositely affect mitochondrial-related stress responses and organismal ageing. To test this hypothesis, we exposed animals to heat stress, CCCP and paraquat. The stress responses that are activated to cope with the stressors mentioned above require functional mitochondria (Castello et al., 2007; Labbadia et al., 2017; Miyazono et al., 2018). We found that DCAP-2 depleted animals are resistant to heat stress in contrast to the NTL-2-deficient ones as compared to their control counterparts (**Figure 22A**).

Additionally, animals were treated with paraquat, which alters ETC function leading to a severe elevation in mtROS production, or CCCP, which specifically perturbs the mitochondrial function by diminishing mitochondrial membrane potential (Δψ). Again, genetic inhibition of *dcap-2* conferred resistance to both paraquat and CCCP treatments (**Figure 22B, 22D**). By contrast, NTL-2 depletion proved to be detrimental as most animals died within the first 24hours following CCCP or paraquat administration (**Figure 22B, 22D**). Interestingly, paraquat sensitivity caused by NTL-2 depletion was observed

even in the *daf-2* mutant background (**Figure 22C**), which is resistant to oxidative stress (Honda and Honda, 1999). Summarizing, these findings indicate that storage body integrity is indispensable for the organism to overcome stress upon mitochondrial dysfunction. Conversely, the organism copes effectively with stress, when degradation bodies are perturbed.

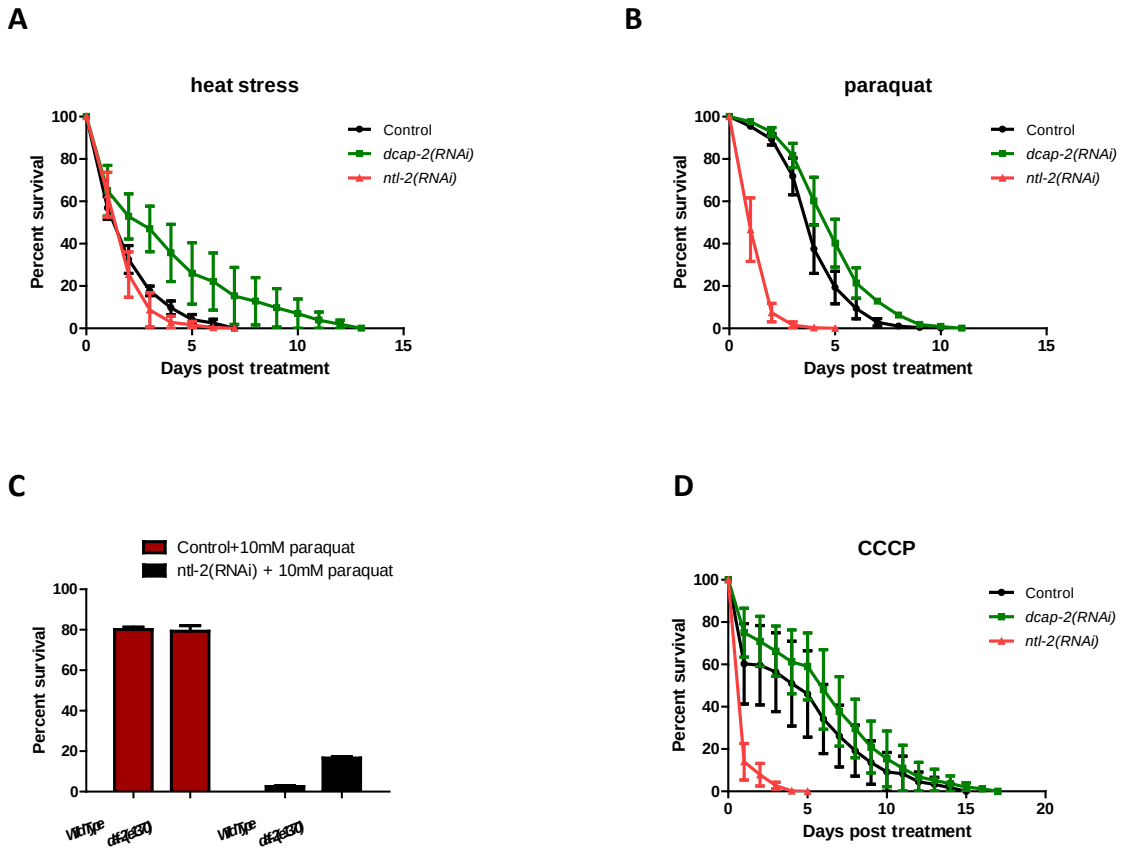

Figure 22. Perturbation of storage and degradation bodies oppositely affects stress resistance. (A) Percent survival of wild type, DCAP-2 and NTL-2 depleted animals exposed to heat stress performed for 5hrs at 37^{o}C counted every 24hours (n=4 independent experiments). Error bars denote s.e.m., (B) Percent survival of wild type, DCAP-2 and NTL-2 depleted animals following paraquat (8mM) administration counted every 24hours (n=4), (C) Percent survival of wild type and *daf-2(e1370)* mutant animals subjected to *ntl-2* knockdown 24hours post paraquat (10mM) administration (n=4), p values, test…. Error bars denote s.e.m., (D) Percent survival of wild type, DCAP-2 and NTL-2 depleted animals counted every 24hours post CCCP (15µM) treatment (n=4). Error bars denote s.e.m.

Next, we examined whether changes in storage and degradation body components affect *C. elegans* lifespan. We found that perturbation of storage bodies, by *ntl-2* genetic inhibition dramatically reduces the lifespan of wild-type animals. By contrast, *ntl-2* overexpression significantly extends lifespan (**Figure 23A & Table 1**). On the other hand, downregulation of specific degradation body components promotes longevity in contrast to their overexpression, as previously shown (Rieckher et al., 2018). It is interesting though that *ntl-2* is also essential for the longevity of long-lived mutants such as *daf-2*, *age-1* and *akt-1* (**Figure 23B, 23C, 23D & Table 1**). Our data indicate that storage body integrity is required both for wild type animal-lifespan and the longevity conferred by the insulin/IGF-1 signaling inhibition.

To investigate whether local translation in the mitochondrial vicinity interfaces mechanistically with *ntl-2* to co-regulate lifespan, we tested the effect of *akap-1* knockdown in control, *ntl-2* overexpressing and *ntl-2* downregulated animals (**Figure 23E, 23F& Table 1**). Interestingly, even though genetic inhibition of *akap-1* extended lifespan in wild type animals, it did not cause further extension in the long-lived *ntl-2* overexpressing worms, implying that the two components function in the same genetic pathway (**Figure 23E & Table 1**). Furthermore, genetic inhibition of *akap-1* ameliorated the short lifespan of NTL-2 depleted animals (**Figure 23F & Table 1**). These findings support our hypothesis that NTL-2 regulates local translation of its target NEMMTs. More specifically, it becomes apparent that genetic inhibition of *ntl-2* shortens lifespan by increasing local translation rates or triggering aberrant local translation of target NEMMTs; this effect ameliorates upon *akap-1* knockdown.

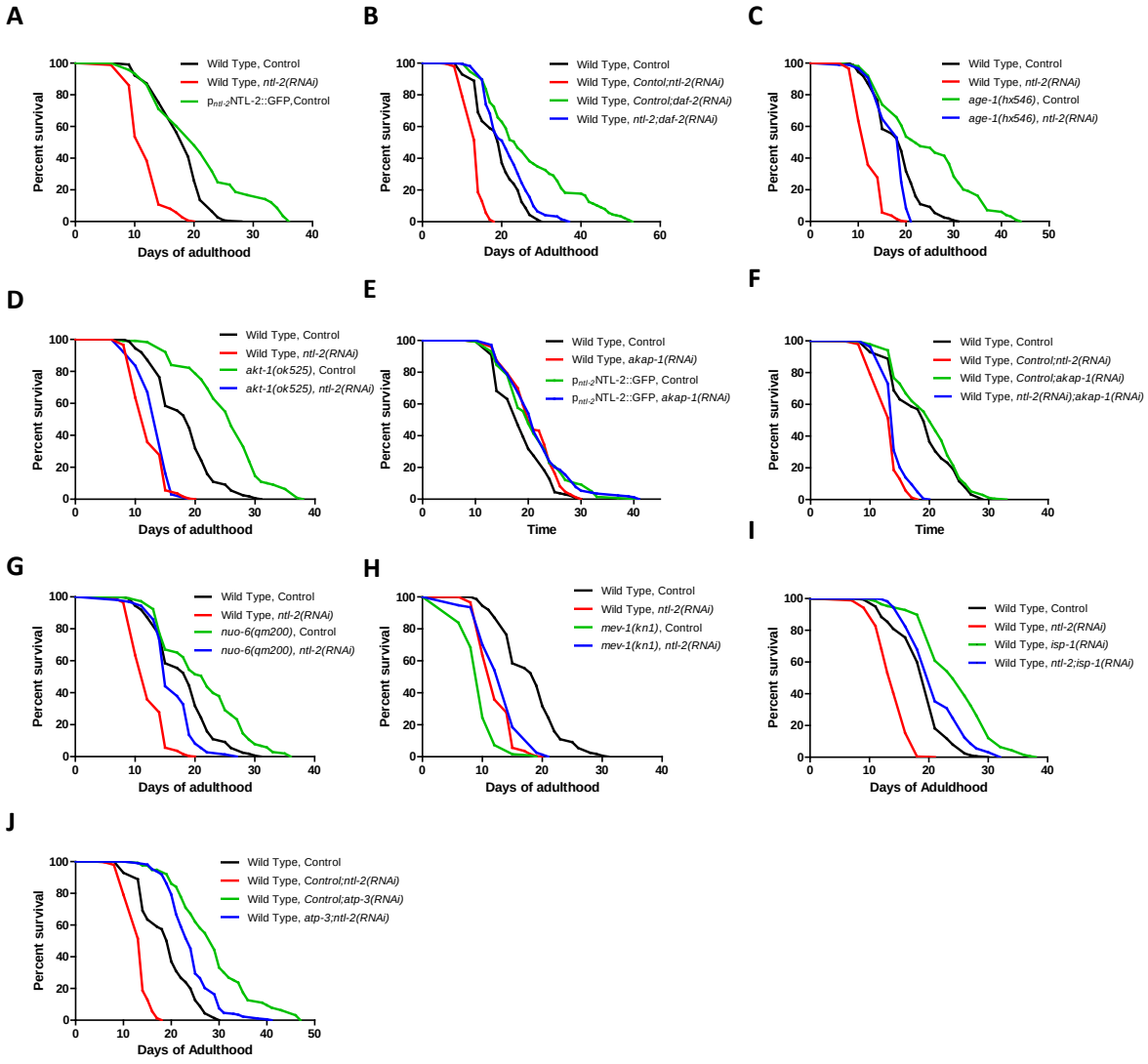

Figure 23. NTL-2 depletion has detrimental effects on *C. elegans* lifespan that are ameliorated upon mutation or downregulation of specific mitochondrial genes, while the overexpression of NTL-2 is beneficial for longevity. (A) Knockdown of *ntl-2* shortens the lifespan of wild type animals in contrast to NTL-2 overexpression, (B) Knockdown of ntl-2 shortens the lifespan of *daf-2(RNAi)* treated long-lived animals, (C) Knockdown of *ntl-2* shortens the lifespan of *age-1(hx546)* mutants, (D) Knockdown of *ntl-2* shortens the lifespan of *akt-1*(ok525) mutants, (E) Knockdown of *akap-1* extends the lifespan of wild type animals while it does not further extend the lifespan of NTL-2 overexpressing animals, (G) *nuo-6(qm200)* mutation alleviates the detrimental effects of *ntl-2* knockdown in longevity, (H) *mev-1(kn1)* mutation alleviates the detrimental effects of *ntl-2* knockdown in longevity, (I) Genetic inhibition of *isp-1* rescues the short lifespan on NTL-2-depleted animals, (J) Knockdown of *atp-3 rescues* the short lifespan on NTL-2-depleted animals.

The fact that downregulation of *akap-1* did not fully restore *ntl-2* toxicity prompted us to hypothesize that the *ntl-2*-mediated lifespan shortening is coupled with the aberrant translation of a specific or select NEMTTs but not of the whole spectrum of AKAP-1 targets (Zhang et al., 2016). Since genetic inhibition of *akap-1*, most possibly, concomitantly affects multiple NEMTTs, we tested the longevity of several NEMTT mutant strains upon NTL-2 depletion. Surprisingly, we found that both *nuo-6* and *mev-1* mutations were beneficial for the lifespan of the *ntl-2*-genetically-silenced animals (**Figure 23G, 23H & Table 1**), while genetic inhibition of *isp-1* and *atp-3* reversed the short lifespan of NTL-2 depleted animals (**Figure 23I, 23J & Table 1**). Collectively, these data suggest a causative relationship between NTL-2-dependent regulation of local translation of specific NEMTTs and longevity/stress resistance in *C. elegans*.

Table 1. Analytical data of the lifespan experiments

Effect of *ntl-2* on longevity							
Strain	**Treatment**	**Mean (+/-) SEM in days**	**Max (+/-) SEM in days**	**Number of animals that died/total**	**P-value**		**Comparison of survival curves**
Wild Type (N2)	Control RNAi	19	28	292/368			
Wild Type (N2)	*ntl-2(RNAi)*	12	20	336/356	P<0.0001	***	vs Wild Type, Control RNAi
N2;*Ex*[p$_{ntl-2}$NTL-2::GFP]	Control RNAi	20	36	218/284	0.0009	***	vs Wild Type, Control RNAi
Wild Type (N2)	Control RNAi	19	31	171/221			
Wild Type (N2)	*ntl-2(RNAi)*	12	20	249/259	P<0.0001	***	vs Wild Type, Control RNAi
N2;*Ex*[p$_{ntl-2}$NTL-2::GFP]	Control RNAi	20	37	127/143	0.0041	**	vs Wild Type, Control RNAi

Wild Type (N2)	Control RNAi	16	26	89/113			
Wild Type (N2)	*ntl-2(RNAi)*	13	16	122/135	P<0.0001	***	vs Wild Type, Control RNAi
Wild Type (N2)	Control RNAi	16	29	177/223			
N2;*Ex*[p_{ntl-2}NTL-2::GFP]	Control RNAi	19	34	171/224	P<0.0001	***	vs Wild Type, Control RNAi
Wild Type (N2)	Control RNAi	18	30	150/179			
Wild Type (N2)	*ntl-2(RNAi)*	14	19	108/130	P<0.0001	***	vs Wild Type, Control RNAi
N2;*Ex*[p_{ntl-2}NTL-2::GFP]	Control RNAi	20	41	140/152	0.0013	**	vs Wild Type, Control RNAi
Wild Type (N2)	Control RNAi	19	29	191/257			
Wild Type (N2)	*ntl-2(RNAi)*	13	18	152/177	P<0.0001	***	vs Wild Type, Control RNAi
Wild Type (N2)	Control RNAi	19	30	191/268			
Wild Type (N2)	*ntl-2(RNAi)*	13	18	152/209	P<0.0001	***	vs Wild Type, Control RNAi

Effect of *akap-1* genetic inhibition on longevity of NTL-2-depleted or -overexpressing animals							
Strain	**Treatment**	**Mean (+/-) SEM in days**	**Max (+/-) SEM in days**	**Number of animals that died/total**	**P-value**		**Comparison**
Wild Type (N2)	Control RNAi	19	31	171/221			
Wild Type (N2)	*akap-1(RNAi)*	21	33	112/126	P<0.0001	***	vs Wild Type, Control RNAi
N2;*Ex*[p_{ntl-2}NTL-2::GFP]	Control RNAi	20	37	127/143	0.0041	**	vs Wild Type, Control RNAi
N2;*Ex*[p_{ntl-2}NTL-2::GFP]	*akap-1(RNAi)*	20	35	130/150	0.1254	ns	vs N2;Ex[pntl-2NTL-2::GFP;unc-119+], Control RNAi
Wild Type (N2)	Control RNAi	20	25	96/209			

Wild Type (N2)	*akap-1(RNAi)*	23	36	180/258	P<0.0001	***	vs Wild Type, Control RNAi
N2;*Ex*[p_{ntl-2}NTL-2::GFP]	Control RNAi	22	28	33/75	P<0.0001	***	vs Wild Type, Control RNAi
N2;*Ex*[p_{ntl-2}NTL-2::GFP]	*akap-1(RNAi)*	21	29	175/203	0.2517	ns	vs N2;Ex[pntl-2NTL-2::GFP;unc-119+], Control RNAi
Wild Type (N2)	Control RNAi	18	30	150/179			
Wild Type (N2)	*akap-1(RNAi)*	20	30	172/183	0.0001	***	vs Wild Type, Control RNAi
N2;*Ex*[p_{ntl-2}NTL-2::GFP]	Control RNAi	20	41	141/153	P<0.0001	***	vs Wild Type, Control RNAi
N2;*Ex*[p_{ntl-2}NTL-2::GFP]	*akap-1(RNAi)*	21	41	171/184	0.6289	ns	vs N2;Ex[pntl-2NTL-2::GFP;unc-119+], Control RNAi
Wild Type (N2)	Control RNAi	19	29	191/257			
Wild Type (N2)	Control;*ntl-2(RNAi)*	14	18	232/257	P<0.0001	***	vs Wild Type, Control RNAi
Wild Type (N2)	Control;*akap-1(RNAi)*	20	33	198/250	0.0427	*	vs Wild Type, Control RNAi
Wild Type (N2)	*ntl-2;akap-1(RNAi)*	14	20	188/221	P<0.0001	***	vs Wild Type, *Control;akap-1(RNAi)*
Wild Type (N2)	Control RNAi	19	30	191/268			
Wild Type (N2)	Control;*ntl-2(RNAi)*	14	18	232/258	P<0.0001	***	vs Wild Type, Control RNAi
Wild Type (N2)	Control;*akap-1(RNAi)*	20	33	197/248	P<0.0001	***	vs Wild Type, Control RNAi
Wild Type (N2)	*ntl-2;akap-1(RNAi)*	14	20	187/216	P<0.0001	***	vs Wild Type, *Control;akap-1(RNAi)*
Effect of *isp-1* genetic inhibition on lifespan NTL-2-depleted animals							
Strain	**Treatment**	**Mean (+/-) SEM in days**	**Max (+/-) SEM in days**	**Number of animals that died/total**	**P-value**		**Comparison**
Wild Type	Control	21	30	188/345			

(N2)	RNAi						
Wild Type (N2)	Control;*ntl-2(RNAi)*	14	21	239/270	P<0.0001	***	vs Wild Type, Control RNAi
Wild Type (N2)	Control; *isp-1(RNAi)*	24	38	192/277	P<0.0001	***	vs Wild Type, Control RNAi
Wild Type (N2)	*ntl-2(RNAi); isp-1(RNAi)*	21	32	196/299	P<0.0001	***	vs Wild Type, *Control; ntl-2(RNAi)*
Wild Type (N2)	*ntl-2(RNAi); isp-1(RNAi)*	21	32	196/299	P<0.0001	***	vs Wild Type, *Control; isp-1(RNAi)*
Wild Type (N2)	Control RNAi	19	27	154/313			
Wild Type (N2)	Control;*ntl-2(RNAi)*	12	19	236/332	P<0.0001	***	vs Wild Type, Control RNAi
Wild Type (N2)	Control; *isp-1(RNAi)*	22	34	322/407	P<0.0001	***	vs Wild Type, Control RNAi
Wild Type (N2)	*ntl-2(RNAi); isp-1(RNAi)*	17	28	229/339	P<0.0001	***	vs Wild Type, *Control; ntl-2(RNAi)*
Wild Type (N2)	*ntl-2(RNAi); isp-1(RNAi)*	17	28	229/339	P<0.0001	***	vs Wild Type, *Control; isp-1(RNAi)*
Wild Type (N2)	Control RNAi	19	29	46/138			
Wild Type (N2)	Control;*ntl-2(RNAi)*	13	17	85/121	P<0.0001	***	vs Wild Type, Control RNAi
Wild Type (N2)	Control; *isp-1(RNAi)*	27	44	106/148	P<0.0001	***	vs Wild Type, Control RNAi
Wild Type (N2)	*ntl-2(RNAi); isp-1(RNAi)*	21	30	74/110	P<0.0001	***	vs Wild Type, *Control; ntl-2(RNAi)*
Wild Type (N2)	*ntl-2(RNAi); isp-1(RNAi)*	21	30	74/110	P<0.0001	***	vs Wild Type, *Control; isp-1(RNAi)*
Effect of *atp-3* genetic inhibition on lifespan of NTL-2-depleted animals							
Strain	**Treatment**	**Mean (+/-)**	**Max (+/-)**	**Number of**	**P-value**		**Comparison**

		SEM in days	SEM in days	animals that died/total			
Wild Type (N2)	Control RNAi	19	30	191/268			
Wild Type (N2)	Control;*ntl-2(RNAi)*	14	18	232/258	P<0.0001	***	vs Wild Type, Control RNAi
Wild Type (N2)	Control;*atp-3(RNAi)*	29	47	76/161	P<0.0001	***	vs Wild Type, Control RNAi
Wild Type (N2)	*atp-3;ntl-2(RNAi)*	24	41	196/247	P<0.0001	***	vs Wild Type, *atp-3(RNAi)*
Wild Type (N2)	Control RNAi	17	30	119/157			
Wild Type (N2)	Control;*ntl-2(RNAi)*	12	20	121/145	P<0.0001	***	vs Wild Type, Control RNAi
Wild Type (N2)	Control;*atp-3(RNAi)*	28	45	129/166	P<0.0001	***	vs Wild Type, Control RNAi
Wild Type (N2)	*atp-3;ntl-2(RNAi)*	22	43	174/193	0.0002	***	vs Wild Type, *atp-3(RNAi)*
Effect of *ntl-2* genetic inhibition on lifespan of DAF-2-depleted animals							
Strain	**Treatment**	**Mean (+/-) SEM in days**	**Max (+/-) SEM in days**	**Number of animals that died/total**	**P-value**		**Comparison**
Wild Type (N2)	Control RNAi	19	30	191/268			
Wild Type (N2)	Control;*ntl-2(RNAi)*	14	18	232/258	P<0.0001	***	vs Wild Type, Control RNAi
Wild Type (N2)	Control;*daf-2(RNAi)*	24	53	182/232	P<0.0001	***	vs Wild Type, Control RNAi
Wild Type (N2)	*ntl-2;daf-2(RNAi)*	21	37	159/250	P<0.0001	***	vs Wild Type, *(daf-2)RNAi*
Wild Type (N2)	Control RNAi	17	29	122/144			
Wild Type (N2)	Control;*ntl-2(RNAi)*	13	20	95/122	P<0.0001	***	vs Wild Type, Control RNAi
Wild Type (N2)	Control;*daf-2(RNAi)*	23	52	182/208	P<0.0001	***	vs Wild Type, Control RNAi
Wild Type (N2)	*ntl-2;daf-2(RNAi)*	20	35	115/137	P<0.0001	***	vs Wild Type, *(daf-2)RNAi*
Effect of *ntl-2* genetic inhibition on lifespan of AGE-1-depleted animals							
Strain	**Treatmen**	**Mean**	**Max**	**Number**	**P-value**		**Comparison**

	t	(+/-) SEM in days	(+/-) SEM in days	of animals that died/total		
Wild Type (N2)	Control RNAi	19	31	171/221		
Wild Type (N2)	*ntl-2(RNAi)*	12	20	249/259	P<0.0001	***	vs Wild Type, Control RNAi
age-1(hx546)	Control RNAi	22	44	99/104	P<0.0001	***	vs Wild Type, Control RNAi
age-1(hx546)	*ntl-2(RNAi)*	19	21	85/96	P<0.0001	***	vs *age-1(hx546),* Control RNAi
Wild Type (N2)	Control RNAi	18	30	131/146		
Wild Type (N2)	*ntl-2(RNAi)*	12	20	89/96	P<0.0001	***	vs Wild Type, Control RNAi
age-1(hx546)	Control RNAi	22	44	178/198	P<0.0001	***	vs Wild Type, Control RNAi
age-1(hx546)	*ntl-2(RNAi)*	18	21	59/73	P<0.0001	***	vs *age-1(hx546),* Control RNAi
Effect of *ntl-2* genetic inhibition on lifespan of AKT-1-depleted animals							
Strain	**Treatment**	**Mean (+/-) SEM in days**	**Max (+/-) SEM in days**	**Number of animals that died/total**	**P-value**		**Comparison**
Wild Type (N2)	Control RNAi	19	31	171/221		
Wild Type (N2)	*ntl-2(RNAi)*	12	20	249/259	P<0.0001	***	vs Wild Type, Control RNAi
akt-1(ok525)	Control RNAi	26	38	110/121	P<0.0001	***	vs Wild Type, Control RNAi
akt-1(ok525)	*ntl-2(RNAi)*	15	19	101/129	P<0.0001	***	vs *akt-1(ok525),* Control RNAi
Wild Type (N2)	Control RNAi	18	29	199/227		
Wild Type (N2)	*ntl-2(RNAi)*	12	20	134/140	P<0.0001	***	vs Wild Type, Control RNAi
akt-1(ok525)	Control RNAi	25	37	159/205	P<0.0001	***	vs Wild Type, Control RNAi
akt-1(ok525)	*ntl-2(RNAi)*	15	20	132/155	P<0.0001	***	vs *akt-1(ok525),* Control RNAi
Effect of *ntl-2* genetic inhibition on lifespan of NUO-6-depleted animals							

Strain	Treatment	Mean (+/-) SEM in days	Max (+/-) SEM in days	Number of animals that died/total	P-value		Comparison
Wild Type (N2)	Control RNAi	19	31	171/221			
Wild Type (N2)	*ntl-2(RNAi)*	12	20	249/159	P<0.0001	***	vs Wild Type, Control RNAi
nuo-6(qm200)	Control RNAi	22	36	103/129	P<0.0001	***	vs Wild Type, Control RNAi
nuo-6(qm200)	*ntl-2(RNAi)*	12	27	121/143	P<0.0001	***	vs *nuo-6(qm200),* Control RNAi
Wild Type (N2)	Control RNAi	18	29	140/166			
Wild Type (N2)	*ntl-2(RNAi)*	13	20	87/102	P<0.0001	***	vs Wild Type, Control RNAi
nuo-6(qm200)	Control RNAi	23	37	176/198	P<0.0001	***	vs Wild Type, Control RNAi
nuo-6(qm200)	*ntl-2(RNAi)*	13	23	93/108	P<0.0001	***	vs *nuo-6(qm200),* Control RNAi
Effect of *ntl-2* genetic inhibition on lifespan of MEV-1-depleted animals							
Strain	**Treatment**	**Mean (+/-) SEM in days**	**Max (+/-) SEM in days**	**Number of animals that died/total**	**P-value**		**Comparison**
Wild Type (N2)	Control RNAi	19	28	292/368			
Wild Type (N2)	*ntl-2(RNAi)*	12	20	336/356	P<0.0001	***	vs Wild Type, Control RNAi
mev-1(kn1)	Control RNAi	7	19	106/170	P<0.0001	***	vs Wild Type, Control RNAi
mev-1(kn1)	*ntl-2(RNAi)*	10	18	102/148	0.0002	***	vs *mev-1(kn1),* Control RNAi
Wild Type (N2)	Control RNAi	19	31	171/221			
Wild Type (N2)	*ntl-2(RNAi)*	12	20	249/259	P<0.0001	***	vs Wild Type, Control RNAi
mev-1(kn1)	Control RNAi	10	19	130/155	P<0.0001	***	vs Wild Type, Control RNAi
mev-1(kn1)	*ntl-2(RNAi)*	15	21	78/115	P<0.0001	***	vs *mev-1(kn1),* Control RNAi

Wild Type (N2)	Control RNAi	16	26	89/113			
Wild Type (N2)	*ntl-2(RNAi)*	13	16	122/135	P<0.0001	***	vs Wild Type, Control RNAi
mev-1(kn1)	Control RNAi	10	16	60/60	P<0.0001	***	vs Wild Type, Control RNAi
mev-1(kn1)	*ntl-2(RNAi)*	13	20	59/59	0.0194	*	vs *mev-1(kn1),* Control RNAi

CHAPTER 4
DISCUSSION

In the present study, we establish that components of the CCR-4/NOT and the decapping complex play distinct roles in mitochondrial abundance, mitochondrial function, lifespan and stress resistance in *C. elegans*. We demonstrated that NTL-2, a CCR-4/NOT complex component, and DCAP-2, a decapping-complex component, consistently to their diverse effect on mitochondrial abundance, oppositely regulate mitochondrial biogenesis. Notably, we unveiled a variety of mechanistic underpinnings describing this event. First, the two factors oppositely influence the abundance of the two master regulators of mitochondrial biogenesis in *C. elegans*, AAK-2 and SKN-1 acting post-transcriptionally. Particularly for SKN-1, we also noticed that its activity is oppositely affected by NTL-2 and DCAP-2 even in mutant backgrounds where SKN-1 is induced. On the other hand, the two components similarly affect mitophagy despite the opposite outcomes on mitochondrial abundance. The inconsistency of the effect of these components on mitophagy stands as evidence of uncoupling of mitophagy from our model, though still, we cannot exclude that it contributes, at least to some extent, on the observed phenotypes.

The semi-autonomous nature of mitochondria renders their biogenesis a quite complex and multi-step process. Following transcription in the nucleus, NEMTTs are possibly transported and translated locally in the mitochondrial vicinity, although in-depth mechanistic insight is still missing. Appreciating the characterized role of the CCR-4/NOT and the decapping complex components in mRNA metabolism, we examined whether they regulate post-transcriptional events in the vicinity of mitochondria apart from their role in SKN-1 and AAK-2 regulation. Notably, we show for the first time *in vivo* that storage bodies enclose NEMTTs by performing RNA immunoprecipitation analysis of the NTL-2:: GFP-bound material and performing real-time PCR for target NEMTTs. In line with our findings, it was lately shown, in yeast, that upon glucose deprivation a different

P-body component can bind on mitochondrial transcripts (Wang et al., 2018a) and, in C. elegans, CAR-1 can bind a specific mitochondrial transcript implicated in modulation of calcium homeostasis in neurons (Tang et al., 2020) highlighting a potential conservation of our model. Our analysis unveiled that storage bodies bind NEMTTs that encode ETC subunits, regulators of the mitochondrial genome and the *skn-1* transcript itself. By contrast, an mRNA encoding a core ER component is not bound, indicative of storage body target specificity. This result suggests that post-transcriptional control of NEMTTs exists. Having observed that the CCR-4/NOT and the decapping complexes oppositely affect the mitochondrial abundance, intervening with the organelle biogenesis mechanisms, we believe that, they oppositely regulate the fate of NEMTTs among other mitochondrial-biogenesis related genes, post-transcriptionally.

Notably, we observed for the first time *in vivo* that the CCR-4/NOT complex and the decapping complex are parts of distinct foci. This finding challenges the prevailing view that both complexes are parts of a single type of foci, the P-body (Behm-Ansmant et al., 2006; Ozgur et al., 2010). Our data are in line with recent crystallographic *in vitro* evidence and *in vivo* proximity-dependent biotinylation (BioID) analyses in human cells (Ozgur et al., 2015; Youn et al., 2018). Moreover, we found that the abundance of storage and degradation bodies is oppositely regulated during ageing. Also, we found that they form antagonistically of each other. Indeed, decapping impairment triggered an elevation of storage body abundance, which correlates with a drop in global translation rates measured in somatic tissues with FRAP. On the contrary, our data show that impairment of the CCR-4/NOT complex by NTL-2 genetic inhibition results in increased abundance of degradation bodies and rise of global translation levels.

Our findings comply with results obtained from human cancer and embryonic kidney cells lines. These *in vitro* data show that CNOT2 depletion blocks deadenylation and enhances

translation rates and toxicity (Ito et al., 2011). While their antagonistic formation suggests that degradation body components would oppositely regulate the storage-body enclosed transcripts indirectly, evidence regarding a direct binding of NEMTTs by the decapping enzymes was not tested in the current study. We believe that the associations of NEMTTs with mRNA degradation components, even if they exist, they are much more dynamic to monitor, than the ones formed with storage bodies components under wild type conditions. More delicate and up-to-date techniques, applicable to *C. elegans* could elucidate the bound mRNAs on decapping components soon.

Collectively, our results support that storage- and degradation-body components post-transcriptionally control the expression of their target NEMTTs affecting the organelle biogenesis. First, we succinctly studied the localization of the two types of bodies. Furthermore, we show that decapping and storage body components form physical associations with mitochondria which are either protein- or post-transcriptional modification-dependent but RNA-independent. Also, the fact that they do affect global translation rates but to a moderate extent compared to the effect caused by the well-characterized global translation regulators *let-363*/TOR and the pharmacological inhibitor of translation cycloheximide, point towards the direction that they control the translation efficacy of only a subset of transcripts and not all transcripts. To further validate that they play a role in local translation events in the vicinity of mitochondria, we focused on storage body localization when perturbing conserved mitochondrial proteins, well-characterized positive regulators of local translation. We demonstrated that perturbation of either *akap-1* or *tomm-20* significantly alters the localization and abundance of storage bodies *in vivo*. In fact, storage bodies fail to specifically localize next to mitochondria as observed under physiological conditions, change also verified by western blotting. This

reveals that the specific localization of storage bodies next to mitochondria is local-translation-dependent.

In line with their opposite effect on mitochondrial biogenesis, our data show that, in contrast to degradation bodies, storage body formation is beneficial both for lifespan and stress resistance. During ageing and in response to various stress insults, mitochondria adapt their metabolism by adjusting their number and function to achieve allostasis (Picard et al., 2018). Accumulating evidence suggests that a quick and effective response upon stress requires rapid translation of target transcripts, as has been shown in neuronal axons during neuronal plasticity (Besse and Ephrussi, 2008; Rangaraju et al., 2019; Sutton and Schuman, 2006). Consistent with this notion, NTL-2 overexpressing animals are long-lived while NTL-2-depleted animals, which have lost the capacity to store NEMTTs, are hypersensitive to mitochondrial stressors. Also, mitochondrial dysfunction leads to storage body disorganization as mRNAs are most probably released upon stress to be translated, rendering storage bodies dispensable.

Additionally, we have observed that DCAP-2 deficiency lowers global translation rates. In this case, the reduction in global translation rates correlates with increased resistance to stress. Previous studies have shown that reduced global protein synthesis increases lifespan and stress resistance in diverse model organisms, including *C. elegans* (Hansen et al., 2007; Syntichaki et al., 2007). Enhanced longevity and adaptation to stress may be due to the increased translation rates of a specific subset of transcripts despite an overall drop in global translation rates, yet the mechanism by which this occurs is not known (Ding et al., 2011). In our case, *dcap-2* genetic inhibition leads to elevated AAK-2 and SKN-1 protein levels and reduced global translation rates in contrast to *ntl-2* knockdown. Together, these data support the notion that storage and degradation bodies could engage in this mechanism.

While the toxic effects of NTL-2-depletion on lifespan were ameliorated by blocking the general regulator of local translation in the vicinity of mitochondria, *akap-1*, genetic inhibition of specific NEMTTs could completely reverse this adverse effect. Nevertheless, we cannot exclude the possibility that the reason why we could not observe a complete rescue in the lifespan of NTL-2-depleted animals upon genetic inhibition of *akap-1* is due to AKAP-1 complementation by TOMM-20 (Eliyahu et al., 2010). Interestingly, combined genetic inhibition of *ntl-2* and either *isp-1* or *atp-3* made animals even more long-lived than wild type animals. The fact that single NEMTT inhibition could reverse the short lifespan of *ntl-2* mutants in contrast to *akap-1* genetic inhibition, which is expected to affect in-parallel several NEMTTs, reveals that aberrant translation of a specific subset of NEMTTs is responsible for *ntl-2* toxicity. Our data suggest that this subset of NEMTTs is overexpressed, and thus alters the organelles' physiology. If there is an over-production of ETC components triggered by *ntl-2* genetic inhibition, this could explain why under this condition mitochondria are less in number, yet hyperactive. It has been previously shown that the fate of mRNAs inside P-bodies is dynamically regulated depending on several factors and that even adjacent molecules can be oppositely regulated. (Eliyahu et al., 2010)

It is the first time that components of the decapping and the CCR-4/NOT complex are implicated in the regulation of mitochondrial function and abundance in response to anterograde and retrograde signaling during ageing. Our findings highlight the significance of accuracy in local translation events and indicate that alteration even of a single factor implicated in the control of NEMTT expression can alter mitochondrial content and function in a manner influencing lifespan and stress resistance.
Of note, impaired mitochondrial biogenesis triggers severe human pathologies and syndromes, such as Huntington's disease (HD) (Rona-Voros and Weydt, 2010;

Taherzadeh-Fard et al., 2011; Weydt et al., 2009), cardiomyopathy and heart failure (Arany et al., 2005; Dorn et al., 2015; Sun et al., 2007), acute kidney injury (AKI) and folic acid nephropathy (Funk and Schnellmann, 2012; Stallons et al., 2014), Alzheimer's disease (AD) (Cabezas-Opazo et al., 2015; Onyango, 2018), multiple sclerosis, depression and Parkinson's disease (Hayashi et al., 2017; Hesham A El-Beshbishy, 2019; Van Laar et al., 2018; Youdim and Oh, 2013; Zheng et al., 2010) and also obesity and type 2 diabetes among others (Baur et al., 2006; Benton et al., 2008; Guarente, 2006; Liang et al., 2009; Nisoli et al., 2007; Zhang et al., 2009). A better understanding of the mitochondrial biogenesis-associated diseases would encourage the identification of compounds or possible molecular targets that would reverse disease-associated phenotypes. Nowadays, comprehensive elucidation of the molecular partners that regulate mitochondrial biogenesis is imperative since many diseases have been associated with mitochondrial biogenesis defects, while efficient therapy is still missing. Intervening with mitochondrial biogenesis regulatory mechanisms is expected to offer significant advantages to combat diseases such as the ones mentioned above. Due to their novel role in mitochondrial biogenesis and their high evolutionary conservation, storage and degradation body components might serve as molecular targets for therapeutic interventions against such pathologies the etiology of which is currently unexplored (Faraji et al., 2016; Maziuk et al., 2017; Vicente et al., 2018; Yoshimi and Abdel-Wahab, 2018).

Akcnowledgements

I thank Aggela Pasparaki for valuable support with confocal microscopy and Konstantinos Palikaras for providing us the *daf-2(e1370)*;*Is*[p_{gst-4}GFP] and the *unc-119(ed3)*;*Ex*[$_{punc-119}$mtRosella;unc-119(+)] strain. Some nematode strains used in this work were provided by the Caenorhabditis Genetics Center, which is funded by NIH Office of Research Infrastructure Programs (P40 OD010440). This work was supported by the European Research Council (GA695190- MANNA), the General Secretariat for Research and Technology of the Greek Ministry of Education (THALIS MIS380228 GEnAge) and by the project “BIOIMAGING-GR” (MIS5002755), which is implemented under the Action “Reinforcement of the Research and Innovation Infrastructure”, funded by the Operational Programme “Competitiveness, Entrepreneurship and Innovation” (NSRF 2014-2020).

CHAPTER 5
REFERENCES

Aboobaker, A.A., and Blaxter, M.L. (2000). Medical significance of Caenorhabditis elegans. Annals of medicine *32*, 23-30.
Aizer, A., Brody, Y., Ler, L.W., Sonenberg, N., Singer, R.H., and Shav-Tal, Y. (2008). The dynamics of mammalian P body transport, assembly, and disassembly in vivo. Molecular biology of the cell *19*, 4154-4166.
Aizer, A., Kalo, A., Kafri, P., Shraga, A., Ben-Yishay, R., Jacob, A., Kinor, N., and Shav-Tal, Y. (2014). Quantifying mRNA targeting to P-bodies in living human cells reveals their dual role in mRNA decay and storage. Journal of cell science *127*, 4443-4456.
Alaynick, W.A. (2008). Nuclear receptors, mitochondria and lipid metabolism. Mitochondrion *8*, 329-337.
Antico Arciuch, V.G., Elguero, M.E., Poderoso, J.J., and Carreras, M.C. (2012). Mitochondrial regulation of cell cycle and proliferation. Antioxidants & redox signaling *16*, 1150-1180.
Arany, Z., He, H., Lin, J., Hoyer, K., Handschin, C., Toka, O., Ahmad, F., Matsui, T., Chin, S., Wu, P.H.*, et al.* (2005). Transcriptional coactivator PGC-1 alpha controls the energy state and contractile function of cardiac muscle. Cell metabolism *1*, 259-271.
Baldelli, S., Aquilano, K., and Ciriolo, M.R. (2013). Punctum on two different transcription factors regulated by PGC-1alpha: nuclear factor erythroid-derived 2-like 2 and nuclear respiratory factor 2. Biochimica et biophysica acta *1830*, 4137-4146.
Barrey, E., Saint-Auret, G., Bonnamy, B., Damas, D., Boyer, O., and Gidrol, X. (2011). Pre-microRNA and mature microRNA in human mitochondria. PloS one *6*, e20220.
Bashkirov, V.I., Scherthan, H., Solinger, J.A., Buerstedde, J.M., and Heyer, W.D. (1997). A mouse cytoplasmic exoribonuclease (mXRN1p) with preference for G4 tetraplex substrates. The Journal of cell biology *136*, 761-773.
Baur, J.A., Pearson, K.J., Price, N.L., Jamieson, H.A., Lerin, C., Kalra, A., Prabhu, V.V., Allard, J.S., Lopez-Lluch, G., Lewis, K.*, et al.* (2006). Resveratrol improves health and survival of mice on a high-calorie diet. Nature *444*, 337-342.
Behm-Ansmant, I., Rehwinkel, J., Doerks, T., Stark, A., Bork, P., and Izaurralde, E. (2006). mRNA degradation by miRNAs and GW182 requires both CCR4:NOT deadenylase and DCP1:DCP2 decapping complexes. Genes & development *20*, 1885-1898.
Benton, C.R., Wright, D.C., and Bonen, A. (2008). PGC-1alpha-mediated regulation of gene expression and metabolism: implications for nutrition and exercise prescriptions. Applied physiology, nutrition, and metabolism = Physiologie appliquee, nutrition et metabolisme *33*, 843-862.
Besse, F., and Ephrussi, A. (2008). Translational control of localized mRNAs: restricting protein synthesis in space and time. Nature reviews Molecular cell biology *9*, 971-980.
Bian, Z., Li, L.M., Tang, R., Hou, D.X., Chen, X., Zhang, C.Y., and Zen, K. (2010). Identification of mouse liver mitochondria-associated miRNAs and their potential biological functions. Cell research *20*, 1076-1078.
Bishop, D.J., Botella, J., Genders, A.J., Lee, M.J., Saner, N.J., Kuang, J., Yan, X., and Granata, C. (2019). High-Intensity Exercise and Mitochondrial Biogenesis: Current Controversies and Future Research Directions. Physiology *34*, 56-70.
Borbolis, F., and Syntichaki, P. (2015). Cytoplasmic mRNA turnover and ageing. Mechanisms of ageing and development *152*, 32-42.
Bouchez, C., and Devin, A. (2019). Mitochondrial Biogenesis and Mitochondrial Reactive Oxygen Species (ROS): A Complex Relationship Regulated by the cAMP/PKA Signaling Pathway. Cells *8*.
Brenner, S. (1974). The genetics of Caenorhabditis elegans. Genetics *77*, 71-94.

Byerly, L., Cassada, R.C., and Russell, R.L. (1976). The life cycle of the nematode Caenorhabditis elegans. I. Wild-type growth and reproduction. Developmental biology *51*, 23-33.
Cabezas-Opazo, F.A., Vergara-Pulgar, K., Perez, M.J., Jara, C., Osorio-Fuentealba, C., and Quintanilla, R.A. (2015). Mitochondrial Dysfunction Contributes to the Pathogenesis of Alzheimer's Disease. Oxidative medicine and cellular longevity *2015*, 509654.
Cassada, R.C., and Russell, R.L. (1975). The dauerlarva, a post-embryonic developmental variant of the nematode Caenorhabditis elegans. Developmental biology *46*, 326-342.
Castello, P.R., Drechsel, D.A., and Patel, M. (2007). Mitochondria are a major source of paraquat-induced reactive oxygen species production in the brain. The Journal of biological chemistry *282*, 14186-14193.
Chacinska, A., Koehler, C.M., Milenkovic, D., Lithgow, T., and Pfanner, N. (2009). Importing mitochondrial proteins: machineries and mechanisms. Cell *138*, 628-644.
Chen, D., Pan, K.Z., Palter, J.E., and Kapahi, P. (2007). Longevity determined by developmental arrest genes in Caenorhabditis elegans. Aging cell *6*, 525-533.
Clemens, M.J. (2001). Translational regulation in cell stress and apoptosis. Roles of the eIF4E binding proteins. Journal of cellular and molecular medicine *5*, 221-239.
Collins, J.J., Huang, C., Hughes, S., and Kornfeld, K. (2008). The measurement and analysis of age-related changes in Caenorhabditis elegans. WormBook : the online review of C elegans biology, 1-21.
Consortium, C.e.S. (1998). Genome sequence of the nematode C. elegans: a platform for investigating biology. Science *282*, 2012-2018.
Corsi, A.K., Wightman, B., and Chalfie, M. (2015). A Transparent Window into Biology: A Primer on Caenorhabditis elegans. Genetics *200*, 387-407.
Coulson, A., Kozono, Y., Lutterbach, B., Shownkeen, R., Sulston, J., and Waterston, R. (1991). YACs and the C. elegans genome. BioEssays : news and reviews in molecular, cellular and developmental biology *13*, 413-417.
Couvillion, M.T., Soto, I.C., Shipkovenska, G., and Churchman, L.S. (2016). Synchronized mitochondrial and cytosolic translation programs. Nature *533*, 499-503.
Curran, S.P., and Ruvkun, G. (2007). Lifespan regulation by evolutionarily conserved genes essential for viability. PLoS genetics *3*, e56.
Daskalaki, I., Markaki, M., and Tavernarakis, N. (2020). Aging in the Nematode Caenorhabditis elegans. In Encyclopedia of Biomedical Gerontology, S.I.S. Rattan, ed. (Oxford: Academic Press), pp. 88-103.
Decker, C.J., and Parker, R. (2012). P-bodies and stress granules: possible roles in the control of translation and mRNA degradation. Cold Spring Harbor perspectives in biology *4*, a012286.
Dickinson, D.J., and Goldstein, B. (2016). CRISPR-Based Methods for Caenorhabditis elegans Genome Engineering. Genetics *202*, 885-901.
Ding, W.-X., Li, M., and Yin, X.-M. (2011). Selective taste of ethanol-induced autophagy for mitochondria and lipid droplets. Autophagy *7*, 248-249.
Dorn, G.W., 2nd, Vega, R.B., and Kelly, D.P. (2015). Mitochondrial biogenesis and dynamics in the developing and diseased heart. Genes & development *29*, 1981-1991.
Duchen, M.R. (2000). Mitochondria and calcium: from cell signalling to cell death. The Journal of physiology *529 Pt 1*, 57-68.
Egea, G., Izquierdo, J.M., Ricart, J., San Martin, C., and Cuezva, J.M. (1997). mRNA encoding the beta-subunit of the mitochondrial F1-ATPase complex is a localized mRNA in rat hepatocytes. The Biochemical journal *322 (Pt 2)*, 557-565.

Eliyahu, E., Pnueli, L., Melamed, D., Scherrer, T., Gerber, A.P., Pines, O., Rapaport, D., and Arava, Y. (2010). Tom20 mediates localization of mRNAs to mitochondria in a translation-dependent manner. Molecular and cellular biology *30*, 284-294.
Eulalio, A., Behm-Ansmant, I., and Izaurralde, E. (2007a). P bodies: at the crossroads of post-transcriptional pathways. Nature reviews Molecular cell biology *8*, 9-22.
Eulalio, A., Behm-Ansmant, I., Schweizer, D., and Izaurralde, E. (2007b). P-body formation is a consequence, not the cause, of RNA-mediated gene silencing. Molecular and cellular biology *27*, 3970-3981.
Faraji, F., Hu, Y., Yang, H.H., Lee, M.P., Winkler, G.S., Hafner, M., and Hunter, K.W. (2016). Post-transcriptional Control of Tumor Cell Autonomous Metastatic Potential by CCR4-NOT Deadenylase CNOT7. PLoS genetics *12*, e1005820.
Filion, A.M., and Laughrea, M. (1985). Translation fidelity in the aging mammal: studies with an accurate in vitro system on aged rats. Mechanisms of ageing and development *29*, 125-142.
Frezal, L., and Felix, M.A. (2015). C. elegans outside the Petri dish. eLife *4*.
Fujiki, M., and Verner, K. (1991). Coupling of protein synthesis and mitochondrial import in a homologous yeast in vitro system. The Journal of biological chemistry *266*, 6841-6847.
Fujiki, M., and Verner, K. (1993). Coupling of cytosolic protein synthesis and mitochondrial protein import in yeast. Evidence for cotranslational import in vivo. The Journal of biological chemistry *268*, 1914-1920.
Funk, J.A., and Schnellmann, R.G. (2012). Persistent disruption of mitochondrial homeostasis after acute kidney injury. American journal of physiology Renal physiology *302*, F853-864.
Galgano, A., Forrer, M., Jaskiewicz, L., Kanitz, A., Zavolan, M., and Gerber, A.P. (2008). Comparative analysis of mRNA targets for human PUF-family proteins suggests extensive interaction with the miRNA regulatory system. PloS one *3*, e3164.
Garcia-Rodriguez, L.J., Gay, A.C., and Pon, L.A. (2007). Puf3p, a Pumilio family RNA binding protein, localizes to mitochondria and regulates mitochondrial biogenesis and motility in budding yeast. The Journal of cell biology *176*, 197-207.
Garcia, M., Darzacq, X., Delaveau, T., Jourdren, L., Singer, R.H., and Jacq, C. (2007). Mitochondria-associated yeast mRNAs and the biogenesis of molecular complexes. Molecular biology of the cell *18*, 362-368.
Garcia, M., Delaveau, T., Goussard, S., and Jacq, C. (2010). Mitochondrial presequence and open reading frame mediate asymmetric localization of messenger RNA. EMBO reports *11*, 285-291.
Garneau, N.L., Wilusz, J., and Wilusz, C.J. (2007). The highways and byways of mRNA decay. Nature reviews Molecular cell biology *8*, 113-126.
Gehrke, S., Wu, Z., Klinkenberg, M., Sun, Y., Auburger, G., Guo, S., and Lu, B. (2015). PINK1 and Parkin control localized translation of respiratory chain component mRNAs on mitochondria outer membrane. Cell metabolism *21*, 95-108.
Gems, D., Pletcher, S., and Partridge, L. (2002). Interpreting interactions between treatments that slow aging. Aging cell *1*, 1-9.
Gerber, A.P., Herschlag, D., and Brown, P.O. (2004). Extensive association of functionally and cytotopically related mRNAs with Puf family RNA-binding proteins in yeast. PLoS biology *2*, E79.
Gingras, A.C., Raught, B., and Sonenberg, N. (1999). eIF4 initiation factors: effectors of mRNA recruitment to ribosomes and regulators of translation. Annual review of biochemistry *68*, 913-963.
Gingras, A.C., Raught, B., and Sonenberg, N. (2004). mTOR signaling to translation. Current topics in microbiology and immunology *279*, 169-197.

Gold, V.A., Chroscicki, P., Bragoszewski, P., and Chacinska, A. (2017). Visualization of cytosolic ribosomes on the surface of mitochondria by electron cryo-tomography. EMBO reports *18*, 1786-1800.
Gonskikh, Y., and Polacek, N. (2017). Alterations of the translation apparatus during aging and stress response. Mechanisms of ageing and development *168*, 30-36.
Gotic, I., and Schibler, U. (2012). The ticking tail: daily oscillations in mRNA poly(A) tail length drive circadian cycles in protein synthesis. Genes & development *26*, 2669-2672.
Guarente, L. (2006). Sirtuins as potential targets for metabolic syndrome. Nature *444*, 868-874.
Guda, P., Guda, C., and Subramaniam, S. (2007). Reconstruction of pathways associated with amino acid metabolism in human mitochondria. Genomics, proteomics & bioinformatics *5*, 166-176.
Gureev, A.P., Shaforostova, E.A., and Popov, V.N. (2019). Regulation of Mitochondrial Biogenesis as a Way for Active Longevity: Interaction Between the Nrf2 and PGC-1alpha Signaling Pathways. Frontiers in genetics *10*, 435.
Hafner, M., Landthaler, M., Burger, L., Khorshid, M., Hausser, J., Berninger, P., Rothballer, A., Ascano, M., Jr., Jungkamp, A.C., Munschauer, M.*, et al.* (2010). Transcriptome-wide identification of RNA-binding protein and microRNA target sites by PAR-CLIP. Cell *141*, 129-141.
Haim, L., Zipor, G., Aronov, S., and Gerst, J.E. (2007). A genomic integration method to visualize localization of endogenous mRNAs in living yeast. Nature methods *4*, 409-412.
Hansen, M., Taubert, S., Crawford, D., Libina, N., Lee, S.J., and Kenyon, C. (2007). Lifespan extension by conditions that inhibit translation in Caenorhabditis elegans. Aging cell *6*, 95-110.
Hardie, D.G. (2011). AMP-activated protein kinase: an energy sensor that regulates all aspects of cell function. Genes & development *25*, 1895-1908.
Hayashi, G., Jasoliya, M., Sahdeo, S., Sacca, F., Pane, C., Filla, A., Marsili, A., Puorro, G., Lanzillo, R., Brescia Morra, V.*, et al.* (2017). Dimethyl fumarate mediates Nrf2-dependent mitochondrial biogenesis in mice and humans. Human molecular genetics *26*, 2864-2873.
Hesham A El-Beshbishy, H.M.E.-R., Hasan S Al-Amry, Rabab A Ali, Mohammed A Hassanien and Ramadan A Saad (2019). Targeting Mitochondrial Biogenesis in Rat Brain for Treatment of Depression. J Biomedical Sci *8*.
Hillier, L.W., Coulson, A., Murray, J.I., Bao, Z., Sulston, J.E., and Waterston, R.H. (2005). Genomics in C. elegans: so many genes, such a little worm. Genome research *15*, 1651-1660.
Hobert, O. (2010). Neurogenesis in the nematode Caenorhabditis elegans. WormBook : the online review of C elegans biology, 1-24.
Hodgkin, J. (2005). Karyotype, ploidy, and gene dosage. WormBook : the online review of C elegans biology, 1-9.
Hodgkin, J., and Doniach, T. (1997). Natural variation and copulatory plug formation in Caenorhabditis elegans. Genetics *146*, 149-164.
Hodgkin, J., Horvitz, H.R., and Brenner, S. (1979). Nondisjunction Mutants of the Nematode CAENORHABDITIS ELEGANS. Genetics *91*, 67-94.
Holcik, M., and Sonenberg, N. (2005). Translational control in stress and apoptosis. Nature reviews Molecular cell biology *6*, 318-327.
Honda, Y., and Honda, S. (1999). The daf-2 gene network for longevity regulates oxidative stress resistance and Mn-superoxide dismutase gene expression in Caenorhabditis elegans. FASEB journal : official publication of the Federation of American Societies for Experimental Biology *13*, 1385-1393.
Horn, D., and Barrientos, A. (2008). Mitochondrial copper metabolism and delivery to cytochrome c oxidase. IUBMB life *60*, 421-429.

Houtkooper, R.H., Mouchiroud, L., Ryu, D., Moullan, N., Katsyuba, E., Knott, G., Williams, R.W., and Auwerx, J. (2013). Mitonuclear protein imbalance as a conserved longevity mechanism. Nature *497*, 451-457.
Huang, L., Mollet, S., Souquere, S., Le Roy, F., Ernoult-Lange, M., Pierron, G., Dautry, F., and Weil, D. (2011). Mitochondria associate with P-bodies and modulate microRNA-mediated RNA interference. The Journal of biological chemistry *286*, 24219-24230.
Hubstenberger, A., Courel, M., Benard, M., Souquere, S., Ernoult-Lange, M., Chouaib, R., Yi, Z., Morlot, J.B., Munier, A., Fradet, M*., et al.* (2017). P-Body Purification Reveals the Condensation of Repressed mRNA Regulons. Molecular cell *68*, 144-157 e145.
Isaac, R.S., McShane, E., and Churchman, L.S. (2018). The Multiple Levels of Mitonuclear Coregulation. Annual review of genetics *52*, 511-533.
Isik, M., and Berezikov, E. (2013). Biolistic transformation of Caenorhabditis elegans. Methods in molecular biology *940*, 77-86.
Islam, H., Edgett, B.A., and Gurd, B.J. (2018). Coordination of mitochondrial biogenesis by PGC-1alpha in human skeletal muscle: A re-evaluation. Metabolism: clinical and experimental *79*, 42-51.
Ito, K., Inoue, T., Yokoyama, K., Morita, M., Suzuki, T., and Yamamoto, T. (2011). CNOT2 depletion disrupts and inhibits the CCR4-NOT deadenylase complex and induces apoptotic cell death. Genes to cells : devoted to molecular & cellular mechanisms *16*, 368-379.
Jager, S., Handschin, C., St-Pierre, J., and Spiegelman, B.M. (2007). AMP-activated protein kinase (AMPK) action in skeletal muscle via direct phosphorylation of PGC-1alpha. Proceedings of the National Academy of Sciences of the United States of America *104*, 12017-12022.
Janssens, G.E., and Veenhoff, L.M. (2016). The Natural Variation in Lifespans of Single Yeast Cells Is Related to Variation in Cell Size, Ribosomal Protein, and Division Time. PloS one *11*, e0167394.
Joo, M.S., Kim, W.D., Lee, K.Y., Kim, J.H., Koo, J.H., and Kim, S.G. (2016). AMPK Facilitates Nuclear Accumulation of Nrf2 by Phosphorylating at Serine 550. Molecular and cellular biology *36*, 1931-1942.
Jornayvaz, F.R., and Shulman, G.I. (2010). Regulation of mitochondrial biogenesis. Essays in biochemistry *47*, 69-84.
Joshi, D.C., and Bakowska, J.C. (2011). Determination of mitochondrial membrane potential and reactive oxygen species in live rat cortical neurons. Journal of visualized experiments : JoVE.
Kaeberlein, M., and Kennedy, B.K. (2008). Protein translation, 2008. Aging cell *7*, 777-782.
Kedersha, N., Stoecklin, G., Ayodele, M., Yacono, P., Lykke-Andersen, J., Fritzler, M.J., Scheuner, D., Kaufman, R.J., Golan, D.E., and Anderson, P. (2005). Stress granules and processing bodies are dynamically linked sites of mRNP remodeling. The Journal of cell biology *169*, 871-884.
Kenyon, C.J. (2010). The genetics of ageing. Nature *464*, 504-512.
Kim, J., Moody, J.P., Edgerly, C.K., Bordiuk, O.L., Cormier, K., Smith, K., Beal, M.F., and Ferrante, R.J. (2010). Mitochondrial loss, dysfunction and altered dynamics in Huntington's disease. Human molecular genetics *19*, 3919-3935.
Kimball, S.R., Vary, T.C., and Jefferson, L.S. (1992). Age-dependent decrease in the amount of eukaryotic initiation factor 2 in various rat tissues. The Biochemical journal *286 (Pt 1)*, 263-268.
Klass, M., and Hirsh, D. (1976). Non-ageing developmental variant of Caenorhabditis elegans. Nature *260*, 523-525.
Kourtis, N., and Tavernarakis, N. (2009). Cell-specific monitoring of protein synthesis in vivo. PloS one *4*, e4547.

Kourtis, N., and Tavernarakis, N. (2017). Protein Synthesis Rate Assessment by Fluorescence Recovery after Photobleaching (FRAP). Bio-protocol *7*.
Kren, B.T., Wong, P.Y., Sarver, A., Zhang, X., Zeng, Y., and Steer, C.J. (2009). MicroRNAs identified in highly purified liver-derived mitochondria may play a role in apoptosis. RNA biology *6*, 65-72.
Kutscher, L.M., and Shaham, S. (2014). Forward and reverse mutagenesis in C. elegans. WormBook : the online review of C elegans biology, 1-26.
Labbadia, J., Brielmann, R.M., Neto, M.F., Lin, Y.F., Haynes, C.M., and Morimoto, R.I. (2017). Mitochondrial Stress Restores the Heat Shock Response and Prevents Proteostasis Collapse during Aging. Cell reports *21*, 1481-1494.
Lamb, R., Bonuccelli, G., Ozsvari, B., Peiris-Pages, M., Fiorillo, M., Smith, D.L., Bevilacqua, G., Mazzanti, C.M., McDonnell, L.A., Naccarato, A.G.*, et al.* (2015). Mitochondrial mass, a new metabolic biomarker for stem-like cancer cells: Understanding WNT/FGF-driven anabolic signaling. Oncotarget *6*, 30453-30471.
LeBleu, V.S., O'Connell, J.T., Gonzalez Herrera, K.N., Wikman, H., Pantel, K., Haigis, M.C., de Carvalho, F.M., Damascena, A., Domingos Chinen, L.T., Rocha, R.M.*, et al.* (2014). PGC-1alpha mediates mitochondrial biogenesis and oxidative phosphorylation in cancer cells to promote metastasis. Nature cell biology *16*, 992-1003, 1001-1015.
Lechler, M.C., and David, D.C. (2017). More stressed out with age? Check your RNA granule aggregation. Prion *11*, 313-322.
Lee, Y.S., Pressman, S., Andress, A.P., Kim, K., White, J.L., Cassidy, J.J., Li, X., Lubell, K., Lim, D.H., Cho, I.S.*, et al.* (2009). Silencing by small RNAs is linked to endosomal trafficking. Nature cell biology *11*, 1150-1156.
Leprivier, G., Remke, M., Rotblat, B., Dubuc, A., Mateo, A.R., Kool, M., Agnihotri, S., El-Naggar, A., Yu, B., Somasekharan, S.P.*, et al.* (2013). The eEF2 kinase confers resistance to nutrient deprivation by blocking translation elongation. Cell *153*, 1064-1079.
Liang, F., Kume, S., and Koya, D. (2009). SIRT1 and insulin resistance. Nature reviews Endocrinology *5*, 367-373.
Lien, L.M., Chiou, H.Y., Yeh, H.L., Chiu, S.Y., Jeng, J.S., Lin, H.J., Hu, C.J., Hsieh, F.I., and Wei, Y.H. (2017). Significant Association Between Low Mitochondrial DNA Content in Peripheral Blood Leukocytes and Ischemic Stroke. Journal of the American Heart Association *6*.
Lill, R., Hoffmann, B., Molik, S., Pierik, A.J., Rietzschel, N., Stehling, O., Uzarska, M.A., Webert, H., Wilbrecht, C., and Muhlenhoff, U. (2012). The role of mitochondria in cellular iron-sulfur protein biogenesis and iron metabolism. Biochimica et biophysica acta *1823*, 1491-1508.
Lopez-Otin, C., Blasco, M.A., Partridge, L., Serrano, M., and Kroemer, G. (2013). The hallmarks of aging. Cell *153*, 1194-1217.
Luo, Y., Na, Z., and Slavoff, S.A. (2018). P-Bodies: Composition, Properties, and Functions. Biochemistry *57*, 2424-2431.
Makrides, S.C. (1983). Protein synthesis and degradation during aging and senescence. Biological reviews of the Cambridge Philosophical Society *58*, 343-422.
Marc, P., Margeot, A., Devaux, F., Blugeon, C., Corral-Debrinski, M., and Jacq, C. (2002). Genome-wide analysis of mRNAs targeted to yeast mitochondria. EMBO reports *3*, 159-164.
Margeot, A., Garcia, M., Wang, W., Tetaud, E., di Rago, J.P., and Jacq, C. (2005). Why are many mRNAs translated to the vicinity of mitochondria: a role in protein complex assembly? Gene *354*, 64-71.
Maziuk, B., Ballance, H.I., and Wolozin, B. (2017). Dysregulation of RNA Binding Protein Aggregation in Neurodegenerative Disorders. Frontiers in molecular neuroscience *10*, 89.

Mello, C.C., and Conte, D., Jr. (2004). Revealing the world of RNA interference. Nature *431*, 338-342.
Miyazono, Y., Hirashima, S., Ishihara, N., Kusukawa, J., Nakamura, K.I., and Ohta, K. (2018). Uncoupled mitochondria quickly shorten along their long axis to form indented spheroids, instead of rings, in a fission-independent manner. Scientific reports *8*, 350.
Moldave, K., Harris, J., Sabo, W., and Sadnik, I. (1979). Protein synthesis and aging: studies with cell-free mammalian systems. Federation proceedings *38*, 1979-1983.
Mori, I. (1999). Genetics of chemotaxis and thermotaxis in the nematode Caenorhabditis elegans. Annual review of genetics *33*, 399-422.
Morris, A.R., Mukherjee, N., and Keene, J.D. (2008). Ribonomic analysis of human Pum1 reveals cis-trans conservation across species despite evolution of diverse mRNA target sets. Molecular and cellular biology *28*, 4093-4103.
Mulcahy, B., Witvliet, D., Holmyard, D., Mitchell, J., Chisholm, A.D., Meirovitch, Y., Samuel, A.D.T., and Zhen, M. (2018). A Pipeline for Volume Electron Microscopy of the Caenorhabditis elegans Nervous System. Frontiers in neural circuits *12*, 94.
Nicholas W L, D.E.C., Hansen E L. (1959). Axenic cultivation of C. briggsae (Nematoda: Rhabditidae) with chemically undefined supplements;--> comparative studies with related nematodes. . Ann NY Acad Sci *77*, 218–236.
Nishimura, T., Padamsi, Z., Fakim, H., Milette, S., Dunham, W.H., Gingras, A.C., and Fabian, M.R. (2015). The eIF4E-Binding Protein 4E-T Is a Component of the mRNA Decay Machinery that Bridges the 5' and 3' Termini of Target mRNAs. Cell reports *11*, 1425-1436.
Nisoli, E., Clementi, E., Carruba, M.O., and Moncada, S. (2007). Defective mitochondrial biogenesis: a hallmark of the high cardiovascular risk in the metabolic syndrome? Circulation research *100*, 795-806.
Nousch, M., Techritz, N., Hampel, D., Millonigg, S., and Eckmann, C.R. (2013). The Ccr4-Not deadenylase complex constitutes the main poly(A) removal activity in C. elegans. Journal of cell science *126*, 4274-4285.
Olsen, A., Vantipalli, M.C., and Lithgow, G.J. (2006). Using Caenorhabditis elegans as a model for aging and age-related diseases. Annals of the New York Academy of Sciences *1067*, 120-128.
Onyango, I.G. (2018). Modulation of mitochondrial bioenergetics as a therapeutic strategy in Alzheimer's disease. Neural regeneration research *13*, 19-25.
Ozgur, S., Basquin, J., Kamenska, A., Filipowicz, W., Standart, N., and Conti, E. (2015). Structure of a Human 4E-T/DDX6/CNOT1 Complex Reveals the Different Interplay of DDX6-Binding Proteins with the CCR4-NOT Complex. Cell reports *13*, 703-711.
Ozgur, S., Chekulaeva, M., and Stoecklin, G. (2010). Human Pat1b connects deadenylation with mRNA decapping and controls the assembly of processing bodies. Molecular and cellular biology *30*, 4308-4323.
Palikaras, K., Lionaki, E., and Tavernarakis, N. (2015). Coordination of mitophagy and mitochondrial biogenesis during ageing in C. elegans. Nature *521*, 525-528.
Pan, K.Z., Palter, J.E., Rogers, A.N., Olsen, A., Chen, D., Lithgow, G.J., and Kapahi, P. (2007). Inhibition of mRNA translation extends lifespan in Caenorhabditis elegans. Aging cell *6*, 111-119.
Partridge, L., and Gems, D. (2002). Mechanisms of ageing: public or private? Nature reviews Genetics *3*, 165-175.
Picard, M., McEwen, B.S., Epel, E.S., and Sandi, C. (2018). An energetic view of stress: Focus on mitochondria. Frontiers in neuroendocrinology *49*, 72-85.
Ploumi, C., Daskalaki, I., and Tavernarakis, N. (2017). Mitochondrial biogenesis and clearance: a balancing act. The FEBS journal *284*, 183-195.

Proud, C.G. (2007). Signalling to translation: how signal transduction pathways control the protein synthetic machinery. The Biochemical journal *403*, 217-234.
Pyle, A., Anugrha, H., Kurzawa-Akanbi, M., Yarnall, A., Burn, D., and Hudson, G. (2016). Reduced mitochondrial DNA copy number is a biomarker of Parkinson's disease. Neurobiology of aging *38*, 216 e217-216 e210.
Quiros, P.M., Mottis, A., and Auwerx, J. (2016). Mitonuclear communication in homeostasis and stress. Nature reviews Molecular cell biology *17*, 213-226.
Rangaraju, V., Lauterbach, M., and Schuman, E.M. (2019). Spatially Stable Mitochondrial Compartments Fuel Local Translation during Plasticity. Cell *176*, 73-84 e15.
Rattan, S.I. (1996). Synthesis, modifications, and turnover of proteins during aging. Experimental gerontology *31*, 33-47.
Regmi, S.G., Rolland, S.G., and Conradt, B. (2014). Age-dependent changes in mitochondrial morphology and volume are not predictors of lifespan. Aging *6*, 118-130.
Ricart, J., Egea, G., Izquierdo, J.M., San Martin, C., and Cuezva, J.M. (1997). Subcellular structure containing mRNA for beta subunit of mitochondrial H+-ATP synthase in rat hepatocytes is translationally active. The Biochemical journal *324 (Pt 2)*, 635-643.
Riddle, D.L., Blumenthal, T., Meyer, B.J., and Priess, J.R. (1997). Introduction to C. elegans. In C elegans II, nd, D.L. Riddle, T. Blumenthal, B.J. Meyer, and J.R. Priess, eds. (Cold Spring Harbor (NY)).
Rieckher, M., Markaki, M., Princz, A., Schumacher, B., and Tavernarakis, N. (2018). Maintenance of Proteostasis by P Body-Mediated Regulation of eIF4E Availability during Aging in Caenorhabditis elegans. Cell reports *25*, 199-211 e196.
Rieckher, M., and Tavernarakis, N. (2017). Caenorhabditis elegans Microinjection. Bio-protocol *7*.
Rogers, A.N., Chen, D., McColl, G., Czerwieniec, G., Felkey, K., Gibson, B.W., Hubbard, A., Melov, S., Lithgow, G.J., and Kapahi, P. (2011). Life span extension via eIF4G inhibition is mediated by posttranscriptional remodeling of stress response gene expression in C. elegans. Cell metabolism *14*, 55-66.
Rona-Voros, K., and Weydt, P. (2010). The role of PGC-1alpha in the pathogenesis of neurodegenerative disorders. Current drug targets *11*, 1262-1269.
Rousakis, A., Vlanti, A., Borbolis, F., Roumelioti, F., Kapetanou, M., and Syntichaki, P. (2014). Diverse functions of mRNA metabolism factors in stress defense and aging of Caenorhabditis elegans. PloS one *9*, e103365.
Scarpulla, R.C. (2012). Nucleus-encoded regulators of mitochondrial function: integration of respiratory chain expression, nutrient sensing and metabolic stress. Biochimica et biophysica acta *1819*, 1088-1097.
Scatena, C., Roncella, M., Di Paolo, A., Aretini, P., Menicagli, M., Fanelli, G., Marini, C., Mazzanti, C.M., Ghilli, M., Sotgia, F.*, et al.* (2018). Doxycycline, an Inhibitor of Mitochondrial Biogenesis, Effectively Reduces Cancer Stem Cells (CSCs) in Early Breast Cancer Patients: A Clinical Pilot Study. Frontiers in oncology *8*, 452.
Short, K.R., Bigelow, M.L., Kahl, J., Singh, R., Coenen-Schimke, J., Raghavakaimal, S., and Nair, K.S. (2005). Decline in skeletal muscle mitochondrial function with aging in humans. Proceedings of the National Academy of Sciences of the United States of America *102*, 5618-5623.
Singh, J., Salcius, M., Liu, S.W., Staker, B.L., Mishra, R., Thurmond, J., Michaud, G., Mattoon, D.R., Printen, J., Christensen, J.*, et al.* (2008). DcpS as a therapeutic target for spinal muscular atrophy. ACS chemical biology *3*, 711-722.

Stallons, L.J., Whitaker, R.M., and Schnellmann, R.G. (2014). Suppressed mitochondrial biogenesis in folic acid-induced acute kidney injury and early fibrosis. Toxicology letters *224*, 326-332.
Steffen, K.K., MacKay, V.L., Kerr, E.O., Tsuchiya, M., Hu, D., Fox, L.A., Dang, N., Johnston, E.D., Oakes, J.A., Tchao, B.N., *et al.* (2008). Yeast life span extension by depletion of 60s ribosomal subunits is mediated by Gcn4. Cell *133*, 292-302.
Sun, C.K., Chang, L.T., Sheu, J.J., Wang, C.Y., Youssef, A.A., Wu, C.J., Chua, S., and Yip, H.K. (2007). Losartan preserves integrity of cardiac gap junctions and PGC-1 alpha gene expression and prevents cellular apoptosis in remote area of left ventricular myocardium following acute myocardial infarction. International heart journal *48*, 533-546.
Sutton, M.A., and Schuman, E.M. (2006). Dendritic protein synthesis, synaptic plasticity, and memory. Cell *127*, 49-58.
Sylvestre, J., Vialette, S., Corral Debrinski, M., and Jacq, C. (2003). Long mRNAs coding for yeast mitochondrial proteins of prokaryotic origin preferentially localize to the vicinity of mitochondria. Genome biology *4*, R44.
Syntichaki, P., Troulinaki, K., and Tavernarakis, N. (2007). eIF4E function in somatic cells modulates ageing in Caenorhabditis elegans. Nature *445*, 922-926.
Taherzadeh-Fard, E., Saft, C., Akkad, D.A., Wieczorek, S., Haghikia, A., Chan, A., Epplen, J.T., and Arning, L. (2011). PGC-1alpha downstream transcription factors NRF-1 and TFAM are genetic modifiers of Huntington disease. Molecular neurodegeneration *6*, 32.
Takahashi, R., Mori, N., and Goto, S. (1985). Accumulation of heat-labile elongation factor 2 in the liver of mice and rats. Experimental gerontology *20*, 325-331.
Tang, N.H., Kim, K.W., Xu, S., Blazie, S.M., Yee, B.A., Yeo, G.W., Jin, Y., and Chisholm, A.D. (2020). The mRNA Decay Factor CAR-1/LSM14 Regulates Axon Regeneration via Mitochondrial Calcium Dynamics. Current biology : CB.
Tavernarakis, N. (2007). Protein synthesis and aging: eIF4E and the soma vs. germline distinction. Cell cycle *6*, 1168-1171.
Tavernarakis, N. (2008). Ageing and the regulation of protein synthesis: a balancing act? Trends in cell biology *18*, 228-235.
Tavernarakis, N., and Driscoll, M. (2002). Caloric restriction and lifespan: a role for protein turnover? Mechanisms of ageing and development *123*, 215-229.
Temme, C., Simonelig, M., and Wahle, E. (2014). Deadenylation of mRNA by the CCR4-NOT complex in Drosophila: molecular and developmental aspects. Frontiers in genetics *5*, 143.
Torrens-Mas, M., Hernandez-Lopez, R., Pons, D.G., Roca, P., Oliver, J., and Sastre-Serra, J. (2019). Sirtuin 3 silencing impairs mitochondrial biogenesis and metabolism in colon cancer cells. American journal of physiology Cell physiology *317*, C398-C404.
Tosato, M., Zamboni, V., Ferrini, A., and Cesari, M. (2007). The aging process and potential interventions to extend life expectancy. Clinical interventions in aging *2*, 401-412.
Van Laar, V.S., Arnold, B., Howlett, E.H., Calderon, M.J., St Croix, C.M., Greenamyre, J.T., Sanders, L.H., and Berman, S.B. (2018). Evidence for Compartmentalized Axonal Mitochondrial Biogenesis: Mitochondrial DNA Replication Increases in Distal Axons As an Early Response to Parkinson's Disease-Relevant Stress. The Journal of neuroscience : the official journal of the Society for Neuroscience *38*, 7505-7515.
Vargas, R., and Castaneda, M. (1981). Role of elongation factor 1 in the translational control of rodent brain protein synthesis. Journal of neurochemistry *37*, 687-694.
Vargas, R., and Castaneda, M. (1983). Age-dependent decrease in the activity of protein-synthesis initiation factors in rat brain. Mechanisms of ageing and development *21*, 183-191.

Verkhusha, V.V., Kuznetsova, I.M., Stepanenko, O.V., Zaraisky, A.G., Shavlovsky, M.M., Turoverov, K.K., and Uversky, V.N. (2003). High stability of Discosoma DsRed as compared to Aequorea EGFP. Biochemistry *42*, 7879-7884.
Vicente, C., Stirparo, R., Demeyer, S., de Bock, C.E., Gielen, O., Atkins, M., Yan, J., Halder, G., Hassan, B.A., and Cools, J. (2018). The CCR4-NOT complex is a tumor suppressor in Drosophila melanogaster eye cancer models. Journal of hematology & oncology *11*, 108.
von der Haar, T., Leadsham, J.E., Sauvadet, A., Tarrant, D., Adam, I.S., Saromi, K., Laun, P., Rinnerthaler, M., Breitenbach-Koller, H., Breitenbach, M.*, et al.* (2017). The control of translational accuracy is a determinant of healthy ageing in yeast. Open biology *7*.
Vyas, S., Zaganjor, E., and Haigis, M.C. (2016). Mitochondria and Cancer. Cell *166*, 555-566.
Wang, C., Schmich, F., Srivatsa, S., Weidner, J., Beerenwinkel, N., and Spang, A. (2018a). Context-dependent deposition and regulation of mRNAs in P-bodies. eLife *7*.
Wang, C., Schmich, F., Srivatsa, S., Weidner, J., Beerenwinkel, N., and Spang, A. (2018b). Correction: Context-dependent deposition and regulation of mRNAs in P-bodies. eLife *7*.
Wang, C., and Youle, R.J. (2009). The role of mitochondria in apoptosis*. Annual review of genetics *43*, 95-118.
Ward, S., and Carrel, J.S. (1979). Fertilization and sperm competition in the nematode Caenorhabditis elegans. Developmental biology *73*, 304-321.
Webster, G.C., and Webster, S.L. (1983). Decline in synthesis of elongation factor one (EF-1) precedes the decreased synthesis of total protein in aging Drosophila melanogaster. Mechanisms of ageing and development *22*, 121-128.
Weydt, P., Soyal, S.M., Gellera, C., Didonato, S., Weidinger, C., Oberkofler, H., Landwehrmeyer, G.B., and Patsch, W. (2009). The gene coding for PGC-1alpha modifies age at onset in Huntington's Disease. Molecular neurodegeneration *4*, 3.
White, J.G., Southgate, E., Thomson, J.N., and Brenner, S. (1986). The structure of the nervous system of the nematode Caenorhabditis elegans. Philosophical transactions of the Royal Society of London Series B, Biological sciences *314*, 1-340.
Williams, C.C., Jan, C.H., and Weissman, J.S. (2014). Targeting and plasticity of mitochondrial proteins revealed by proximity-specific ribosome profiling. Science *346*, 748-751.
Yoshida, Y., Hasegawa, J., Nezu, R., Kim, Y.K., Hirota, M., Kawano, K., Izumi, H., and Kohno, K. (2011). Clinical usefulness of mitochondrial transcription factor A expression as a predictive marker in colorectal cancer patients treated with FOLFOX. Cancer science *102*, 578-582.
Yoshimi, A., and Abdel-Wahab, O. (2018). Targeting mRNA Decapping in AML. Cancer cell *33*, 339-341.
Youdim, M.B., and Oh, Y.J. (2013). Promise of neurorestoration and mitochondrial biogenesis in Parkinson's disease with multi target drugs: an alternative to stem cell therapy. Experimental neurobiology *22*, 167-172.
Youn, J.Y., Dunham, W.H., Hong, S.J., Knight, J.D.R., Bashkurov, M., Chen, G.I., Bagci, H., Rathod, B., MacLeod, G., Eng, S.W.M.*, et al.* (2018). High-Density Proximity Mapping Reveals the Subcellular Organization of mRNA-Associated Granules and Bodies. Molecular cell *69*, 517-532 e511.
Zeitelhofer, M., Karra, D., Vessey, J.P., Jaskic, E., Macchi, P., Thomas, S., Riefler, J., Kiebler, M., and Dahm, R. (2009). High-efficiency transfection of short hairpin RNAs-encoding plasmids into primary hippocampal neurons. Journal of neuroscience research *87*, 289-300.
Zhang, B.B., Zhou, G., and Li, C. (2009). AMPK: an emerging drug target for diabetes and the metabolic syndrome. Cell metabolism *9*, 407-416.
Zhang, C., and Rabouille, C. (2019). Membrane-Bound Meet Membraneless in Health and Disease. Cells *8*.

Zhang, X., Zuo, X., Yang, B., Li, Z., Xue, Y., Zhou, Y., Huang, J., Zhao, X., Zhou, J., Yan, Y.*, et al.* (2014). MicroRNA directly enhances mitochondrial translation during muscle differentiation. Cell *158*, 607-619.
Zhang, Y., Chen, Y., Gucek, M., and Xu, H. (2016). The mitochondrial outer membrane protein MDI promotes local protein synthesis and mtDNA replication. The EMBO journal *35*, 1045-1057.
Zheng, B., Liao, Z., Locascio, J.J., Lesniak, K.A., Roderick, S.S., Watt, M.L., Eklund, A.C., Zhang-James, Y., Kim, P.D., Hauser, M.A.*, et al.* (2010). PGC-1alpha, a potential therapeutic target for early intervention in Parkinson's disease. Science translational medicine *2*, 52ra73.
Zheng, D., Ezzeddine, N., Chen, C.Y., Zhu, W., He, X., and Shyu, A.B. (2008). Deadenylation is prerequisite for P-body formation and mRNA decay in mammalian cells. The Journal of cell biology *182*, 89-101.

CURRICULUM VITAE

Ioanna Daskalaki accomplished her Bachelor's Degree in the Biology Department of the University of Crete in Greece in 2011. During her Bachelor's, she initially worked as a volunteer in 2007 in the laboratory of Systems Biology and Biogeography of Chilopoda. Later, in 2008, she worked in the laboratory of Molecular Systematics and Evolution. Both labs are at the Natural History Museum in Heraklion, Greece. In 2011 she performed her Bachelor's Degree Thesis in Dr. Joseph Papamatheaki's lab, where she studied the regulation of the cancer stem cell markers CD44 and CD24 in human cancer cell lines.

From 2011 to 2013 she performed her Master's in Molecular Biology and Biotechnology operated by the Biology Department and the School of Medicine, University of Crete, Greece and the Institute of Molecular Biology and Biotechnology, FORTH, Heraklion, Greece. During her Master's she worked in the laboratory of Bioinformatics and the laboratory of Pharmacology in the School of Medicine, University of Crete, Greece. She conducted her master thesis in Prof. Nektarios Tavernarakis lab. By that time she was awarded graduate studies fellowship from the State Scholarships Foundation. In prof. Tavernaraki's lab she continued for her PhD studies.

During her PhD, she worked on the model organism *C. elegans* towards understanding the complex interplay between mRNA metabolism components and mitochondria and also defining the role of this association in stress resistance and ageing.

Overall, she has published 15 posters in national, European and international conferences. Six posters are related to her main PhD project while the rest are related to her involvement in two additional projects. Furthermore, Ioanna has published four review papers and one book chapter and has performed three public oral presentations.

Last, she was part of the organizing Committee in the 1st FORTH YouR Night event (https://www.forth.gr/YouRnight/index.html).